ISSN 0385-2520

Rock Magnetism and Paleogeophysics

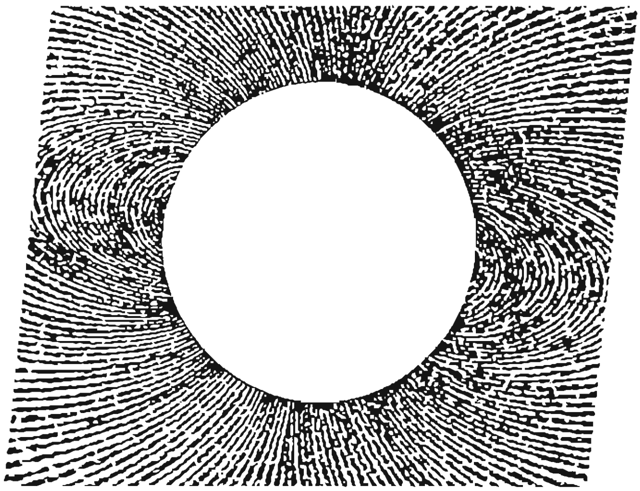

Volume 18

December 1991

Published by

Rock Magnetism and Paleogeophysics
Research Group in Japan

Preface

This volume is the annual progress report of the Rock Magnetism and Paleogeophysics Research Group in Japan for the year of 1991. We have published annual reports with a title Annual Progress Report of the Rock Magnetism (Paleogeophysics) Research Group in Japan in 1963, 1964, 1965, and 1967. Since 1973, the title changed to Rock Magnetism and Paleogeophysics and the reports were published annually (except 1976).

This volume contains a collection of summaries, extended abstracts or brief notes of research works carried out in our group this year. Many reports contain materials which may undergo a significant change or may be revised as the research activity continues. In this respect, readers are warned to regard them as tentative and are also requested to refer from a complete paper if published as a final results. (Names of journal appear at the end of individual articles if they are in press, submitted, or in preparation for submission to some scientific journals.

The editor of Rock Magnetism and Paleogeophysics has been Professor Masaru Kono of Tokyo Institute of Technology since 1973. However, as stated in the preface of volume 16,1989, he decided to retire from the editorial charge. After some debate about the continuation of the annual report in our group, we decided to continue the publication of this annual report for more several years. During this extension period, M. Torii of Kyoto University is the editor of this report for even-number years and Y. Hamano of University of Tokyo for odd-number years.

This publication is partly supported by a Grant-in-Aid for Scientific Research on Priority Areas (Central Core of the Earth) from the Japanese Ministry of Education, Science and Culture (No. 02246105).

Tokyo
December 1991

Yozo Hamano
Editor of 1991

Rock Magnetism and Paleogeophysics
Research Group in Japan

Rock Magnetism and Paleogeophysics, Volume 18
Table of Contents

Tectonics

ROCK MAGNETIC PROPERTIES OF SEDIMENTS FROM SITE 797, JAPAN SEA
(Extended abstract)

M. Torii[1], A. Hayashida[2], L. Vigliotti[3], and J. Wippern[4]

[1] Department of Geology and Mineralogy, Kyoto University, Kyoto 606-01, Japan
[2] Laboratory of Earth Sciences, Doshisha University, Kyoto 602, Japan
[3] Istitute di Geologia Marina, CNR, I-40127 Bologna, Italy
[4] Institute Angewandte Geophysik, Universität Müchen, D-8000 Müchen, Germany

Paleomagnetic and rock magnetic studies of the sediment samples from ODP Site 797 (western part of the Yamato basin; Tamaki, Pisciotto, Allan, et al., 1990) were carried out. The primary purpose of this study is to identify magnetic minerals in the sediments to help interpretation of the shipboard paleomagnetic results. We collected cubic samples mainly from silt and clay layers; 11 sampling horizons were selected from the cores recovered by using Advanced Piston Corer, 5 horizons from Extended Core Barrel, and 7 horizons from conventional Rotary Core Barrel. The diagenetic change of biogenic silica in the sediments, which was accelerated by the increase of temperature and duration time of burial (Tada, 1991) is also a good indicator to show physicochemical change in the sediments. Two distinct diagenetic boundaries were recognized in Site 797 sediments (Tamaki, Pisciotto, Allan, et al., 1990). The opal-A zone to opal-CT zone transition occurs between 294.3 and 299.1 mbsf and the opal-CT zone to quartz zone transition occurs between 428 and 438 mbsf. From each horizon, we obtained two vertically adjacent samples. Six additional samples were obtained from the Brunhes-Matuyama transition zone (around 40 mbsf). Total numbers of studied samples are 52 from 29 horizons. Our experiments were carried out on bulk samples. We did not make any kind of magnetic separation and/or condensation of magnetic mineral. We thought that the magnetic separation may bias mineral identification by overestimating larger grains. And also the volume of our sample from each horizon is only 7cm3 which is not practically enough for any kind of magnetic separation. The followings are results and conclusions:

(1) The stability of remanent magnetization was examined by progressive AF and thermal demagnetizations. AF method is generally not effective in eliminating secondary overprinting because of easy acquisition of ARM. Thermal demagnetization is more effective in revealing a high-temperature component, but was occasionally impaired by the production of new magnetic minerals. The ratio of $\chi 450/\chi$ was a useful parameter to describe production of new magnetic minerals during the demagnetization. We could not find significant difference of $\chi 450/\chi$ ratio between dark and light color layers in the APC zone.

(2) Magnetic mineralogy was investigated by thermal demagnetization of three orthogonal (composite) IRM's (Lowrie, 1989). Unblocking temperature of the three coercivity ranges revealed that there are at least four types of magnetic mineral assemblage (Fig. 1). In the opal-A zone, a mixture of pyrrhotite and (titano)magnetite is dominant. The mixing ratio of (titano)magnetite and pyrrhotite is changeable from sample to sample judging from the pattern of the thermal demagnetization curves. Magnetite is more dominant in the lower part

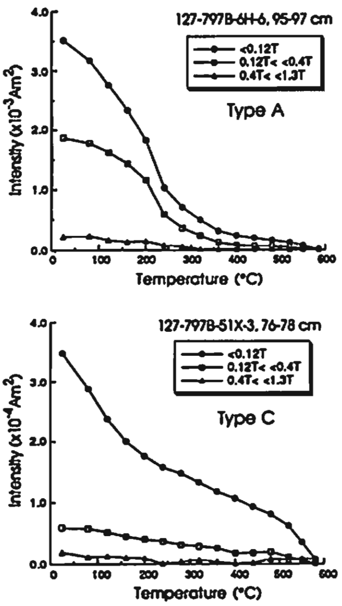

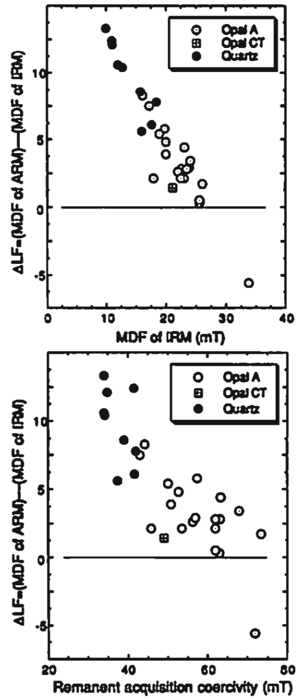

Figure 1 (above). Four types of thermal demagnetization curves of orthogonal IRM's. Closed circles indicate thermal decay of IRM intensity imparted by the field of 0.1 T. Open squares and open triangles indicate demagnetization curves of medium (0.4 T to 1.3 T) and hard (1.3 T) IRM's, respectively.

Figure 2 (right). Plot of ΔLF [(MDF of ARM) - (MDF of IRM)] vs. MDF of IRM (above). Plot of ΔLF vs. remanent acquisition coercivity, (below).

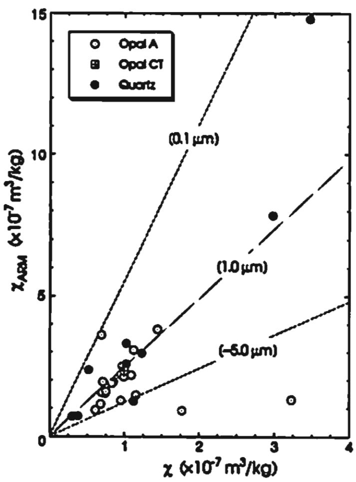

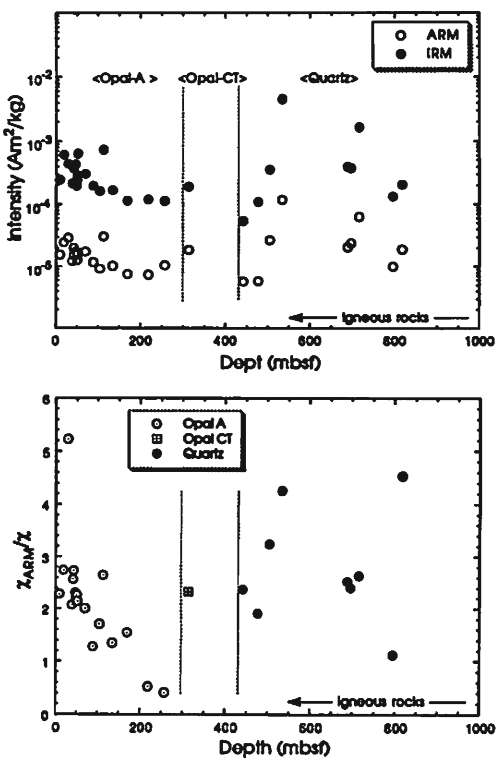

Figure 3 (above). Plot of mass susceptibility of ARM (χ_{ARM}) against mass initial susceptibility (χ). Lines denoted 0.1mm to ~5.0 mm are defined after King et al. (1982).

Figure 4 (right). Downcore plot of ARM and IRM intensities (above), and χ_{ARM}/χ ratio (below).

of the hole (opal-CT and quartz zones).

(3) Apparent grain size of the magnetic minerals were estimated by the modified Lowrie-Fuller test (Johnson et al., 1975) and by using the χ_{ARM}/χ ratio (King et al., 1982). We pointed out that magnetic minerals of most samples from Site 797 are of SD/PSD or small MD size (Fig. 2 and Fig. 3), and resemble that of normal deep-sea sediments such as from the South Atlantic (Petersen et al., 1986), the Northeast Pacific (Karin, 1990), and the North Pacific (Doh et al., 1988). Magnetic mineralogy and grain size distribution are not identical in the opal-A zone and in the quartz zone. The ΔLF values make separate clusters when plotted against MDF of IRM and/or remanent acquisition coercivity.

(4) Some rock magnetic parameters such as ARM and IRM intensities, and the χ_{ARM}/χ ratio showed characteristic downcore decrease within the opal-A zone (Fig. 4). This fact implies diagenetic dissolution of finer magnetic minerals in the sediments. In the lower part of the hole, production of magnetic minerals is suggested. The intrusion of igneous rocks might accelerate production of magnetite. Paleomagnetic directions might have been safely preserved in the upper part of opal-A zone, but severely overprinted in the quartz zone.

References

Doh, S. J., J. W. King, and M. Leinen (1988): Paleoceanography, **3**, 89.
Johnson, H. P., W. Lowrie, and D. V. Kent (1975): Geophys. J. R. Astr. Soc., **41**, 1.
Karlin, R. (1990): J. Geophys. Res., **95**, 4421.
King., J. W., S. K. Banerjee, J. Marvin, and Ö. Ödemir (1982): Earth Planet. Sci. Lett., **59**, 404.
Lowrie, W. (1990): Geophys. Res. Lett., **17**, 159.
Petersen, N., T. von Dobeneck, and H. Vali (1986): Nature, **320**, 611.
Tada, R. (1991): in Einsele, Ricken, and Seilacher (Eds.) *Cycle and Event in Stratigraphy, Heidelberg*, (Springer), 480.
Tamaki, K., K. Pisciotto, J. Allan, et al. (1990): Proc. ODP, Init. Rept., **127**, College Station, TX (Ocean Drilling Program).

*(to be published in Proc. ODP, Sci. Results, **127/128**, College Station, TX, 1992)*

ALTERATION OF FERROMAGNETIC CONSTITUENTS OF OCEANIC BASALT UNDER PRESSURIZED HYDROTHERMAL LIQUIDS IN LABORATORY

Tomoko OGISHIMA and Hajimu KINOSHITA

Earthquake Res. Inst., Univ. of Tokyo, Yayoi 1 chome, Bunkyo-ku, Tokyo 113

Introduction

Low temperature oxidation which is believed to occur in the oceanic basement has been investigated intensively (e.g. Readman and O'Reilly, 1970; Bleil and Petersen, 1983; Furuta, 1983; Akimoto et al., 1984). Laboratory experiments for the effect on its magnetic characteristics by simulating hydrothermal condition have not been studied enough.

In the present experiment one of fresh oceanic basalts was altered under pressurized hydrothermal environment to induce some change in magnetic characteristics of ferromagnetic minerals (titanomagnetite). In order to reveal the effect of initial pH values of solution, acid and alkaline solutions were used. It was reported that strong acid (about pH 3) fluid poured out around oceanic ridge (Von Damm et al., 1985; private communication by Kinoshita from Hole 504B, ODP). The term "fresh" in this text is meant that the titanomagnetite has reversible Js-T curves and low Curie temperature as low as 200°C.

Sample selection and magnetic measurements

The ten minicore basalt samples which were identified to contain fresh titanomagnetites were obtained from Hole 412A, Leg 49 referring to the thermomagnetic data of the Initial Report of Deep Sea Drilling Project (Kobayashi et al., 1979). Hole 412A is located near the Mid-Atlantic Ridge and its formation age is 1.6 Ma (Luyendyk and Cann, 1979). The minicore samples were pulverized in stainless mortar and pestle roughly and magnetic characteristics were detected by thermomagnetic analyses and magnetic parameters measurement by use of vibration sample type magnetometer (Riken-denshi Co.). Thermomagnetic analyses were conducted in vacuum 1.3×10^{-3} Pa using powder samples from 50 to 100 mg. Heating and cooling rate was 4.5°C/min, maximum temperature was 780°C and the magnetic field intensity was about 1.0 T. Heating and cooling was repeated twice for all runs. As magnetic parameters, saturation moment (Js), remanent saturation moment (Jrs), coercive force (Hc), remanent coercive force (Hrc) were measured in the magnetic field intensity as high as 1.4 T. No magnetic separation of samples was attempted due to difficulty in obtaining pure magnetic minerals from a restricted volume of the specimen. In this experiment we had no means to controlling size effect on various magnetic parameters in the experiment in spite of importance of this factor described previously (Sakamoto et al., 1968; Hamano et al., 1979).

Eight out of ten minicore samples are magnetically fresh in

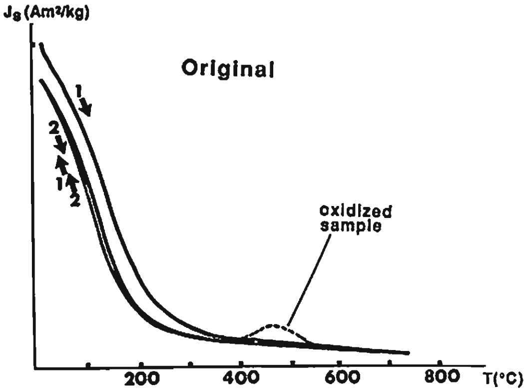

Fig.1 Js-T curves of a fresh sample before hydrothermal treatment. Reversible curves with low Curie point (about 200°C) are shown by solid lines. Those of a sample which had been subject to low temperature oxidation to some extent in natural indicated small Js increase shown by dashed line. Arrows and numbers indicate 1st and 2nd heating and cooling directions.

thermomagnetic analyses i.e. monotonous change against temperature. These samples showed reversible Js-T curves with low Curie point (around 200°C). The rest of two original samples indicated small increase of Js at around 450°C in first heating cycle of Js-T curves, which suggests that they had been subject to low temperature oxidation to some extent under the seawater (Fig.1).

Magnetic parameters can be characterized from the plots of Fig.2 that the ferromagnetic carrier of the present samples are small grains of titanomagnetites of pseudo-single domain size by referring to Day's method (Day et al., 1977).

One of the most fresh minicore samples (Core 3, section 1, interval 175.92-175.94 m) was selected for the present hydrothermal experiment.

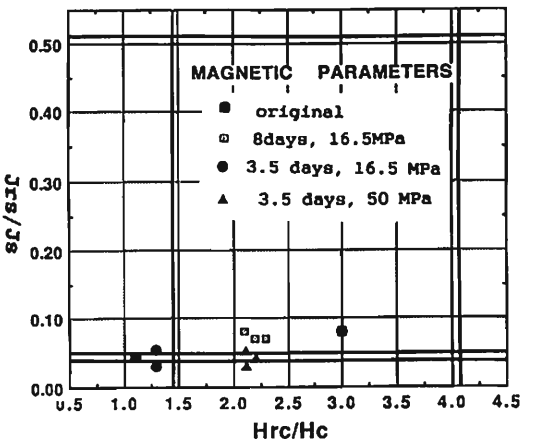

Fig.2 Magnetic parameters and their ratios of individual samples before and after various treatments are plotted. The vertical and horizontal axes are Jrs/Js and Hrc/Hc respectively. The sample which fall in a region within a rectangle bordered by double lines are identified as "effectively pseudo-single domain grains" after Day's method (Day et al., 1977).

Hydrothermal experiment

Each 100 mg powder sample was sealed up in Au-pipe (sample holder) with acid and alkaline fluid and heated up to 350°C.

Three hydrothermal experiments were conducted: 1. 8 day heating at 16.5 MPa with varying pH of initial solution. Three samples were heated up with 0.15 ml solutions whose initial pH values were 3 (H_2SO_4), pure water and 9 (NaOH) respectively. 16.5

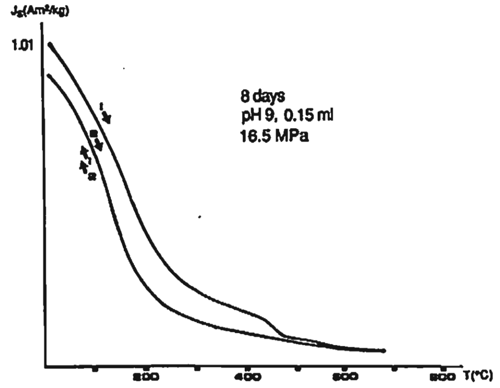

Fig.3 Js-T curves of a hydrothermally altered sample. Metastable phase converts at around 480°C. Magnetic moment is lost at 650°C. Arrows and numbers indicate 1st and 2nd heating and cooling cycle.

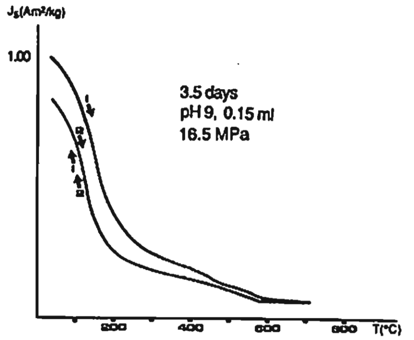

Fig.4 Alkaline environment seems to prevent alteration compared to the result of the case otherwise processed in the some conditions.

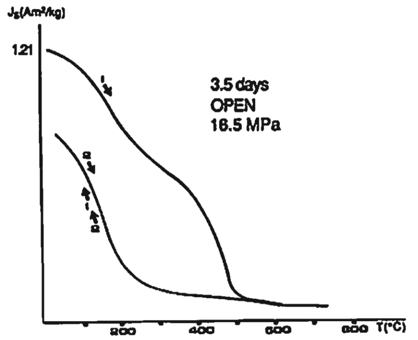

Fig.5 Sample exposed to confining water produces considerable amount of altered phase.

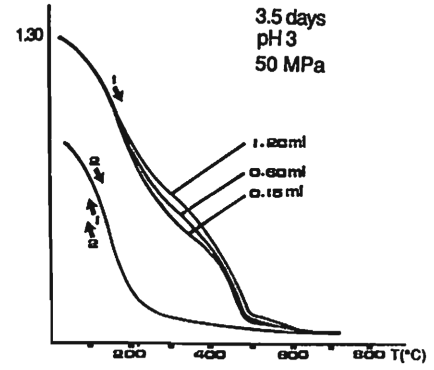

Fig.6 Js-T curves of hydrothermally altered samples by different volume of initial pH 3 fluid. Drop of Js at around 480°C becomes much more pronounced as the volume of initial reaction fluid increases.

MPa is the pressure of vapor at 350°C. 2. 3.5 day heating at 16.5 MPa with varying pH of initial solution. Two samples were altered by 0.15 ml solution with initial pH values 3 and 9. And a sample was put in a sample holder with some pin holes i.e. open to confining pressurizing water as much as 25 ml in the autoclave. 3. 3.5 day heating at 50 MPa with fixed pH of initial solution with various volume. Three samples were altered by pH 3 solution whose volumes were 0.15, 0.6 and 1.2 ml respectively. 50 MPa was made by intruding water into the autoclave. The pressure corresponds to that at 5000 meter depth.

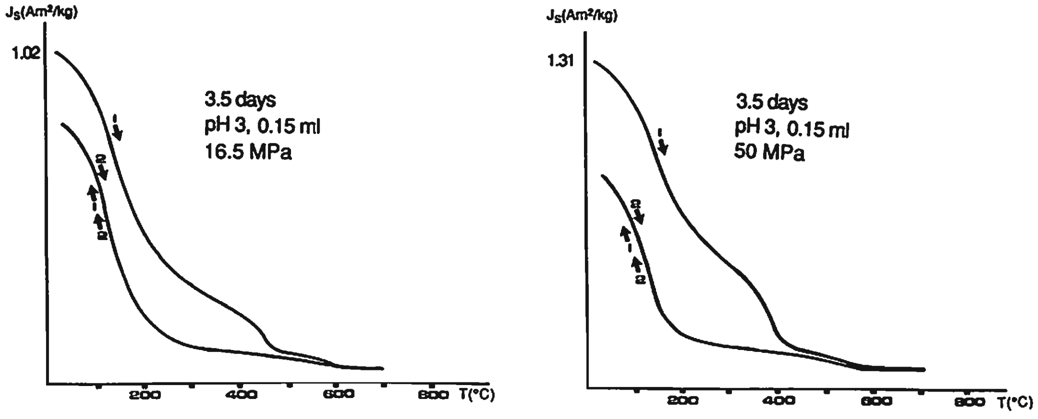

Fig.7 Js-T curves of hydrothermal altered samples by different pressure. High pressure induces the alteration of magnetic phase. Right:by 50 MPa. Left:by 16.5 MPa.

Results

In 8 day heating at 16.5 MPa with varying pH of initial solution, a clear change was revealed by thermomagnetic analyses in any cases in a similar sense. Each Js-T curve showed a distinct drop of magnetic moment at around 480°C and lost it at around 600°C in the first heating process (Fig.3). In the cooling precess Curie temperature was observable at around 200°C and also in consecutive heating and cooling cycles.

In 3.5 day heating at 16.5 MPa with varying pH of initial solution, Js-T curves of the individual samples showed the same tendency as previous cases of 8 day heating. However, the sample altered by pH 9 showed slightly small change compared to that by pH 3 (Fig.4), and the sample exposed to pressurizing water indicated a remarkable alteration compared to these of acidic alkaline initial mixture (Fig.5).

In 3.5 day heating at 50 MPa with fixed pH value of initial solution with various volume, gradual magnetic change was observed in Js-T curves depending on volume variation of initial solutions. As the volume of solution increases, the ratio of new magnetic phase seems to increase (Fig.6). Comparing to the results of 1.65 MPa, it was revealed that alteration was induced by high pressure (Fig.7).

4. Discussion

The fresh DSDP cores indicated reversible Js-T curves with low Curie point (around 200°C) suggesting that the ferromagnetic component, titanomagnetite, is composed of 60 atomic per cent ulvöspinel after the Curie temperature scheme proposed by Nishitani and Kono (1983) on an assumption of stoichiometric composition. Magnetic parameters showed to have a pseudo-single magnetic domain structure based upon discussion by Day et al.(1977).

From the results of the 8 day heating of samples, it was revealed that the fresh titanomagnetite changed in a sense of producing meta-stable phase which had been regarded as a production by low temperature oxidation. It decomposed and was converted to a new phase at around 450°C in vacuum (1.3×10^{-3} Pa). The formation of new magnetic phase occurred in any pH values of fluid. However, less pronounced change was observed in the Js-T curve of pH 9 than in the case of pH 3. This shows that the reaction proceeds faster rather in the acidic environment than in the alkaline one.

Three samples altered in the different volume of pH 3 solution revealed that the more hydrothermal fluid the more volume of the new phase can be produced. It seems likely that abundance of anion in the reaction system which is certainly related to the oxygen fugacity of fluid must be fundamental reagent of the alteration.

Comparing samples which were altered at 16.5 MPa and 50 MPa, it was revealed that high pressure induced the production of new magnetic phase.

Conclusions

It was revealed that titanomagnetite in the oceanic basalt can easily be subject to hydrothermal alteration in short length of time. Acid solution and high pressure induce the production of meta-stable magnetic phase. The new magnetic phase seems to be produced by a change similar to the low temperature oxidation in which the metallic ions would be lost ultimately out of the cubic crystal system.

References

Akimoto, T., H. Kinoshita and T. Furuta (1984) Earth planet. Sci. Lett., 71, 263.
Bleil, U. and N. Petersen (1983) Nature, 301, 384.
Day, R., M. Fuller and V. A. Schmidt (1977) Earth and Planet. Interiors, 13, 260.
Furuta, T. (1983) Init. Repts. DSDP, 69, 711.
Hamano, Y., T. Nishitani and M. Kono (1980) Init. Repts. DSDP, 52, 1391.
Kobayashi, K., M. Steiner, A. Faller, T. Furuta, T. Ishi, P. Shive and R. Day (1979) Init. Repts. DSDP, 49, 793.
Luyendyk, B. P. and J. R. Cann (1979) Init. Repts. DSDP, 49, 339.
Nishitani, T. and M. Kono (1983) Geophs. J. R. astr. Soc., 74, 585.
Readman, P. W. and W. O'Reilly (1970) Phys. Earth Planet.

Interiors, 4, 121.
Sakamoto, N., P. I. Ince and W. O'Reilly (1968) Geophys. J., 15, 509.
Von Damm, K. L., J. M. Edmond, B. Grant, C. I. Measures, B. Walden and R. F. Weiss (1985) Geochim. Cosmochim. Acta, 49, 2197.

(To be submitted to J. Geomag. Geoelectr.)

COAGULATION DUE TO MAGNETOSTATIC INTERACTION IN FLUIDS

Koji FUKUMA
Department of Geology and Mineralogy, Kyoto University, Kyoto 606-01

Behavior of magnetic particles in a fluid and the accompanying net magnetization change are simulated with the Monte-Carlo technique under the effect of the magnetostatic interaction between particles. The simulated assembly comprises of a hundred of spherical single-domain magnetites within a two-dimensional unit cell. Periodic boundary condition is used to calculate the interacting field due to nearest neighbors and the concentration of assembly is variable. The dilute assemblies showed the monotonic relaxation and acquisition patterns of magnetization (Fig. 1), which are expected from analytical solution for the non-interacting state (Collinson, 1965). On the other hand, more complicated patterns were produced for the concentrated assemblies. These patterns are consistent with the experimental results for suspension with comparable concentrations (Yoshida & Katsura, 1985). In the concentrated assemblies, it was also found that coagulation of particles occurs and the particle moments in a chain-like cluster are aligned along its elongated direction (Fig. 2). Coagulation of particles in the concentrated assembly modifies the net magnetization change pattern through the dominance of the interacting field in a cluster. Thus magnetostatic interaction could play an important role for the behavior of magnetic particles in a fluid. Such a numerical simulation incorporating the other interaction effects (e.g. Van der Waals force which is invoked by Deamer & Kodama, 1990) will give insight into the acquisition process of detrital remanent magnetization.

References
Collinson, D. W., (1965) *J. Geophys. Res.*, **70**, 4663-4668.
Deamer, G. A. & K. P. Kodama, (1990) *J. Geophys. Res.*, **95**, 4511-4529.
Yoshida, S. & I. Katsura, (1985) *Geophys. J. R. astr. Soc.*, **82**, 301-317.

(Submitted to Geophys. J. Int.)

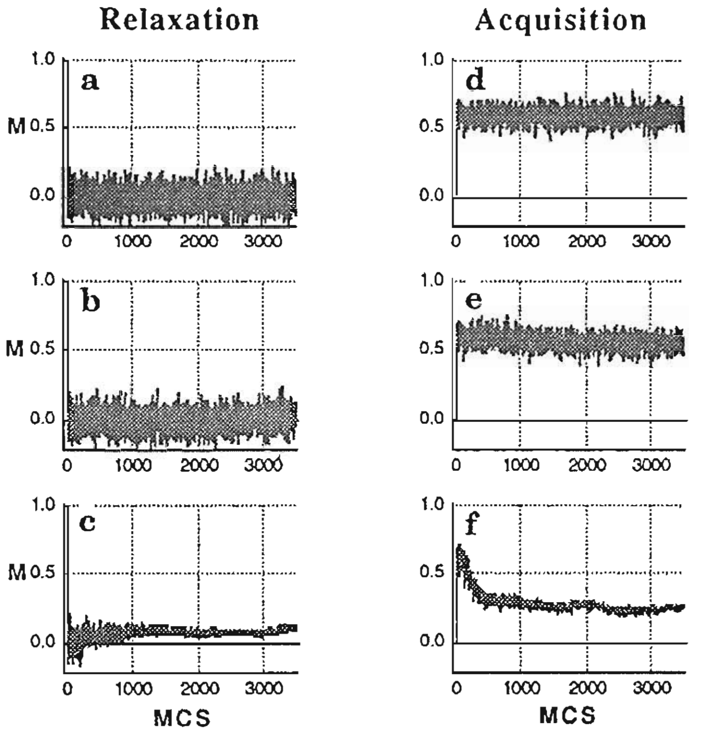

Fig. 1 Magnetization relaxation and acquisition patterns with Monte-Carlo steps (MCS). Relaxation patterns are shown for (a)non-interacting, (b)dilute (p=0.01ppm) and (c)concentrated (p=10ppm) assembly. Acquisition patterns are also shown for (d)non-interacting, (e)dilute and (f)concentrated assembly.

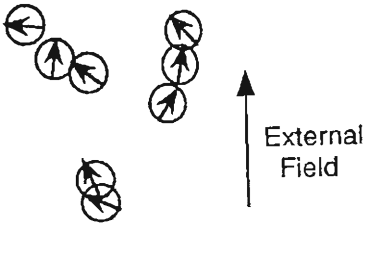

Fig. 2 An enlarged view of the clusters in the interacting assembly. The arrows indicate the vectors of particle magnetic moments.

MAGNETIZATION OF OCEANIC GABBROS

Eiichi KIKAWA*# & Kazuhito Ozawa+%

*Texas A&M University, Department of Geophysics and Geodynamics Research Institute, College Station, TX 77843-3114, USA
#Geological Survey of Japan, Marine Geology Department, Tsukuba 305, Japan
+Department of Geology and Geophysics, Yale University, P.O. Box 6666, New Haven, CT 06511-8130,USA
%University of Tokyo, Geological Institute, Tokyo 113, Japan

Our present concept of oceanic crustal magnetization is much more complex than the original, uniformly magnetized block model of Vine-Matthews-Morley[1,2]. Previous magnetic inversion studies concluded that layer 2A (upper 500 m oceanic extrusive basalts) is the only magnetic layer[3,4]. Direct measurements of DSDP/ODP samples, however, have shown (1) that magnetization of layer 2A is insufficient to give the required size of the magnetic anomaly, (2) that this layer also has overlapping of different magnetic polarities in vertical section, which would lower the effective magnetization responsible for marine magnetic anomalies, and that (3) contribution from the lower intrusive layers is necessary[5,6,7]. Magnetic studies for the oceanic intrusive layers have reported the relatively high and stable magnetization in oceanic gabbros, which was not expected for these coarse-grained igneous rocks, and showed that substantial contribution to marine magnetic anomalies may come from these layers[8,9,10]. But these studies were conducted on unoriented dredged and ophiolite samples and on intermittent DSDP cores because of the difficulty in sampling.

A total of 500.7 m of continuous, vertical oceanic gabbroic section was first recovered during ODP Leg 118 (Hole 735B at Southwest Indian Ridge). Because of the extremely high recovery rate of 87 %, Hole 735B may represent an excellent type section for layer 3 at this suite. Olivine gabbro, olivine-bearing gabbro, two pyroxene gabbro, Fe-Ti oxide gabbro, troctolite, and microgabbro with rare basalt and tronhjemite were recognized in the sequence, based upon igneous mineralogy, mineral compositions, and degree and style of deformation. We summarize magnetic properties of these gabbros below[11].

Rather large variations and very high values in magnetic properties were obtained from paleomagnetic measurements of 264 minicore samples from Hole 735B; NRM intensities range between 2.6×10^{-3} to 1.3×10^{2} A/m and magnetic susceptibilities vary from 3.4×10^{-5} to 3.4×10^{-2} cgs. NRM inclinations were about equally divided between normal and reversed

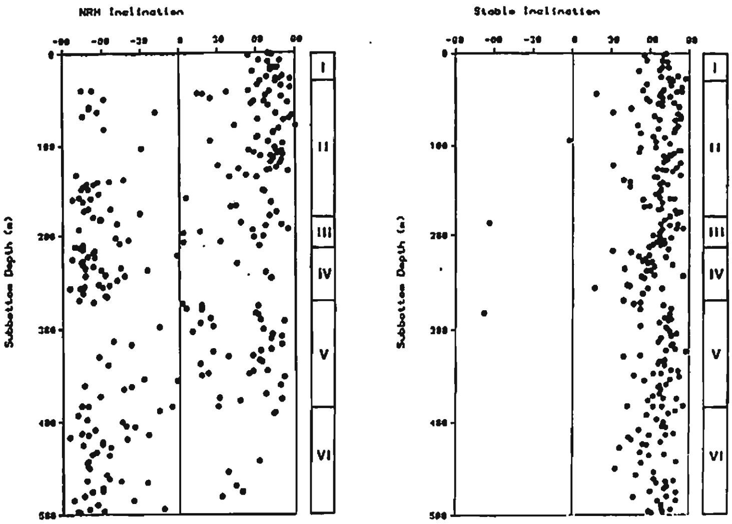

Fig. 1. Plots of NRM inclinations vs. depth (left) and of stable inclinations vs. depth for Hole 735B (right).

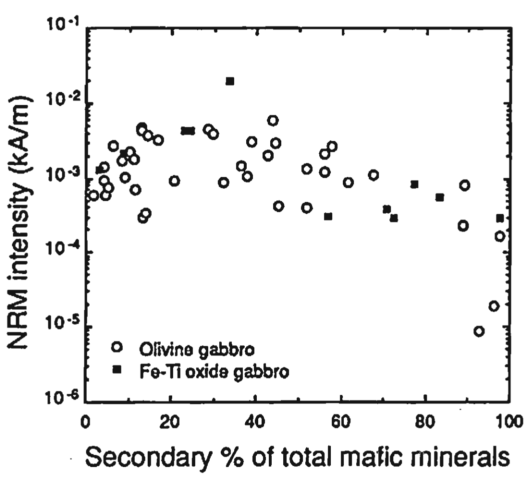

Fig. 2. Plot of NRM intensity vs. volume percentage of secondary mafic minerals in total volume of mafic minerals for respective Leg 118 samples.

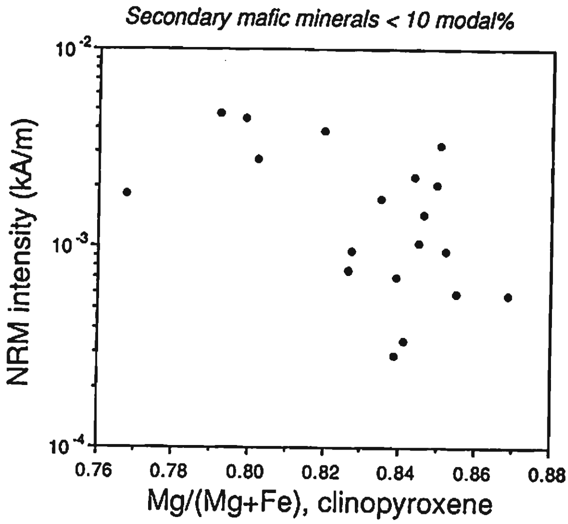

Fig. 3. Plot of NRM intensity vs. Mg# of clinopyroxene for fresh olivine gabbros of which secondary mafic minerals are less than 10 modal %.

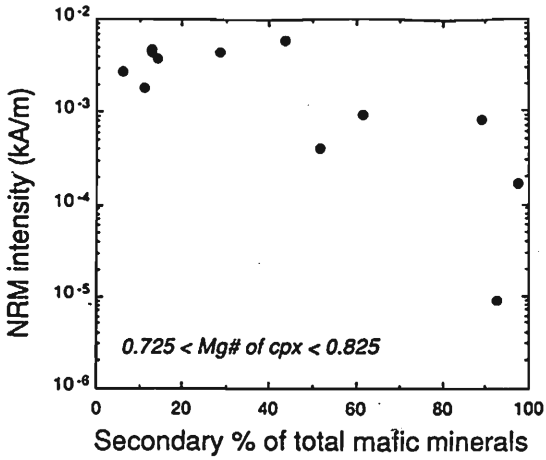

Fig. 4. Plot of NRM intensity vs. volume percentage of secondary mafic minerals in total volume of mafic minerals for olivine gabbros of which Mg#s of clinopyroxene range between 0.725 and 0.825.

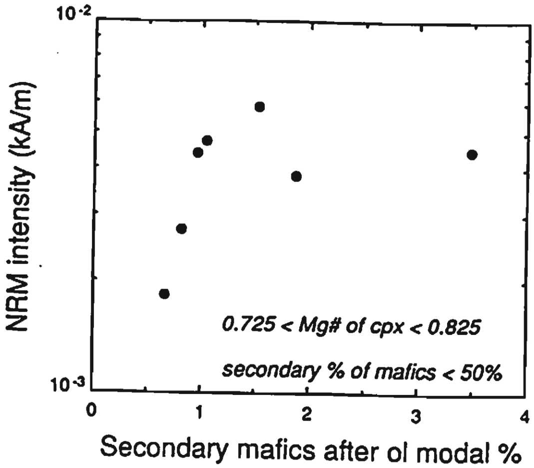

Fig. 5. Plot of NRM intensity vs. modal % of secondary mafics after olivine for olivine gabbros which have less than 50 % of secondary mafics and show Mg# from 0.725 to 0.825.

polarity. However, all samples showed a reversed stable inclination with an average of 66°(+/- 5°), which is consistent with the location of Hole 735B (Fig. 1). Several experiments to determine the origin of the unstable component of normal polarity, together with magnetic logging study, showed that this component was probably IRM created during drilling and coring, and that in situ magnetization may be close to that of the stable reversed magnetization. This indicates that the stable remanent magnetizations of reversed polarity, which was probably acquired during a single polarity epoch of short duration (0.7 m.y. or less), are capable of contributing to marine magnetic anomalies as a whole section. The average intensity for these stable magnetizations is 1.6 A/m, which would provide most of the amplitude of magnetic anomalies observed at sea surface, if distributed uniformly throughout 4.5 km-thick layer 3.

In this study we further examine the relationship between NRM intensity of ODP Leg 118 gabbros and the degree of metamorphism. The volume percentage of secondary mafic minerals in total volume of mafic minerals was used as an indicator for the degree of metamorphism(Fig. 2). Fig. 2 shows that with increasing the degree of metamorphism, NRM intensities of oceanic gabbros likewise increase, show a broad peak at about 40 %, and then decrease with greater metamorphic degrees. Further study of the relationship between the metamorphic degree and NRM intensity, by considering the difference in initial compositions of the gabbros, provides a closer look at this relationship. Most of the samples studied here are olivine gabbros, although many Fe-Ti oxide gabbros were obtained during the Leg 118. Most of the Fe-Ti oxide gabbros showed a strong secondary magnetization most likely acquired during drilling. As Fig. 3 shows, fresh olivine gabbros of which secondary mafic minerals are less than 10 modal % depict a relatively wide range in magnetization (about an order) and an increase in magnetization with decreasing Mg# of clinopyroxene (as gabbros become evolved). However, a close examination of the olivine gabbros for which MG# of cpx ranges between 0.725 and 0.825 showed the same tendency in the relationship between the degree of metamorphism and NRM intensity as the previously reported overall results (Fig. 4). The olivine gabbros which have less than 50 % of secondary mafics also showed a rapid increase in magnetization (several factors) with increasing the modal % of secondary mafics after olivine (Fig. 5). This may support our interpretation that the increase in magnetization with the metamorphic degree corresponds to replacement of olivine by magnetite. The significant change in magnetization observed in Leg 118 oceanic gabbros may overscore, or underscore the importance of contribution of oceanic gabbros to marine magnetic anomalies in response to the actual occurrence of the respective gabbros in the oceanic crust. As we are unable to estimate this, we suggest that oceanic gabbros, together with consideration of the effects of metamorphism and of magmatic evolution, may account for up to most of seafloor spreading magnetic anomalies.

References

1. Vine F.J., and Matthews, D.H. (1963) Nature, 199:947-949
2. Morley, L.W. (1981) In *The Sea and Observations on the Progress in the Study of the Seas,* Vol. 7, edited by C. Emiliani, pp. 1717-1719. Wiley-Interscience.
3. Talwani et al. (1971) J. Geophys. Res. 76:473-517
4. Atwater, T., and Mudie, J.D. (1973) J. Geophys. Res. 78:8665-8686
5. Harrison, C.G.A. (1981) In *The Sea* , ed. C. Emiliani, 7:219-239. New York: Wiley
6. Banerjee, S.K. (1984) Tectonophys. 105: 15-27
7. Harrison, C.G.A. (1987) *Ann. Rev. Earth Plant.Sci.*, 15: 505-543
8. Fox, P.J. and Opdyke, N.D. (1973) J. Geophys. Res., 78: 5139-5154
9. Kent et al. (1978) Geophys. J. Royal Astron. Soc., 55: 513-537
10. Dunlop, D.J., and Prevot, M. (1982) Geophys. J. Royal Astron. Soc., 69: 763-802
11. Kikawa, E. and Pariso, J.E. (1991) *In* Von Herzen, R.P., and Robinson, P.T. et al., 1991. *Proc. ODP, Sci. Results, 118* : College Station, TX (Ocean Drilling Program): 285-307

(To be submitted to *Nature*)

OPAQUE MINERALOGY IN THE HYDROTHERMAL ALTERATION ZONE OF THE TSUCHIHATA MINE, IWATE PREFECTURE, JAPAN.

Hirotomo UENO

Department of Geology, College of Liberal Arts,
Kagoshima University, Kagoshima 890

Opaque minerals, which are inclusive of primary rock-forming Fe-Ti oxide minerals in igneous rocks, secondary Fe-Ti oxide minerals and new sulfide minerals changed from Fe-Ti oxide minerals, are examined in the hydrothermal alteration zone of the Tsuchihata mine. Continuous sections from fresh to altered within the same igneous rock body are selected for this purpose.

The Hatabira rhyolite dome of the Tsuchihata mining district is host rock of the network copper veins which are believed to be the Keiko-type ores of the Kuroko deposits (Goto and Kubota, 1984). Samples of the Hatabira rhyolite body collected from the 5th Gallery of Level 0 (Fig. 1). Consisting rocks of this body are massive rhyolite being flow-banded. The principal phenocrysts are of quartz and plagioclase. The constituents of the groundmass are quartz, chalcedonic quartz and glass. The most fresh rock among collected samples is 300m of the ore body at the near portion to the entrance adit of Level 0. The rocks become more altered as the distance to the ore body decreases. Opaque minerals were observed under an ore microscope. Even if the most fresh part with brownish gray in color, primary magnetite changes partly to hematite (Fig. 2-A). Altered samples contain hematite and pyrite (Figs. 2-B and 2-C). Distinctly altered samples contain pyrite and fine grained hematite (Fig. 2-D). Finally hematite changes to pyrite. Microscopic hematite are not found in TUC-24 and TUC- 25. No maghemite is observed in this alteration zone.

Clay minerals are determined by X-ray powder diffraction. Chlorite and sericite are detected, and these clay minerals increase as the alteration proceeds. Perlite zones resulted from rapid cooling of original rock appear in this section. Although the clay mineral is mordenite instead of chlorite and sericite, hematite occurs as a continuously changing phase of opaque minerals.

Remanences of altered samples may be the chemical remanent magnetizations due to hematite (Ueno and Tonouchi, 1987). The paleomagnetical analysis are now being continued.

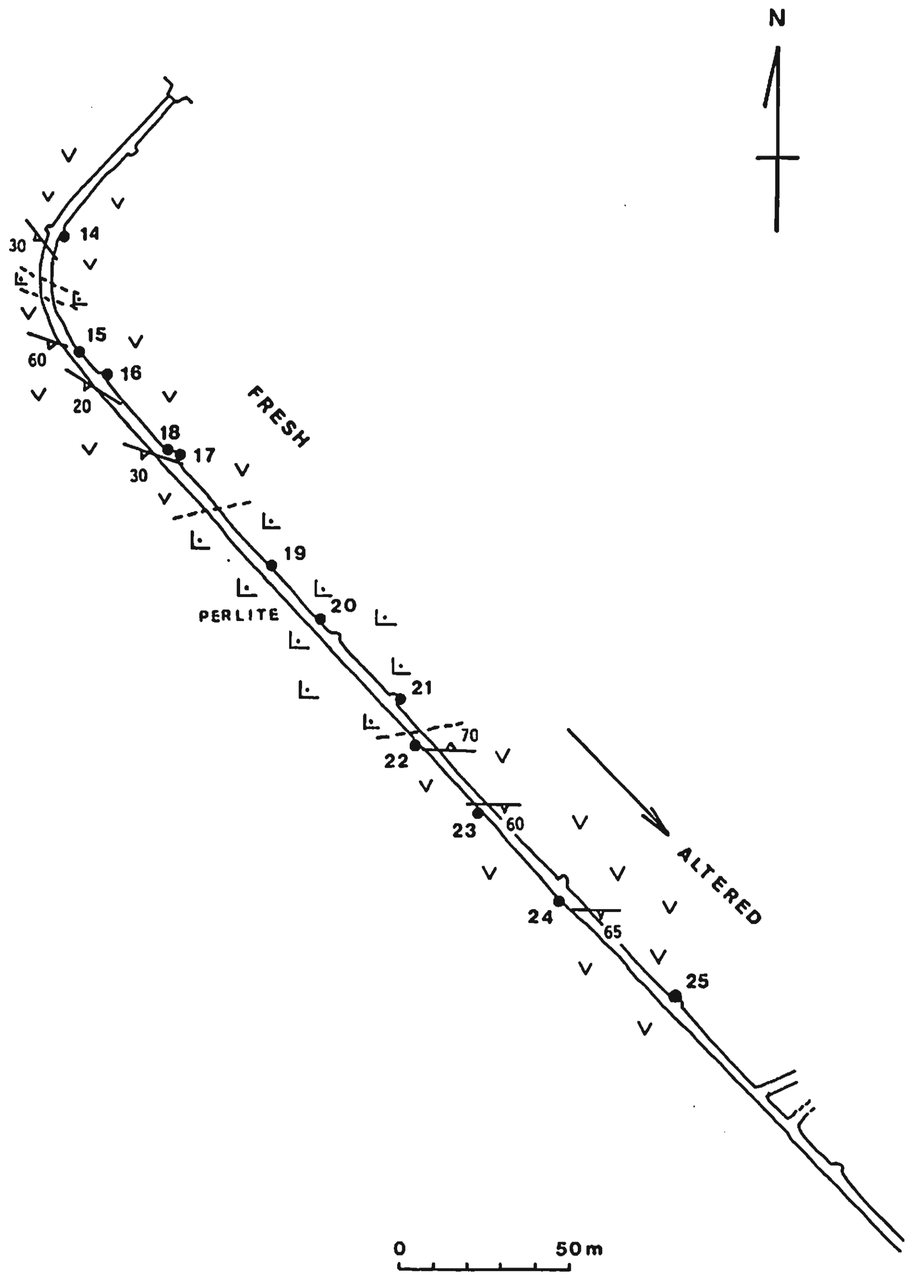

Fig. 1. Underground geological map of the 5th Gallery, Level 0, Tsuchihata mine.
Sample numbers are indicated. Small numerical letters show dips of flow bands of rhyolite.

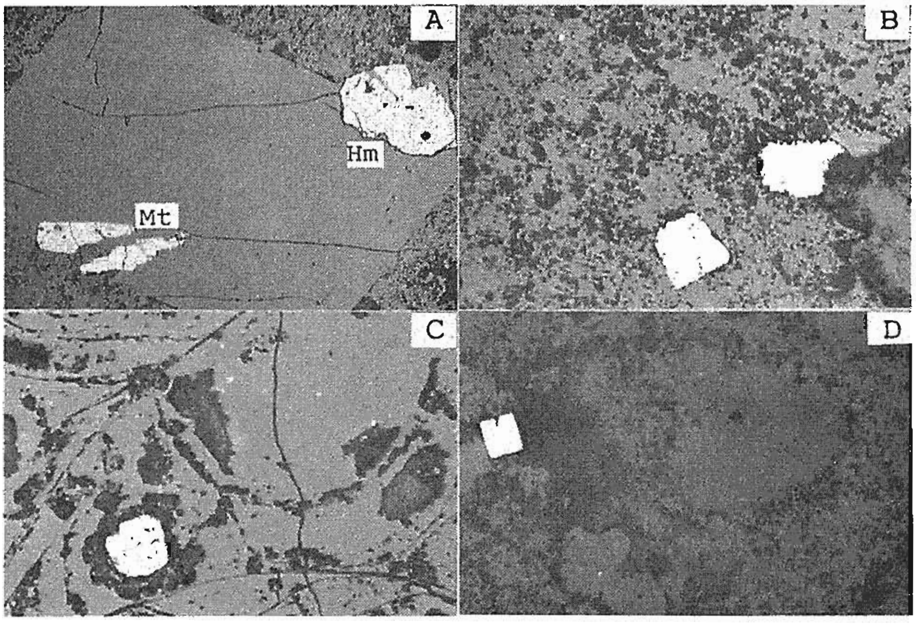

Fig. 2. Photomicrographs of opaque minerals in rhyolite samples from Tsuchihata mine. (Width of field = 0.6 mm)
A: TUC-17, magnetite(Mt) and hematite(Hm).
B: TUC-16, large and fine grained hematite.
C: TUC-19, large and fine grained hematite in perlite.
D: TUC-22, pyrite and fine grained hematite.

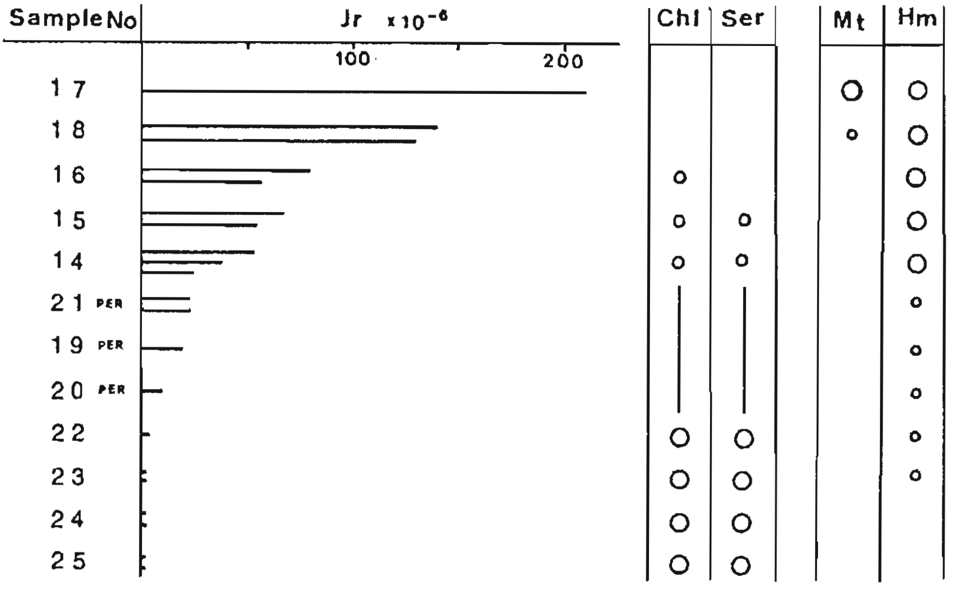

Fig. 3. Clay and opaque minerals and remanent intensity(emu/cc). Chl;chlorite, Ser;sericite, Mt;magnetite, Hm;hematite, PER;perlite.

In Fig. 3, samples are rearranged in descending order of remanent intensities. Both clay and Fe-Ti oxide minerals are changing systematically.

References

Goto, S. and Kubota, Y. (1984) in; Soc. Mining Geol.(Ed), Exploration in Japan, 2, 27.

Ueno, H. and Tonouchi, S. (1987) Econ. Geol., **82**, 1723.

THERMAL HISTORY OF THE SHIMANTO ACCRETIONARY PRISM; FISSION-TRACK ANALYSES

Noriko HASEBE, Takahiro TAGAMI and Susumu NISHIMURA

Dept. Geol. Mineral., Kyoto Univ., Kyoto 606, Japan

Sampling

To place thermotectonic constraints on the evolution of the Cretaceous to Neogene Shimanto Belt, we carried out fission-track (FT) analyses of detrital apatite and zircon collected from both sandstone turbidites and blocks in melanges on the Muroto Peninsula, Shikoku, southwest Japan (Fig. 1).

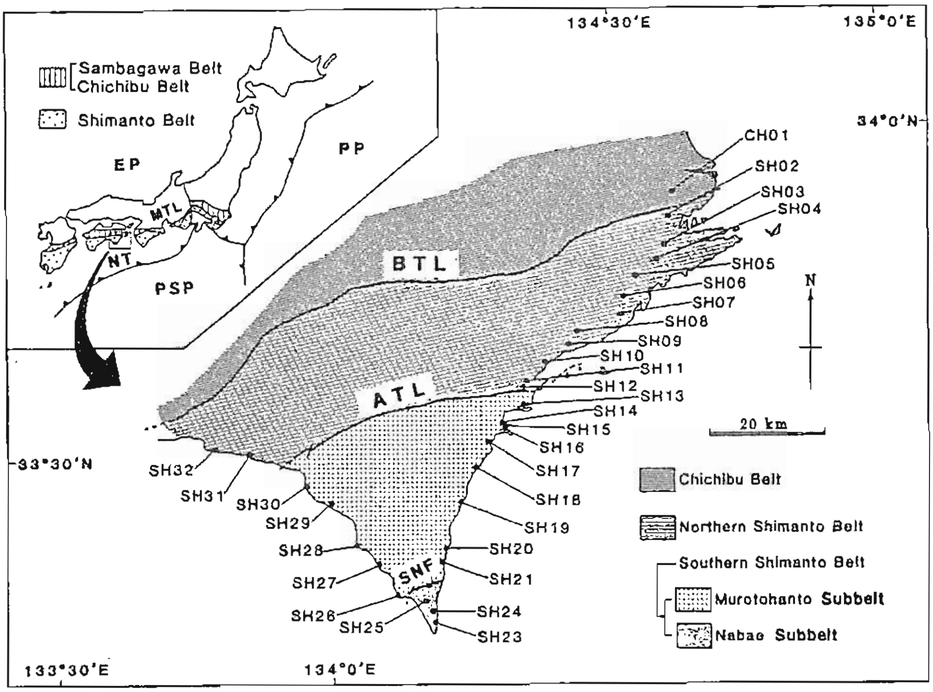

Fig. 1. Map showing the location of the Shimanto Belt and sampling sites in the Muroto peninsula, modified from Taira and Tashiro (1987), Taira et al. (1989) and geological map published by the Regional Forestry Office of Kochi Prefecture in 1977. SH03-04, SH10-12, SH31-32 are collected from blocks in melanges, and others are from turbidites.
MTL ; Median Tectonic Line. BTL ; Butsuzo Tectonic Line. ATL ; Aki Tectonic Line. SNF ; Shiina Narashi Fault. NT ; Nankai Trough. EP ; Eurasia Plate. PSP ; Philippine Sea Plate. PP ; Pacific Plate.

Mineral separation and sample preparation procedures were described by Tagami et al. (1988).

Results and thermal history

Eight FT apatite ages show good agreement around 10 Ma (Table 1), with all data except for one passing the χ^2 test at the 5 % criterion (Galbraith, 1981). These results, in conjunction with depositional ages of Cretaceous to Early Oligocene, demonstrate that the Shimanto Belt was heated hotter than ~125°C (apatite total annealing temperature, Gleadow et al., 1983) and subsequently cooled below ~100°C at ~10 Ma.

Table 1. Apatite fission track analytical results.

site	Ps (x10^6/cm^2)	Ns	Pi (x10^6/cm^2)	Ni	Pd x10^6/cm^2)	Nd	T ±2σ (Ma)	n	P(x^2) (%)	Sampling site
CH01	0.29	119	2.45	1018	0.5437	2527	10.2 ±2.1	7	4	Chichibu Belt
SH02	0.21	189	1.48	1331	0.5017	2332	11.4 ±1.9	16	85	Hinotani U.
SH19	0.34	77	1.12	251	0.2841	3301	13.5 ±3.7	10	99	Naharigawa U., C
SH28	0.16	23	0.76	110	0.2841	3301	9.2 ±4.3	4	40	Naharigawa U., C
SH20	0.41	49	2.47	299	0.2841	3301	7.2 ±2.3	6	95	Muroto U.
SH21	0.22	106	1.08	525	0.2841	3301	8.9 ±2.0	12	95	Muroto U.
SH26	0.10	23	0.53	122	0.2841	3301	8.3 ±3.8	6	90	Muroto U.
SH27	0.29	38	1.31	170	0.2841	3301	9.8 ±3.6	7	60	Muroto U.

Table 2. Zircon fission track analytical results.

site	Ps (x10^6/cm^2)	Ns	Pi (x10^6/cm^2)	Ni	Pd (x10^6/cm^2)	Nd	T ±2σ (Ma)	n	P(x^2) (%)	Sampling site
CH01	9.63	3469	1.72	620	0.1514	2462	147.7 ±14.6	11	<0.1	Chichibu Belt
SH02	6.41	3106	1.31	635	0.1514	2462	129.1 ±12.8	16	<0.1	Hinotani U.
SH03	11.03	1884	2.01	342	0.1514	2462	145.4 ±18.4	6	<0.1	Akamatsu U.
SH04	6.91	948	2.24	307	0.1514	2462	81.5 ±11.4	7	5	Taniyama U.
SH32	11.98	1281	2.99	320	0.0969	2026	68.6 ±9.9	12	1	Tei Melange
SH06	6.08	1271	1.98	414	0.1514	2462	81.0 ±9.9	7	<0.1	Hiwasa U.
SH07	4.98	585	1.51	1922	0.1514	2462	86.7 ±9.2	10	<0.1	Hiwasa U.
SH09	7.89	2027	1.64	422	0.1287	2093	107.8 ±12.7	9	<0.1	Hiwasa U.
SH31	11.33	3186	1.99	560	0.097	2028	97.6 ±11.4	22	<0.1	Mugi U.
SH30	8.94	3596	2.62	1054	0.0978	2045	58.8 ±5.9	29	<0.1	Oyamamisaki U.
SH13	5.26	1663	1.08	340	0.1287	2093	109.7 ±14.2	11	<0.1	Naharigawa U., A
SH17	7.18	6043	1.20	1017	0.1006	2104	112.4 ±10.9	27	<0.1	Naharigawa U., B
SH18	8.35	6918	1.53	1266	0.1026	2145	100.8 ±9.4	29	<0.1	Naharigawa U., B
SH29	9.35	3944	1.55	654	0.0939	1964	113.9 ±12.4	20	<0.1	Naharigawa U., B
SH19	9.87	929	0.95	89	0.1086	2271	215.0 ±49.9	6	1	Naharigawa U., C
SH28	8.12	2592	1.54	491	0.0948	1983	100.9 ±12.1	21	<0.1	Naharigawa U., C
SH20	8.67	4073	1.30	611	0.1024	2142	127.8 ±14.2	20	<0.1	Muroto U.
SH21	7.52	4337	1.24	713	0.0941	1969	105.0 ±11.3	28	<0.1	Muroto U.
SH26	8.07	2120	1.73	454	0.1081	2260	94.0 ±11.6	14	1	Muroto U.
SH27	8.54	3433	1.63	653	0.1100	2300	107.8 ±11.7	19	<0.1	Muroto U.
SH25	2.84	2943	1.82	1891	0.1051	2199	30.4 ±2.8	47	<0.1	Hioki Complex
SH24	7.38	4431	1.73	1037	0.0774	1618	59.9 ±6.2	34	<0.1	Tsuro U.

ρs : Density of spontaneous tracks
Ns : Number of spontaneous tracks counted to determine ρs
ρi : Density of induced tracks in a sample
Ni : Number of induced tracks in a muscovite external detector to determine ρi
ρd : Density of induced tracks in NBS-SRM612 dosimeter glass
Nd : Number of induced tracks in a muscovite external detector to determine ρd
T : FT age calculated from pooled Ns and Ni for all grains counted
n : Number of counted grains
P (χ^2) : Probability of χ^2 for N degrees of freedom (N=n-1) quoted to the nearest 5 or 10% except for those under 5% and over 95% (Galbraith, 1981).

On the other hand, twenty three zircon samples show a large range of sample ages from 150 Ma to 17 Ma, with all failing the χ^2 test except for one from a melange (Table 2). Hence, most parts of the Shimanto Belt have not been heated above the zircon partial annealing zone (ZPAZ; ~190-260°C, Zaun and Wagner, 1985), whereas some parts of the melanges have experienced temperatures above 260°C. To investigate the degree of track annealing in zircon, we also examine the FT age spectrum using single-grain ages (Hurford et al., 1984). At deposition, individual detrital grains retain a variety of FT ages older than the timing of deposition, reflecting their provenances. When the rock has been heated over the FT total retain zone after deposition, grain ages are progressively reduced, resulting in a shift of the initial pattern of spectrum toward the timing of heating. In this case, some peaks could be younger than the depositional age. FT zircon age spectra from the Northern Shimanto Belt (NSB) show, in general, the youngest peak in each sample is younger than its depositional age, suggesting the maximum temperature was in the ZPAZ (Fig. 2). In contrast, all age peaks from the Southern Shimanto Belt (SSB), are consistently older than depositional ages, providing no evidence of heating up to ZPAZ (Fig. 2).

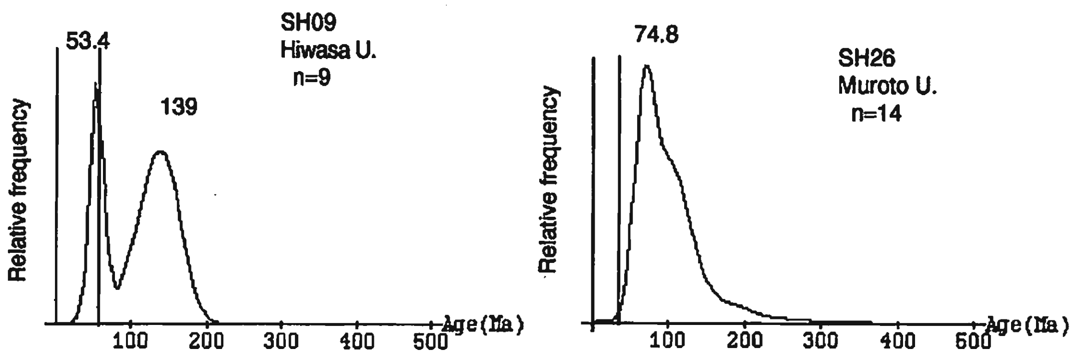

Fig. 2. FT zircon age spectra of SH09 from the Northern Shimanto Belt and SH26 from the Southern Shimanto Belt with crystal number and peak ages. Vertical line represents the youngest limit of the depositional age determined by fossils (Taira et al., 1980).

These contrasting patterns probably reflect systematic differences in the maximum temperature reached during the evolution of the Shimanto Belt (Fig. 3).

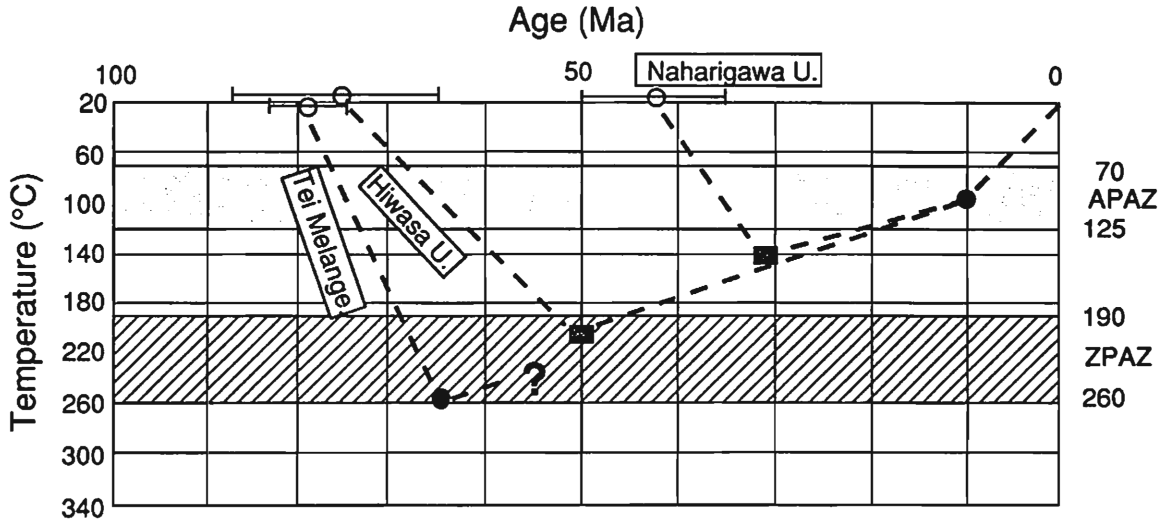

Fig. 3. Thermal history of the Tei Melange, Hiwasa Unit and Naharigawa Unit, which are representative example of Cretaceous melange, Cretaceous turbidite and Eocene turbidite, respectively. Open circles show the depositional ages with possible depositional duration. Solid circles show time-temperature points determined by FT ages. The timing of maximum temperature of the melange was inferred from the peak ages of their age spectra. Solid squares show the maximum possible temperature derived from FT zircon data, and their timing are based on K-Ar cleavage ages (Ager and others, 1989).

Tectonic implication

A plausible evolution of the Cretaceous to Eocene Shimanto Belt is reconstructed schematically in Fig. 4 under the asumption of steady-state geometry and geothermal gradient on the basis of the age-temperature paths estimated for individual tectonic units. The Northern Shimanto Belt, represented by the Hiwasa Unit, accreted at the trench at ~75 Ma and was dragged down to ~10 km depth at ~50 Ma. It subsequently rebounded to migrate from the slab with gradual exhumation, followed by rapid unroofing since ~10 Ma to the present. The Murotohanto Subbelt, represented by the Naharigawa Unit, yields a similar pattern of evolution since the accretion at 43 Ma to the exposure at present, except that the path stays consistently at shallower depth. The Tei Melange was subducted at ~80 Ma prior to accretion, underplated below offscraped sedimentary piles and was dragged down to ~12 km depth at ~65 Ma. Then it rebounded to leave slab, although the subsequent unroofing history remains ambiguous.

The cooling pattern of ~10 Ma is attributed to higher thermal gradients and/or uplift caused by rapid subduction of the newly formed Shikoku Basin plate at ~15 Ma.

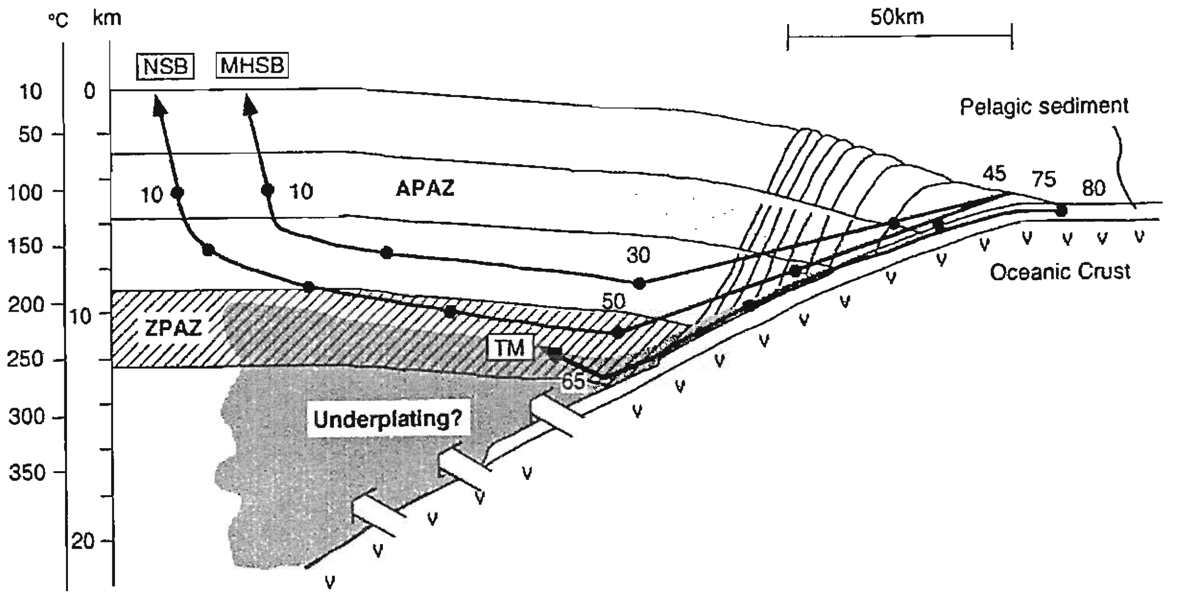

Fig. 4. Schematic diagram which represents the tectonic history of the offscraped and underplated materials under the frameworks of constant wedge shape and 20°C/km thermal gradient (Takasu and Dallmeyer, 1990, Toriumi and Teruya, 1988) with surface temperature of 10°C. NSB; path for the offscraped sediments in the Northern Shimanto Belt. MHSB; path for the offscraped sediments in the Murotohanto Subbelt. TM; path for the underplated materials in the Northern Shimanto Belt. Solid circles on trajectories depict positions every 10 Ma. Figures in the diagram indicate timings inferred on the basis of thermal histories.

Conculusion

1) The turbidites in the Northern Shimanto Belt should have been heated up to the ZPAZ (190-260°C) while those of the Southern Shimanto Belt show no evidence of such heating. These contrasting results suggest the systematic difference in the maximum temperature and thus evolutionary paths during the accretionary process. The age-temperature paths estimated for individual tectonic units imply successive accretion, growth and uplift of sedimentary piles.

2) Melanges in the Northern Shimanto Belt sustained variable maximum temperatures, presumably reflecting their different evolutional processes. They should have underplated at the bottom of imbricated sedimentary piles and subsequently dragged down to within or below ZPAZ.

3) The Cretaceous to Eocene Shimanto Belt was cooled through ~100°C isotherm at ~10 Ma, which would be attributable to increased geothermal gradient and/or unroofing related to the newly formed Shikoku Basin plate.

References

Ager, S. M., Cliff, R. A., Duddy, I. R. and Rex, D. C. (1989) *J. Geol. Soc. London,* **146**, 893.

Galbraith, R. F. (1981) *Math. Geol.,* **13**, 471.

Gleadow, A. J. W., Duddy, I. R. and Lovering, J. F. (1983) *Aust. Petrol. Explor. Assoc.,* **23**, 93.

Tagami, T., Lal, N., Sorkhabi, R. B., Ito, H. and Nishimura, S. (1988) *Mem. Fac. Sci., Kyoto Univ.,* **53**, 14.

Taira, A., Katto, J., Tashiro, M. and Okamura, M. (1980) *Geology and paleontology of the Shimanto Belt* (Rinyakosaikai Press, Kochi), 319.

Taira, A. and Tashiro, M. (1987) *Historical biogeography and plate tectonic evolution of Japan and eastern Asia* (Terra Scientific Publishing Company, Tokyo) 1.

Taira, A., Tokuyama, H. and Soh, W. (1989) *The evolution of the Pacific ocean margins* (Oxford Univ., Press), 100.

Takasu, A. and Dallmeyer, R. D. (1990) *Tectonophysics,* **185**, 111.

Toriumi, M. and Teruya, J. (1988) *Modern Geol.,* **12**, 303.

Zaun, P. E. and Wagner, G. A. (1985) *Nucl. Tracks Rad. Meas.,* **10**, 303.

(Submitted to GSA Special Publication)

HARD SECONDARY MAGNETIZATION OF MIOCENE MARINE SEDIMENTS FROM THE JOBAN AREA, NORTHEAST JAPAN

Daisuke MIKI and Masayuki TORII

Dept. Geol. Mineral., Kyoto Univ., Kyoto 606-01, Japan

Tertiary marine sediments are widely distributed in the Joban area, along the eastern coast of Northeast Japan. A paleomagnetic and rock magnetic study was carried out on those sediments of Miocene age. The original purpose of the study is to clarify tectonic movements in the area at Miocene time, however, we could not find any *primary* paleomagnetic direction. We report paleomagnetic and rock magnetic characteristics of the sediments, whose natural remanent magnetization (NRM) is dominated by the hard secondary remanence.

We collected 130 paleomagnetic samples from the Yunagaya Group, Shirado Group, Takaku Group, and Taga Group; 27 sites as a total. These Miocene sediments mainly consist of sandstones, mudstones, and tuffaceous sediments (Sugai *et al.*, 1957). These rocks yield abundant age-diagnostic marine micro fossils such as diatoms and foraminifera (*e.g.* Yanagisawa *et al.*, 1989).

Each sample was cut into 1 to 3 cylindrical specimens of the standard size, and NRMs of all specimens were measured by using a cryogenic magnetometer (ScT C112). Some pilot specimens from each site were subjected to the progressive alternating field demagnetization (PAFD) and progressive thermal demagnetization (PThD). At each step of PThD, we measured initial susceptibility to check chemical alterations during heating process by using Bartington susceptibility meter (M.S.2.B.). High temperature measurements of the initial susceptibility were also carried out continuously from the room temperature to 700°C by using bartington M.S.2.F. susceptibility meter (Torii *et al.*, 1989). Some samples showed drastic change in the initial susceptibility after heating above 350°C. We tried PAFD for those samples after heating up to 200°C.

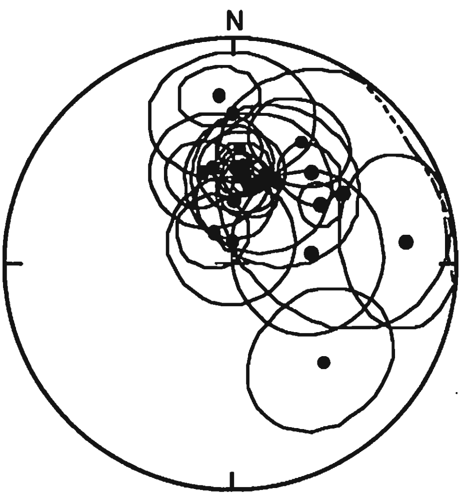

Fig. 1. In situ site mean directions before demagnetizations with 95% confidence limit, plotted on an equal area projection.

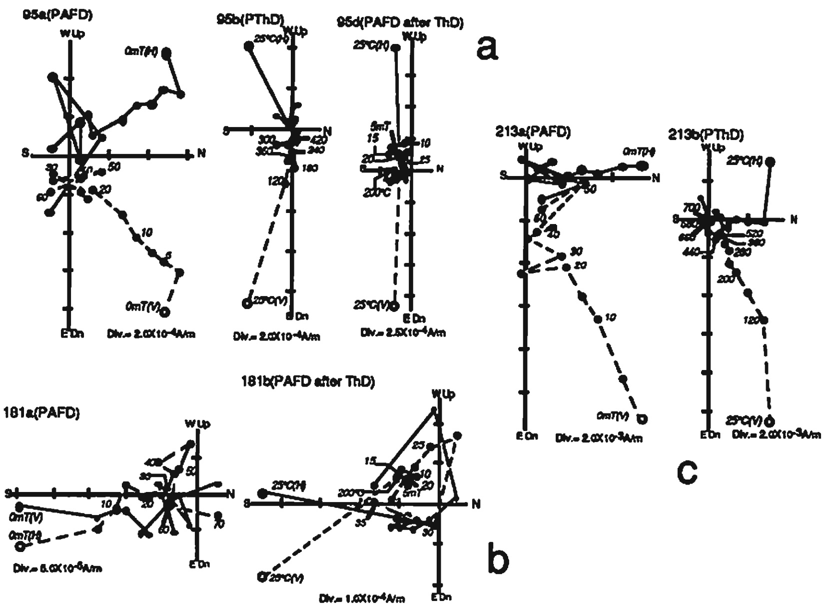

Fig. 2. Typical examples of the demagnetization experiments of NRM plotted on the vector demagnetization diagrams. Dots and solid lines indicate projection on holizontal plane; circles and dashed lines are vertical plane.

Heating cycles below 200°C gave almost reversible change of the initial susceptibility.

We applied isothermal remanent magnetization (IRM) acquisition experiments and the thermal demagnetization of composite IRMs (Lowrie, 1990) to identify magnetic minerals in the sediments. For such experiments, we used a spinner magnetometer (Schonstedt SSM-1A).

Intensity of NRM was very weak; the order of 10^{-4}A/m for most sites, and 10^{-3}A/m for tuffaceous rocks. Site mean direction with neither demagnetizations and tilt corrections are shown in Fig. 1. Most of these indicate apparently same direction as the present geomagnetic field. This fact suggests that the NRMs are governed by viscous overprintings which are parallel to the present geomagnetic field.

Samples can be divided into two categories in terms of behavior against PAFD and PThD. The first category is typically shown as Figure 2a and 2b; the remanent magnetization scatters in early stages of AF demagnetization, less than 20mT. These kind of samples showed very rapid decrease of NRM when heated up to 200°C or less. Above the thermal demagnetizing step of about 400°C, specimens obtained a huge amount of spurious remanence which may be viscous origin acquired under the laboratory magnetic field. Such the viscous remanent

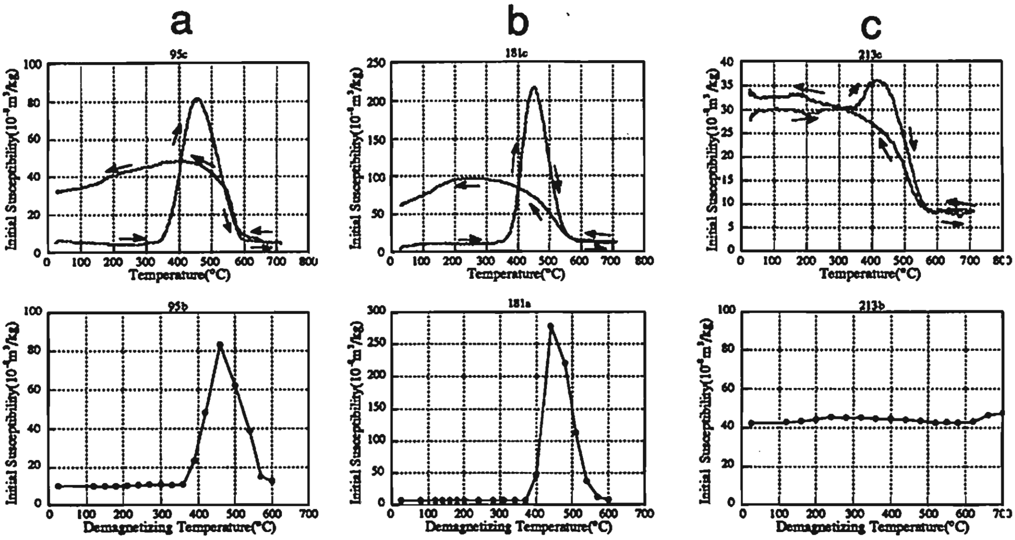

Fig. 3. Typical examples of the initial susceptibility. Continuous record of thermal variation (upper row). And, initial susceptibility measured after each step of thermal demagnetization (lower row). a, b, and c correspond to the examples in Fig. 2.

magnetizations (VRMs) made measurement of there original weak remanence extremely difficult. The initial susceptibility of those samples increased typically 20 times or more of the initial value by heating above 350°C (Fig. 3a, 3b). The dramatic increase of the initial susceptibility may suggest production of highly magnetic minerals by the heating. We found that the conventional demagnetizing methods, PAFD and PThD, were not effective for these samples. Although we applied PAFD after heating samples up to 200°C, we could not determine any stable direction for the most of samples. Only small amount of samples indicated northwest declination of positive inclination and/or southeast declination of negative inclination. These directions are just indications and not enough for further paleomagnetic discussions.

The other category of demagnetization behavior is shown in Fig. 2c. Both of PAFD and PThD seem to be successful, and the chemical change by heating are not very serious as shown in Fig. 3c. The stable component of remanence which was observed in both PAFD and PThD diagrams show almost the same direction as the present geomagnetic field. Unfortunately the studied formations are monotonously inclined to the east, which make an effective fold test difficult.

The difference between the two categories obviously corresponds to the difference of the rock type of samples. The rock type of the former category is sandstone and mudstone which contains little amount of volcanic ash. The latter is tuff or tuffaceous sandstone. The results of IRM acquisition (Fig. 4) and the thermal demagnetization of composite IRMs (Fig. 5), however, show no clear difference between the two categories. It may be said that the disturbing magnetic minerals produced during the laboratory heating are originated from non-magnetic minerals. The non-magnetic minerals, such as clay minerals, may be reduced to produce highly magnetic minerals, possibly magnetite, by the laboratory heating above 350°C.

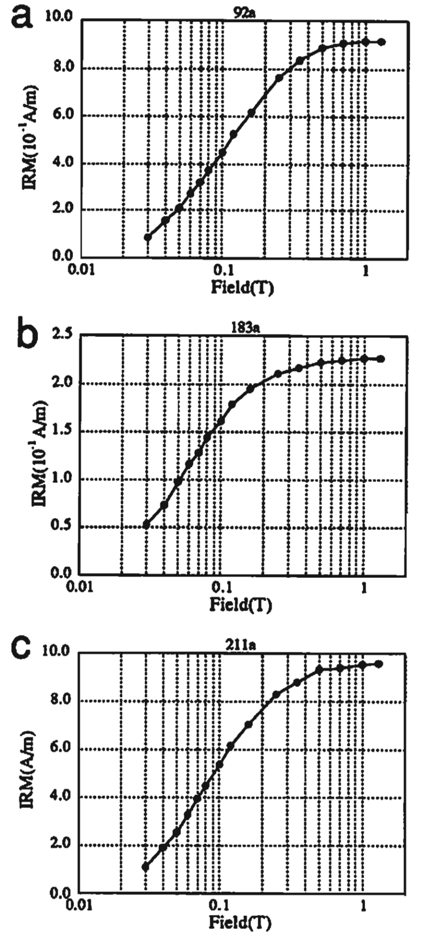

Fig. 4. The examples of IRM acquisition curve. a, b, and c : see caption of Fig. 3.

The results of the IRM acquisition (Fig. 4) and the thermal demagnetization of composite IRM (Fig.5) suggest that the dominant carriers of remanent magnetization are possibly magnetite and iron sulfides such as pyrrhotite. In Fig. 4, IRM acquisition curves increase gently and does not saturate beyond 0.5T or more. The presence of high coercivity (over 0.4T) components is also confirmed by the compatible curves between the medium (0.1T to 0.4T) and soft (less than 0.1T) IRMs as shown in Fig. 5. It is notable that unblocking temperature of the hard IRM is about 300°C. Although higher unblocking such as the case of Fig. 5c is also observed, the main phase of the unblocking is observed around 300°C. The medium and soft IRMs are slightly concaved at about 300°C. The main phase is clearly indicated at about 550°C. These lines of evidence suggest that magnetic constituents of these samples are magnetite, pyrrhotite, and minor hematite. The intensity ratio of the medium IRM to soft one at room temperature is considerably high as shown in Fig.5. The medium coercivity is possibly attributed to the presence of pyrrhotite (Dekkers, 1988). It may be said that stable secondary remanence is carried by pyrrhotite. Thermal instability of pyrrhotite may responsible to the unsuccessful PThD experiments.

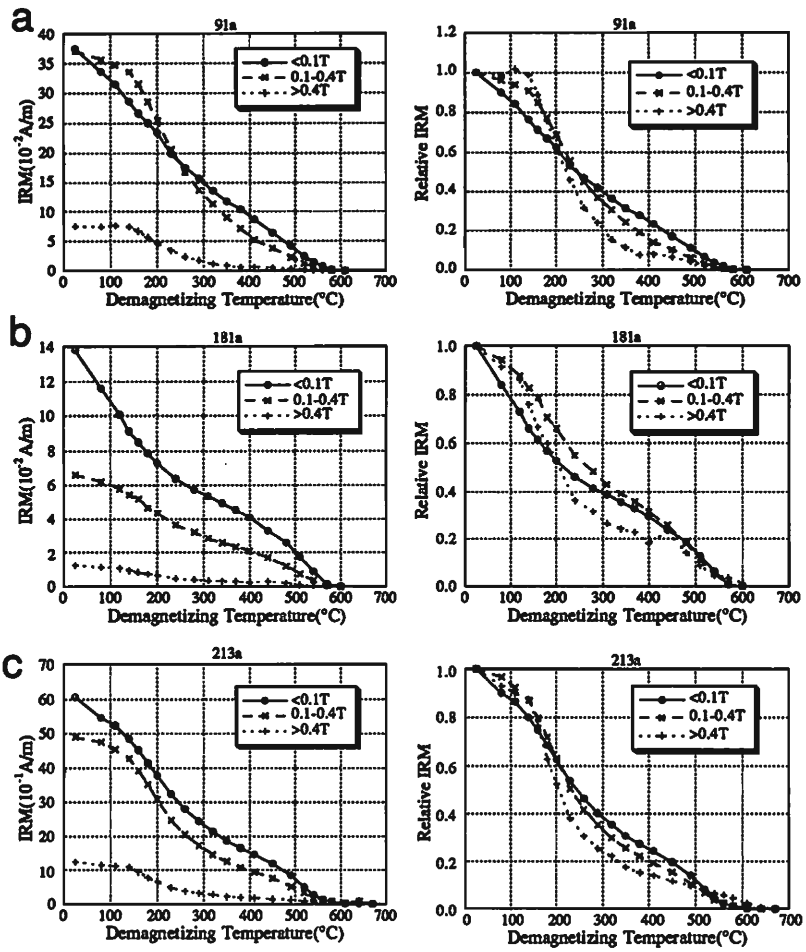

Fig. 5. Typical results of thermal demagnetization of composite IRMs. Intensity of the left column are absolute value, while right column are relative ones. a, b, and c : see caption of Fig. 3.

References

Dekkers, M. J. (1988) *Phys. Earth Planet. Inter.*, **52**, 376.

Lowrie, W (1990) *Geophys. Res. Lett.*, **17**, 159.

Sugai, K., H. Matsui, S. Sato, Y. Kitagawa, M. Sasaki, M. Miyashita, and H. Kawauchi (1957) *Geological Map of Joban Coalfield* (Goel. Surv. Japan), 143.

Torii, M., H. Oda, and H. Shibuya (1989) *Rock Mag. Paleogeophys.*, **16**, 20.

Yanagisawa, Y., K. Nakamura, Y. Suzuki, K. Sawamura, F. Yoshida, Y. Tanaka, Y. Honda, and M. Tanahashi (1989) *Bull. Geol. Surv. Japan*, **40**, 405.

(to be submitted to J. Geomag. Geoelectr)

PALEOMAGNETIC DATING OF A CORE FROM LAKE SUIGETSU, CENTRAL JAPAN

Chizu ITOTA[1], Masayuki HYODO[1], Akira HAYASHIDA[2], Hiroyuki KITAGAWA[3] and Yoshinori YASUDA[3]

1. The Graduate School of Science and Technology, Kobe University, Kobe 657
2. Laboratory of Earth Sciences, Doshisha University, Kyoto 606
3. International Research Center for Japanese Studies, Oeyama 3-2, Nishikyo-ku, Kyoto 610-11

Introduction

A paleomagnetic study was carried out on a core of sediment from Lake Suigetsu, Central Japan. The core was sampled for rock magnetic and paleomagnetic measurements as one of the research project of recovering the past environment of the earth around the area. In addition to magnetic analyses, the project covers the studies of sedimentology, tephrochronology, pollen - analyses, geochemistry and so on. In this report, we present preliminary results of paleomagnetic experiments, and attempt dating of the core by comparing the vertical change of magnetization directions with a record of the geomagnetic secular variation in Japan.

Sampling

Lake Suigetsu is a coastal lake faced on Wakasa Bay of Japan Sea, at latitude of 35.55°N and longitude of 135.88°E. It is about 10 km round and 4.3 km^2 in area, and a maximum water depth is 33.7 m. This lake is connected to the adjacent lake Mikata with a natural channel. Lake Suigetsu is further connected with the artificial channel constructed in AD1800 to Lake Hiruga, which has been artificially connected to Japan Sea in AD1630 (Okada, 1984). Therefore, the water of the lake is stratified into salt water in the base and fresh water in the subsurface.

The boring was made at the flat bottom of depth 30 m around the center using a Mackereth-type corer (Mackereth, 1958). The corer is characterized by penetration of a core tube with compressed air so that undisturbed cores of sediment which are suitable for paleomagnetic study are obtained. We have taken a core 7 cm in diameter and 4 m long, which has been sealed up quickly with vinyl plastic sheets on board to avoid drying of the sample.

The core was split into halves along the core length in the laboratory and the individuals were named SG1-W and SG1-E. Cubic specimens of volume about 10 cm^3 were taken from both halves. For the segment SG1-W, a total of 169 specimens were collected directly pushing in polycarbonate cubic boxes. For the segment SG1-E, a total of 170 specimens were cut out with a tool made of aluminum plate 0.2 mm thick and subsequently put into polycarbonate cubic boxes. The procedure for the latter is to avoid the deformation of sediment structure due to compression by the direct penetration of thick (1mm) polycarbonate boxes. This report presents only the magnetic results for SG1-E.

Experimental results

Thirty five pilot specimens selected from the segment SG1-E were subjected to progressive AF-demagnetizations with more than 15 steps. All the remanences have a single stable component and a viscous remanent magnetization (VRM) of coercivity < 5mT, as shown in Fig.1. The average direction of remanences after demagnetizations in AFs of 10 and 20 mT and the direction of stable component by the principal component analysis (Kirschvink, 1980) agree within a difference of 1°. Therefore all the remaining specimens were demagnetized in AFs of 10 and 20 mT only, and the average direction of the two remanences after AF-demagnetization was adopted as a stable direction.

The depth-dependency plot of NRM intensity for SG1-E is shown in the left of Fig.2. The NRM intensity shows high fluctuations in the uppermost part of 50cm. The intensity fluctuations correlate with fluctuations of material as in the lithology in the right of Fig.2.

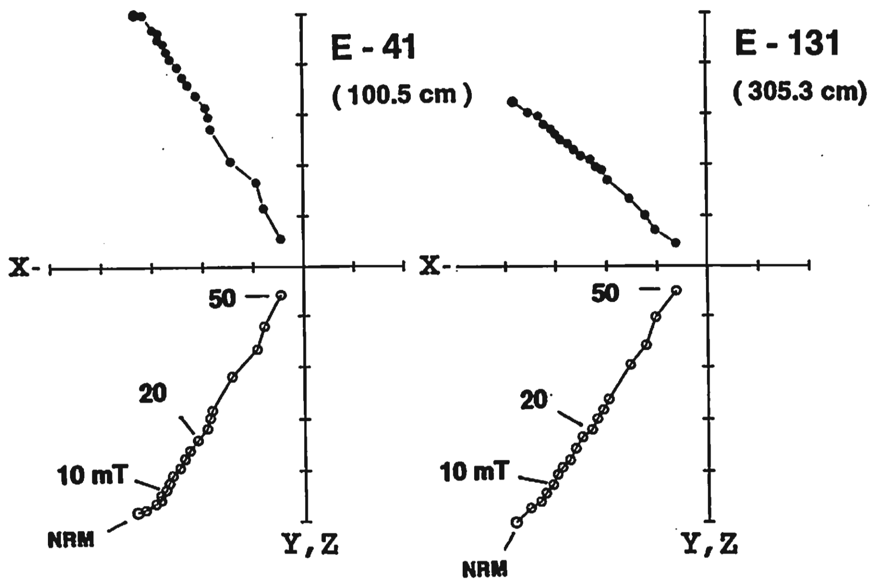

Fig.1 Progressive demagnetizations for samples at depths of 100.5 and 305.3 cm for SG1-E at Af-levels of 5, 6.7, 8.3, 10, 11.7, 13.3, 15, 16.7, 18.3, 20, 21.7, 23.3, 25, 30, 35, 40 and 50 mT. Open (solid) symbols show the magnetic vectors projected on the vertical (horizontal) plane.

Below a depth of 50 cm, the NRM intensity represents a gradual and smooth decrease with depth, accompanied by some spikes of high intensity. The smooth change is due to relatively homogeneous material mainly of dark grey clay, and all the spikes are pale grey clays. The trend may represent the slow change of material suggesting some long-term environmental changes.

The depth-dependency plots of declination and inclination of NRMs in Fig.2 show relatively small amplitude cahnges. They represent almost same changes with those of declination and inclination of stable components in Fig.3. The absence of difference in the two directional changes suggests that the NRMs are less affected by secondary VRMs. Therefore the small amplitude of change is not due to overprints of VRMs pointing to the present field.

Paleomagnetic dating

Secular variation of the geomagnetic field direction in Japan has been obtained from archaeomagnetism for the last 2000 years (Hirooka, 1971; 1983) and from sedimentary magnetism for the time span from 500 to 11500 yrBP (Hyodo et al., 1991). The former is from thermoremanent magnetizations of baked clays in archaeological places and the latter from depositional detrital remanent magnetizations of shallow marine and lacustrine sediments in central Japan. The two geomagnetic records derived from the different sources are in good agreement for the last 2000 years. The present core can be dated by correlating its magnetization directions with the geomagnetic secular variation records.

The declination change of the geomagnetic fields for the last 11500 years in Japan (SVJ) is characterized by ; (a) a large-scale swing from 4000-6000 yrBP with amplitude of 70° in peak-to-peak value and (b) a long-term westerly deflection persisting from 7000 yrBP to at least 11500 yrBP (Fig.3). These two features should be recorded in magnetizations of sediments even if their sedimentation rates are as slow as those of deep-sea sediments (> several mm/kyr). The changes of declination for SG1-E are within 40° of peak-to-peak value suggesting no recording of the feature (a). Therefore it is reasonable to assume that the bottom of the core is younger than 4000 yrBP.

Deficiencies of data in the curve of SVJ for the last 500 years can be covered by the archaeomagnetic data. The present declination 6°w around the area moves gradually to easterly directions to the past passing zero-declination around 200 yrBP and reaches to the first easterly peak which is <10°E around 400 yrBP. After that it has the second easterly peak between 700 and 800 yrBP, the easterly declination maintained. From 900 to 2300 yrBP, the declination is swinged to westerly directions with an pulsatile deflection > 20°W about 1500 yrBP. From 2300 yrBP, the declination becomes easterly again until 3300 yrBP and after that it becomes westerly. These series of features for declination changes in Japan are well reproduced in the record of SG1-E as in Fig.3. The bottom age is thus estimated about 3500 yrBP.

The inclination of the geomagnetic secular variation in Japan (SVJ) is characterized by small amplitudes of change. The archaeomagnetic data show that the present inclination 48° around the area becomes somewhat shallower to the past to within 40-45 °. It becomes deeper again, passing the line of 50° between 600 and 700 yrBP, and has a peak > 55° about 800 yrBP. The curve of inclination for SVJ is consistent with the archaeomagnetic one until the peak 800 yrBP. Although the archaeomagnetic data further show two high peaks in inclination

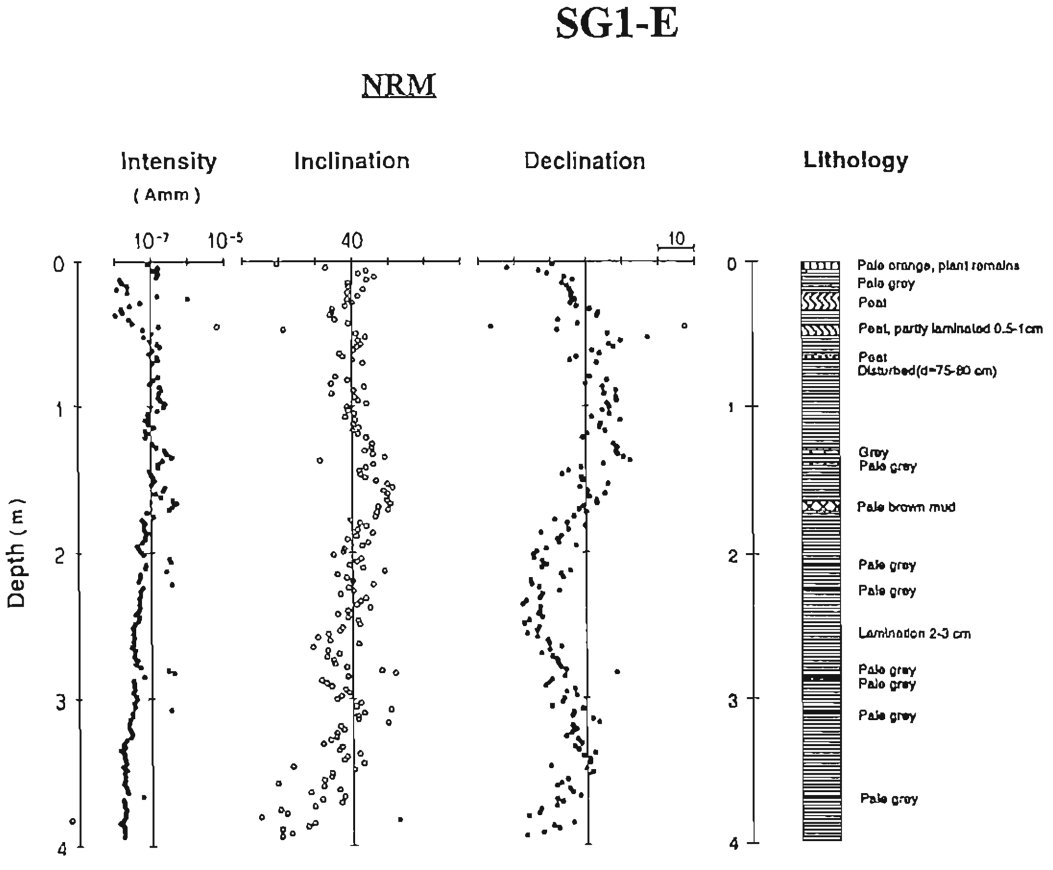

Fig.2 Depth-dependency plots of the intensity, inclination and relative declination of NRMs for the core segment SG1-E. In the lithology (right), most parts except descriptions show dark greenish grey clay and the descriptions by only color show clays.

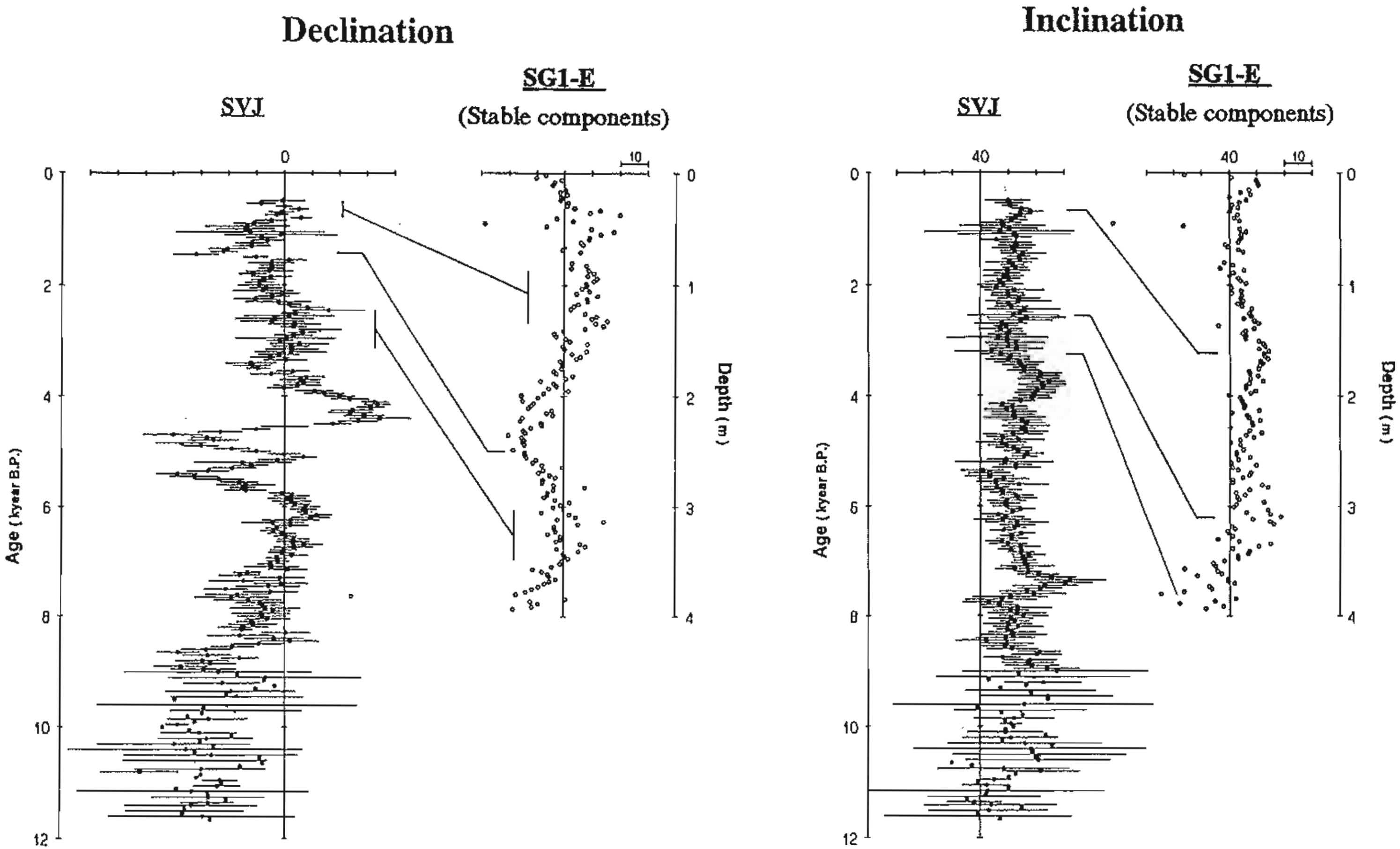

Fig.3 A standard curve of the geomagnetic secular variation in Japan (SVJ) and the depth-dependency plot of the directions of stable magnetization components (SG1-E). The data of SVJ have been constructed from magntization directions of seven cores of marine and lacustrine sediments in central Japan (Hyodo et al., 1991). The solid circles in the curve of SVJ are the directions averaged within a window of 50 years and the error bars show limits of 95 % confidence circle. The age scale is based on the calibrated (Klein et al., 1982; Shove, 1983; Stuiver, 1982) radiocarbon dates. See text for the stable components of magnetization of SG1-E.

about 1350 and 1750 yrBP., the inclination of SVJ has no such peaks. The inclination of SG1-E is well correlated with that of SVJ rather than the archaeomagnetic record for the duration 1000-2000 yrBP (Fig.3). The small peak at depths 310-340 cm may be correlated with the peak around 2500 yrBP in the curve of SVJ. The tie-lines in the curves of inclination shown in Fig.3 are consistent with those of declination curves. The bottom age can be again estimated about 3500 yrBP independently.

Discussion

Most of the features in declination and inclination of SVJ for the last 3500 years are recorded in the remanent magnetizations of the core from Lake Suigetsu. This suggests that the magnetizations are less affected by filtering due to post-depositional magnetization process of sediments (Hyodo, 1984). The only exception is absence of the pulsatile westerly deflection around 1500 yrBP, which may be due to the filtering effect. Some of the source data of secular variation used for construction of the curve of SVJ have been subjected to deconvolution fitting amplitudes of changes to the biggest one. In addition, the curve of SVJ for the past 2000 years shows consistent and almost same amplitude changes with the archaeomagnetic data. Hence, the curve of SVJ is least affected by filtering and may represent the geomagnetic secular variation fairly faithfully.

An average sedimentation rate of 1.1 mm/yr is obtained from the estimation of 3500 yrBP at a depth of 400 cm. This is about three times of the sedimentation rate of 0.4 mm/yr in Lake Mikata (Yasuda, 1982). However the high average sedimentation rate for Lake Suigetsu is due to the extremely high rate 1.6 mm/yr above a depth of 250 cm which is correlated with the age of 1500 yrBP. Below 250 cm in depth, the average sedimentation rate becomes only 0.6 mm/yr. Since the estimated rate in Lake Mikata is based on the conventional radiocarbon age 15000 yrBP at depths 579-600 cm, the time span for calculating an average sedimentation rate is different from that for Lake Suigetsu. It may be that there is no difference in sedimentation rate between the two adjacent lakes.

In conclusion, the sediments of the core from Lake Suigetsu have magnetizations of very stable directions. The vertical changes of declination and inclination of magnetizations are well correlated with the secular variation of geomagnetic field direction in Japan. The core was dated by correlating the features of declination and inclination changes. As a result, the age of the base in the core was estimated 3500yrBP. Furthermore, it was suggested that the sedimentation rate increased after about 1500 yrBP while it was as slow as the estimated rate in Lake Mikata before 1500 yrBP.

References

Hirooka, K.(1971) Mem. Fac. Sci. Kyoto Univ., 38, 167-207.

Hirooka, K.(1983) Geomagnetism of baked clays and recent sediments, edited by K.M. Creer, P. Tucholka and C.E. Barton, Elsevier, Amsterdom, 150-157.

Hyodo, M.(1984) J. Geomag. Geoelectr., 36, 45-62.

Hyodo, M., C. Itota and K. Yaskawa (1991), To be submitted to J. Geomag. Geoelectr..

Kirschvink, J.L.(1980) Geophys. J. R. Astr. Soc., 62, 699-718.

Klein, J., J.C. Lerman, P.E. Damon and E.K. Ralph (1982) Radiocarbon, 24, 103-150.

Mackereth, F.J.H.(1958) Limnol. Oceanog., 3, 181-191.

Okada, T.(1984) Torihama-Kaizuka, 9-42 (in Japanese).

Shove, D.J.(1983) Geomagnetism of baked clays and recent sediments, edited by K.M. Creer, P. Tucholka and C.E. Barton, Elsevier, Amsterdom, 45-56.

Stuiver, M. (1980) Radiocarbon, 24, 1-26.

Yasuda, Y. (1982) The Quat. Res.(Daiyonkikenkyu), 21, 255-271 (in Japanese).

ANOMALOUS PALEOMAGNETIC FIELD DIRECTIONS IN LATE MATUYAMA MARINE CLAYS IN TAKATSUKI, CENTRAL JAPAN

Kaori TAKATSUGI [1] and Masayuki HYODO [2]

1 Department of Earth Sciences, Faculty of Science, Kobe University, Kobe 657
2 The Graduate School of Science and Technology, Kobe University, Kobe 657

[Introduction]

The earth's magnetic field is often approximated by a geocentric dipole field. It is since William Gilbert (1600) proposed a model of a uniformly magnetized sphere. More than 90 % of components in the present geomagnetic field can be accounted by a central dipole field. The approximation is valid for the past geomagnetic fields as well as the present field. It has been revealed by paleomagnetism that the past geomagnetic fields in the geological era are dipolar. However, paleomagnetism also revealed existence of the two major geomagnetic behaviors in which field directions deflect largely from a dipole field. One is a reversal and the other is an excursion. A short geomagnetic event is often classified into excursions.

History of the geomagnetic field reversals was first clarified from paleomagnetic measurements and radiometric dating of volcanic rocks. The reversal history was recognized by the marine magnetic anomalies and magnetizations of cores of deep-sea sediments. Magnetizations of oceanic crusts, calculated from marine magnetic anomalies, extended the time span of the reversal history to the past 150 million years. Magnetostratigraphy was thus established. On the other hand, only a few examples of geomagnetic excursion whose reliability is sufficiently examined have been reported, so that even its behavior is still obscure. However, as often discussed, an excursion or a short geomagnetic event may become a trigger of a reversal, so that they may play an important role in the dynamo process. The importance of observing new excursions or short events also lies in the magnetostratigraphic dating.

In this paper, we report a sequence of paleomagnetic field directions largely deflected from a geocentric axial dipole field obtained from marine clays in the Osaka Group, Central Japan. This may be a geomagnetic excursion or a short event.

[Sampling]

The Osaka Group, Plio-Pleistocene sequences in the Kinki district, is distributed in and around Osaka Bay. It is composed with unconsolidated fluvio-lacustrine and marine deposits. The marine facies form fourteen continuous clay markers named Ma 0 to Ma 13 in ascending order, corresponding to progressions. The forth marine clay Ma 3, which is mainly sampled in this study, is interbeded with the Azuki Tuff, a widespread volcanic ash, dated at 0.87 ± 0.07 m.y. by fission-track method (Nishimura and Sasajima, 1970). The Brunhes/Matuyama polarity boundary is assigned in the fifth marine clay Ma 4 (Hayashida and Yokoyama, 1989).

Paleomagnetic sampling was made in a hill of Nasahara area (34.86°N,135.58°E), Takatsuki city. In the area, there was a fresh section from the bottom of marine clays Ma 3 up to the top of the marine clay Ma 4. The thickness of the Azuki Tuff was about 50 cm in the section. The level of the bottom of the Azuki Tuff was used as a standard level for sampling horizons. We sampled mainly fine marine clays and sometimes marine clays rather silty. Some samples of marine silts and sands were also collected, but no fluviatile sediments was taken.

All the samples were hand oriented. The sediments were excavated and then a horizontal surface of about a few hundreds cm^2 was constructed, from which a block sample about 10 cm on a side was collected. In laboratory, small cubic specimens of sediment were cut out and sealed in polycarbonate cubic boxes about 10 cm^3 in volume. In total, 473 specimens were taken from 76 horizontal levels.

[Experiment]

The following procedures were taken as a routine work in paleomagnetic experiments. 1) Preparation of cubic specimens was carefully made by hand work subjected to no compressive stress. 2) Specimens in cubic boxes were stored in a hermetically sealed case until measurements to prevent desiccation. 3) All the specimens were progressively demagnetized in alternating fields (AF). These procedures were taken because the following precautions were obtained empirically before the routine work.

First, compaction or vibration of a sample damages the magnetization. To save time for field work, we tried to take some samples by penetrating a polycarbonate cubic box directly to a sediment surface leveled. Sometimes a cubic box was penetrated hit by a wooden hammer. The samples represent unstable remanent magnetizations in progressive AF-demagnetizations. A typical AF-demagnetization pattern for these samples is shown in Fig.1 (b) comparing with that of a specimen taken by the normal method from the same block shown in Fig.1 (a). The unstable demagnetization pattern may be caused by rotation of mobile magnetic particles in the cracks made by compressive stress.

Second, drying of a sample also seems to destroy a magnetization structure. Fig.2 shows results of demagnetization of specimens from a same stratigraphic level 1.40 m above the Azuki Tuff. Progressive AF-demagnetization of a specimen 10 hours after preparation of specimens shows a clear pattern of reverse polarity of remanence, as in Fig.2 (a). Such a stable magnetization was not obtained from AF- and thermal demagnetizations of dried specimens. The lower diagrams in Fig.2 show the results of (b) AF-demagnetization of a dried specimen stored in a non-zero magnetic field for a month, (c) AF-demagnetization of the dried specimen stored in a desiccator with silica gel for 10 days in a zero-field and (d) thermal demagnetization

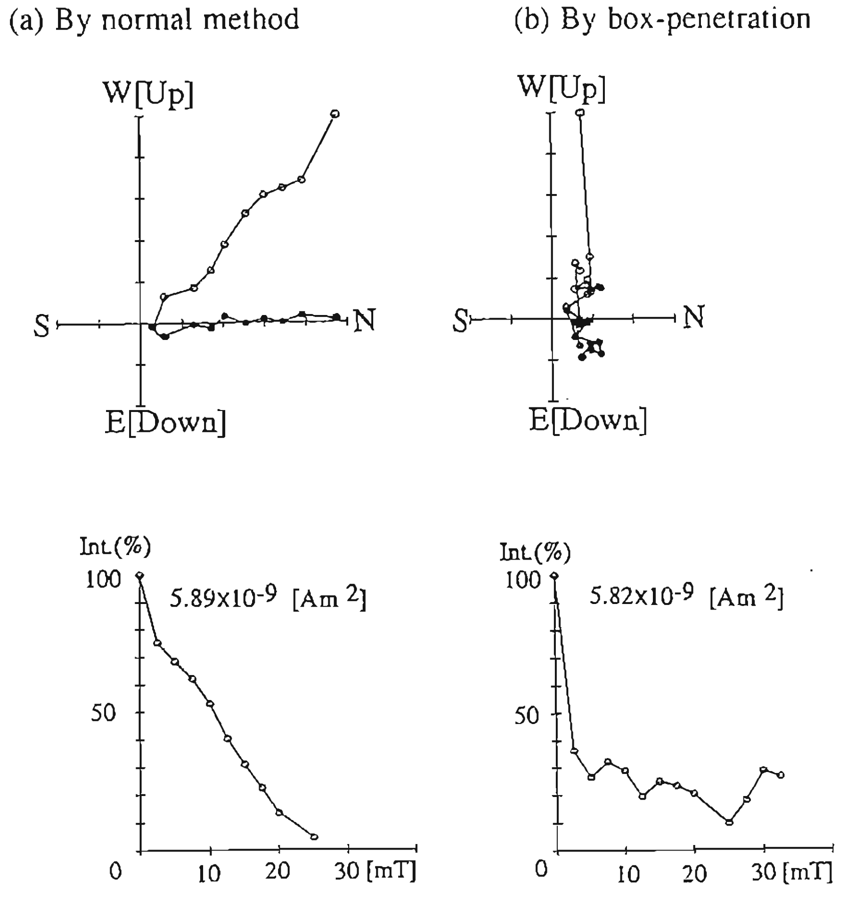

Fig.1 Progressive AF-demagnetizations of (a) a specimen taken by a normal method (see text) and (b) a specimen taken by penetrating a cubic box directly to a sediment surface. These two are from a same horizon.

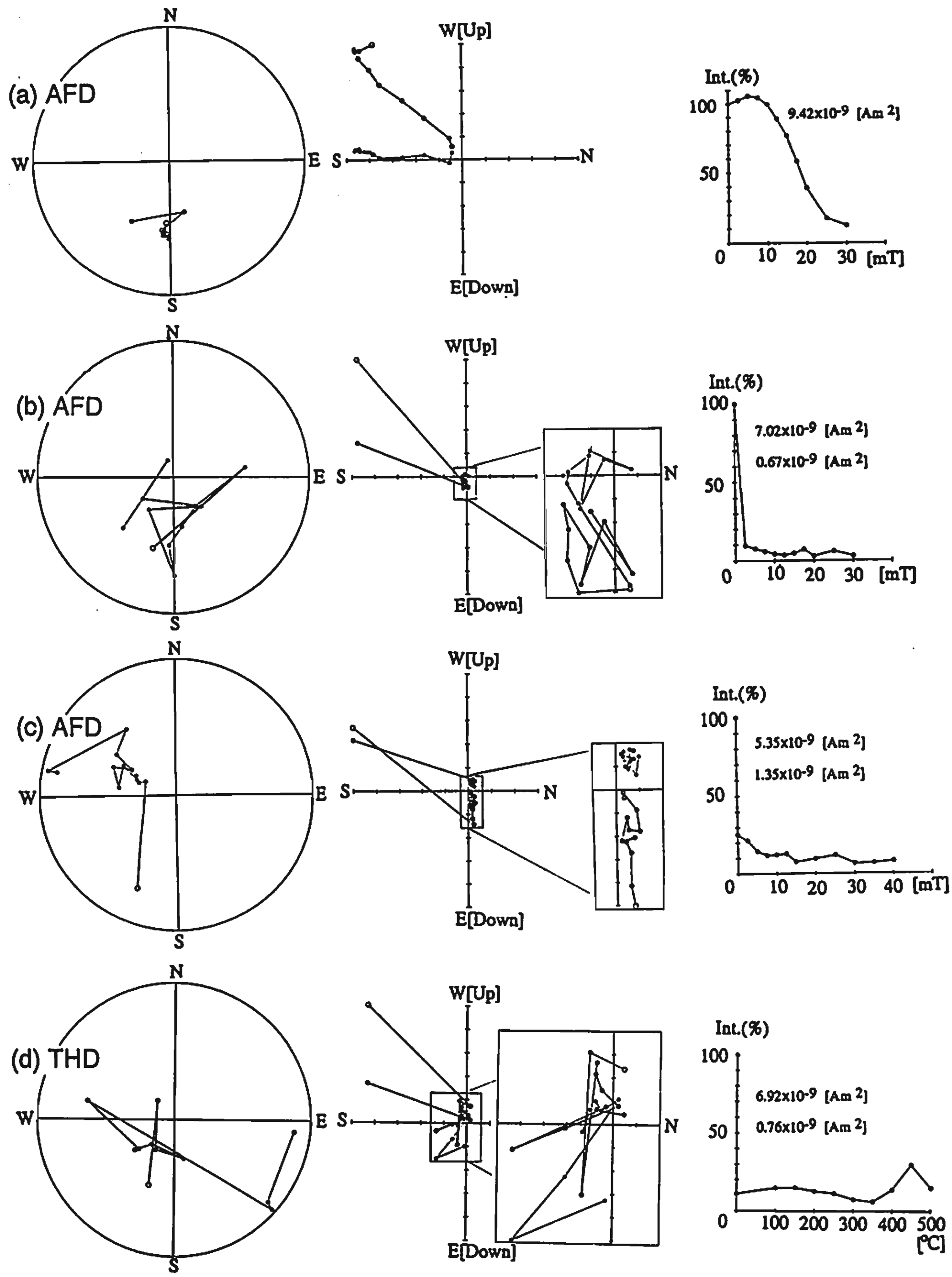

Fig.2 Progressive AF- and thermal demagnetizations of specimens from a same horizon. (a) A specimen taken by the normal method (see text). (b) A specimen after natural drying. (c) A specimen artificially dried in a desiccator. (d) Thermal demagnetization of a specimen artificially dried in a desiccator.

of a specimen dried like (c). About 40 weight percent of water was removed in the specimens of (c) and (d). Any results show that the NRMs have anomalous directions before demagnetization and unstable remanence directions during progressive demagnetization. The intensity decrease due to the drying effect (Otofuji et al., 1982) was about 10-25 % of NRM intensities of wet samples in the samples (c) and (d). Furthermore they show a sudden intensity drop at the first step of AF-demagnetization. The intensity drop may be due to physical rotations of mobile grains resulting in random alignments.

[Paleomagnetic results]

All the specimens were progressively demagnetized in AFs of at least 2.5, 5, 7.5, 10, 12.5, 15, 20, 25 and 30 mT, and sometimes until 90 mT at intervals of 5 mT. The remanence of most samples was separated to higher (>7.5 mT) and lower (<5mT) coercivity components by the principal component analysis (Kirschvink, 1980). The remanence of samples from 37 horizons could not be separated into components. Most of such samples are silts and sands, and some others are clays. They may be subjected to chemical alterations. Although we avoided to sample the clays partly discolored suggesting limonites, we may have looked over some slight discoloration. Anyway, only the remanences possessing components which can be isolated by the principal component analyses is used in the later discussion.

In the two components of remanence, the lower coercivity components are all directed to the present field direction, suggesting viscous remanent magnetizations (VRM). Most of the higher components have reverse polarity suggesting the Matuyama reversed chron. Three normal polarity fields were obtained in the upper part of the marine clay Ma 4 suggesting the Brunhes normal chron. Fig.3 shows a mean direction of higher components for specimens in the same horizon. The sequence of magnetization directions of high coercivity components

Fig.3 Mean directions of high coercivity components of remanence by the principal component analysis (Kirschvink, 1980). Error bars show limits of 95 % confidence circle.

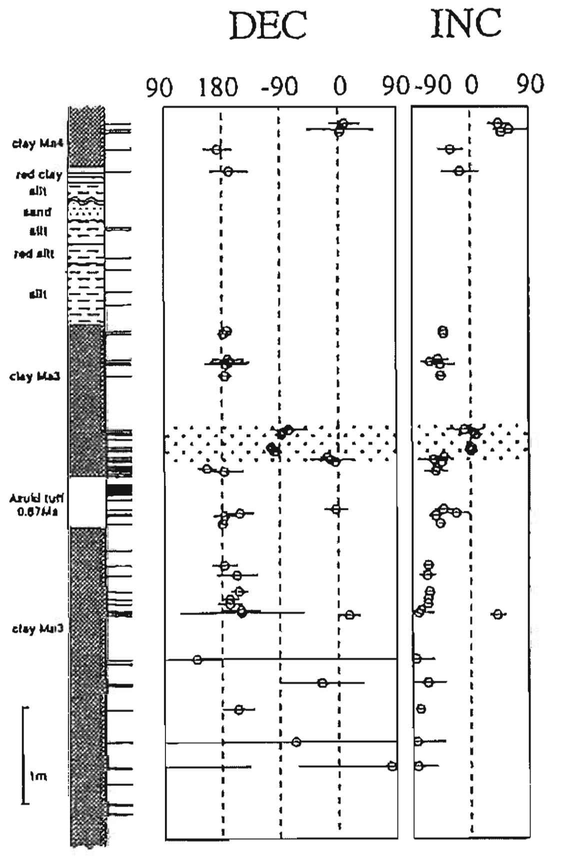

shows the existence of a zone of fields largely deflected from reverse polarity fields 10 - 45 cm above the Azuki Tuff. The field directions in the zone are characterized by shallowly inclined westerly directions (Fig.4 (a)) and northward-pointing directions with negative inclination (Fig.4 (b)). As shown in Fig.4, they are the components isolated by removing a low coercivity component magnetized along the present field direction. The right diagrams in Fig.4 show the consistent paleomagnetic directions of other specimens in the same horizon.

VGPs of the horizon mean directions in Fig.3 are plotted in Fig.5, in which those of field directions in the deflection zone are numbered in ascending order. The VGPs of Nos. 1 - 3 are from the northward-pointing directions with shallow inclinations and the other numbered VGPs are from the westerly directions. All of the VGPs in the deflection zone are departed more than 45° from the south pole, satisfying the condition of a geomagnetic excursion. The zone of fields with deflected directions would be an excursion or transitional fields in a short geomagnetic event. The latter case is possible because the upper boundary of the zone could not be defined. Stable remanence components was not obtained due to no fine clays above the zone.

[Discussion]

The excursion or short event obtained in the marine clay Ma 3 is in the late Matuyama chron. It is clearly distinct from the short normal event in the Kamikatsura tuff dated at 0.85 ± 0.03 Ma by fission track dating (Maenaka, 1983). The Kamikatsura tuff is intercalated in the fluviatile sediments between the marine clays Ma 2 and Ma 3, which may be in the Jaramillo event. There are some other reports of short normal event in other places of the globe; near the

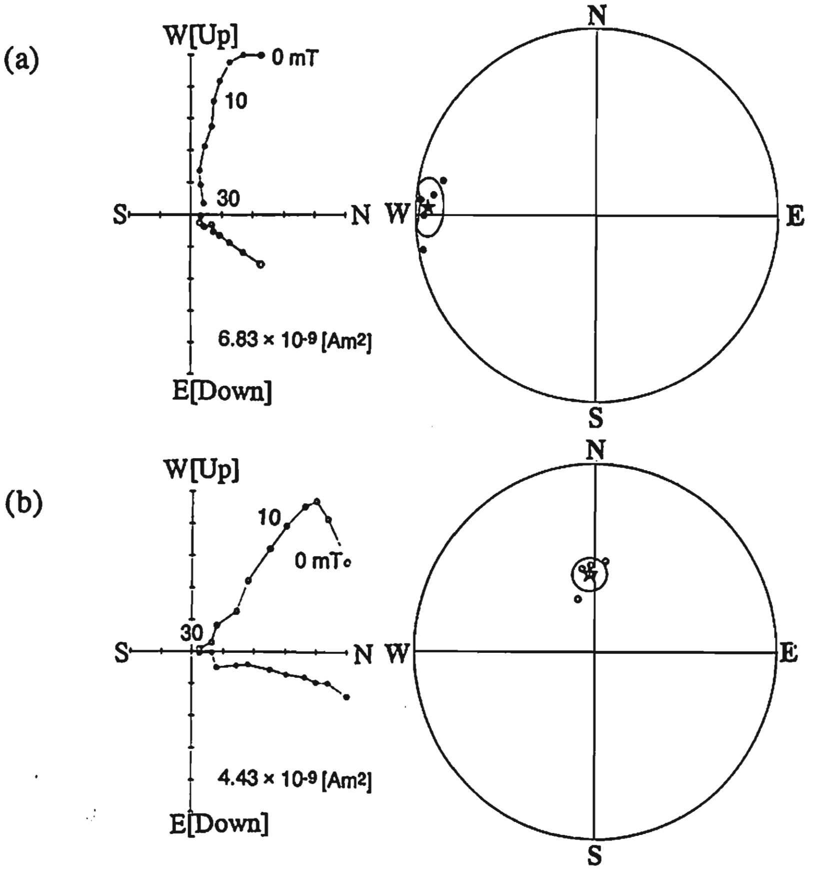

Fig. 4 Progressive AF-demagnetizations for magnetizations of two typical directions in the zone of deflected field directions just above the Azuki Tuff in the marine clay Ma 3.

Fig.5 VGPs of the mean paleomagnetic field directions in each horizon. Open (solid) circles show the northern (southern) hemisphere. The data points from the zone of deviated fields hatched in Fig.3 are numbered in ascending order.

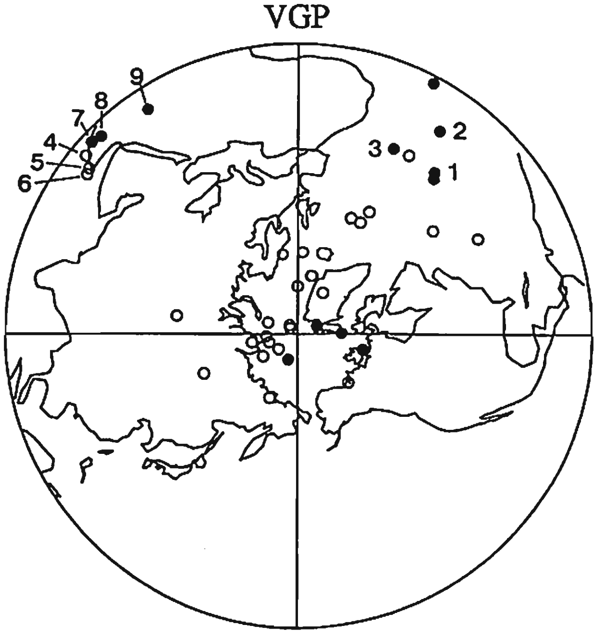

Clear Lake of California at 0.84 ± 0.03 Ma (Mankinen et al., 1981), in a deep-sea core about 0.85 Ma (Watkins et al., 1968) and in the Bonneville Basin, Utah about 0.86 Ma (Eardley et al, 1973). All of these events can be correlated with the zone of deflected fields discovered in this study, suggesting the global instability of geomagnetic field.

The thickness of the zone of deflected fields is 35 cm. This is a minimum value because the upper boundary of the zone could not be defined. The thickness of 35 cm is roughly estimated 350 years in duration from the present sedimentation rate in the bottom of Osaka Bay (Hyodo and Yaskawa, 1980), where the marine clay Ma 13 is now in deposition. The duration is close to the estimate about 1000 years or less for the Mono Lake excursion of age 24 - 25 Ka (Denham, 1974; Liddicoat and Coe, 1979). There may be no difference in the mechanism of occurrence between the excursion (or short event) in the late Matuyama epoch and the excursion in the late Brunhes epoch.

In conclusion, a sequence of paleomagnetic fields largely deviated from a geocentric dipole field was observed in the marine clay Ma 3 of the Osaka Group in Takatsuki City, Central Japan. The sequence is recorded in a zone of sediments at levels from 15 cm to 50 cm above the Azuki Tuff, which is above the Jaramillo subchron and below the Brunhes/Matuyama polarity boundary. The field directions are characterized by shallowly inclined westerly directions and full northward-pointing directions with negative inclinations. The geomagnetic sequence may suggest a geomagnetic excursion or a transitional record of a geomagnetic short normal event in the late Matuyama epoch.

[References]

Denham, C.R. (1974) J. Geomag. Geoelectr., 26, 487-498.
Eardley, A.J., et al. (1973), Geol. Suc. Am. Bull., 84, 211-216.
Gilbert, W. (1600) De Magnete.
Hayashida, A. and T. Yokoyama (1989) Paleogeograph. Paleoclim. Paleoecol., 72, 195-201.
Hyodo, M. and K. Yaskawa (1980) J. Geomag. Geoelectr., 32, 581-584.
Liddicoat, J.C. and Coe, R.S. (1979) J. Geophys. Res., 268, 22-25.
Maenaka, K. (1983), Mem. Hanazono Univ., 14, 1-65.
Mankinen, E.A. et al. (1981) Geol. Surv. Prof. Pap., 1141, 67-82.
Nishimura, S. and S. Sasajima (1970) Chikyu Kagaku, 24, 222-224.
Otofuji, Y., I. Katsura ans S. Sasajima (1982) Geophys. J. R. Astr. Soc., 70, 191-203.
Takatsugi, K. (1987) The thesis of Kobe Univ., 50pp.
Watkins, N.D. (1968) Earth Planet. Sci. Let., 4, 341-349.

(To be submitted to J. Geomag. Geoelectr.)

RESULTS OF PALEOMAGNETIC MEASUREMENT AND NANNOFOSSIL ANALYSIS OF THE DAITA BOREHOLE CORE, SETAGAYA, TOKYO

Toshikazu INOUE[1], Mitsuo YOSHIDA[2] and Masamichi YAMAZAKI[1]

[1] Department of Resources and Environmental Geology,Geoscience Co.,Ltd., 2-1, Higashi-Ueno 6 chome,Taito-ku,Tokyo 110,JAPAN.

[2] Department of Resources and Environmental Geology,Geoscience Co.,Ltd., 2-1, Higashi-Ueno 6 chome,Taito-ku,Tokyo 110,JAPAN (presently at Geoscience Laboratory,Geological Survey of Pakistan, c/o JICA,P.O.Box 1772,Islamabad,PAKISTAN)

Introduction

The subsurface geology of the Kanto Plain recently becomes clear by a lot of borehole data for civil engineering survey. The Daita borehole is one of these boreholes (Figure 1). It penetrated 100m thick continuous sedimentary sequence which could be correlated with the Shimousa Group and Kazusa Group of the Upper and the Middle Pleistocene. Paleomagnetic measurement and nannofossil analysis could successfully determine a detailed chronology of the sequence.

Paleomagnetic Measurements

Total 74 specimens were collected from the borehole cores, especially from the parts of fine sediments, such as silt and silty sand. Paleomagnetic samples were put in nonmagnetic poli-carbonate cubic capsules 2.5cm on a side ($10cm^3$). Intensities of natural remanent magnetizations indicated from 10^{-4} to 10^{-5} emu which can be measured by a spinner magnetometer. We selected four pilot samples (25.12m,29.82m, 57.25m and 90.30m in depth) for progressive alternating field demagnetization (AFD) analysis. The results are shown in Figure 2. In the progressive demagnetization treatment, remanent magnetization vectors of the pilot samples decayed toward origin after small randomly oriented components were removed at low inductions of less than 20mT. Therefore we chosed 20mT in a peak field AFD as the demagnetization condition for estimating characteristic components.

Three horizons of 29.82-31.45m, 38.48m and 42.95-43.48m in depth show normal polarity, but the other horizons show reversed polarity.

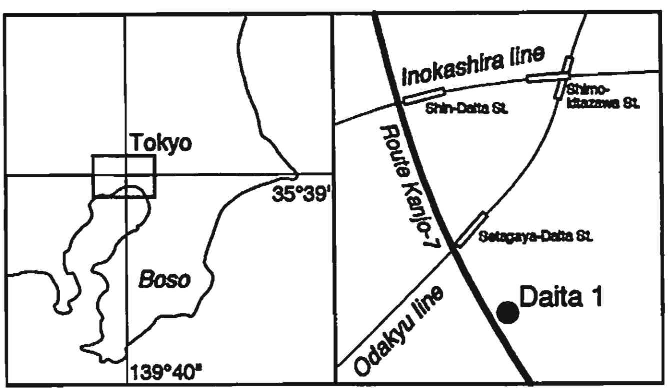

Figure 1: Locality map of the Daita borehole site.

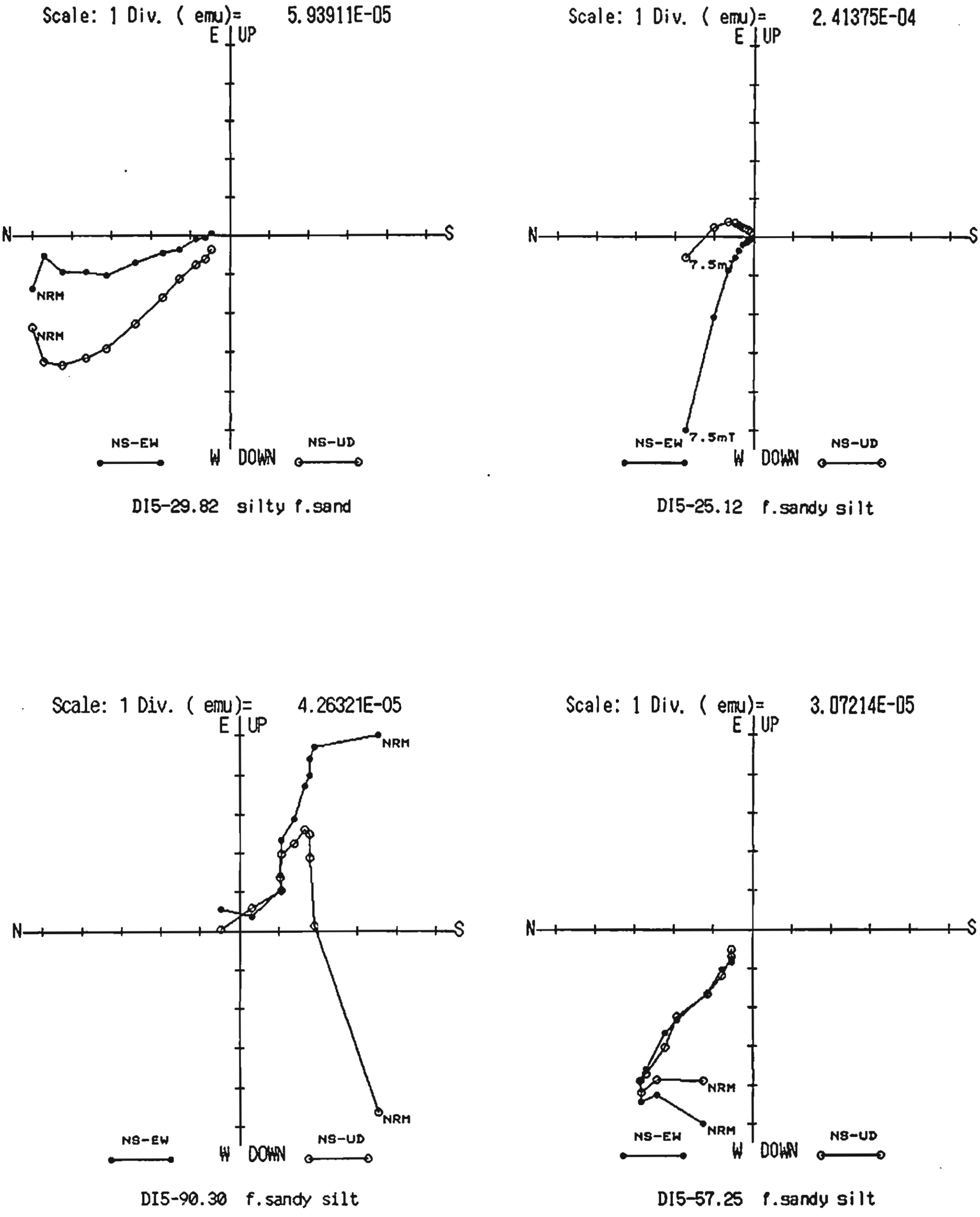

Figure 2: Results of progressive demagnetization analysis.

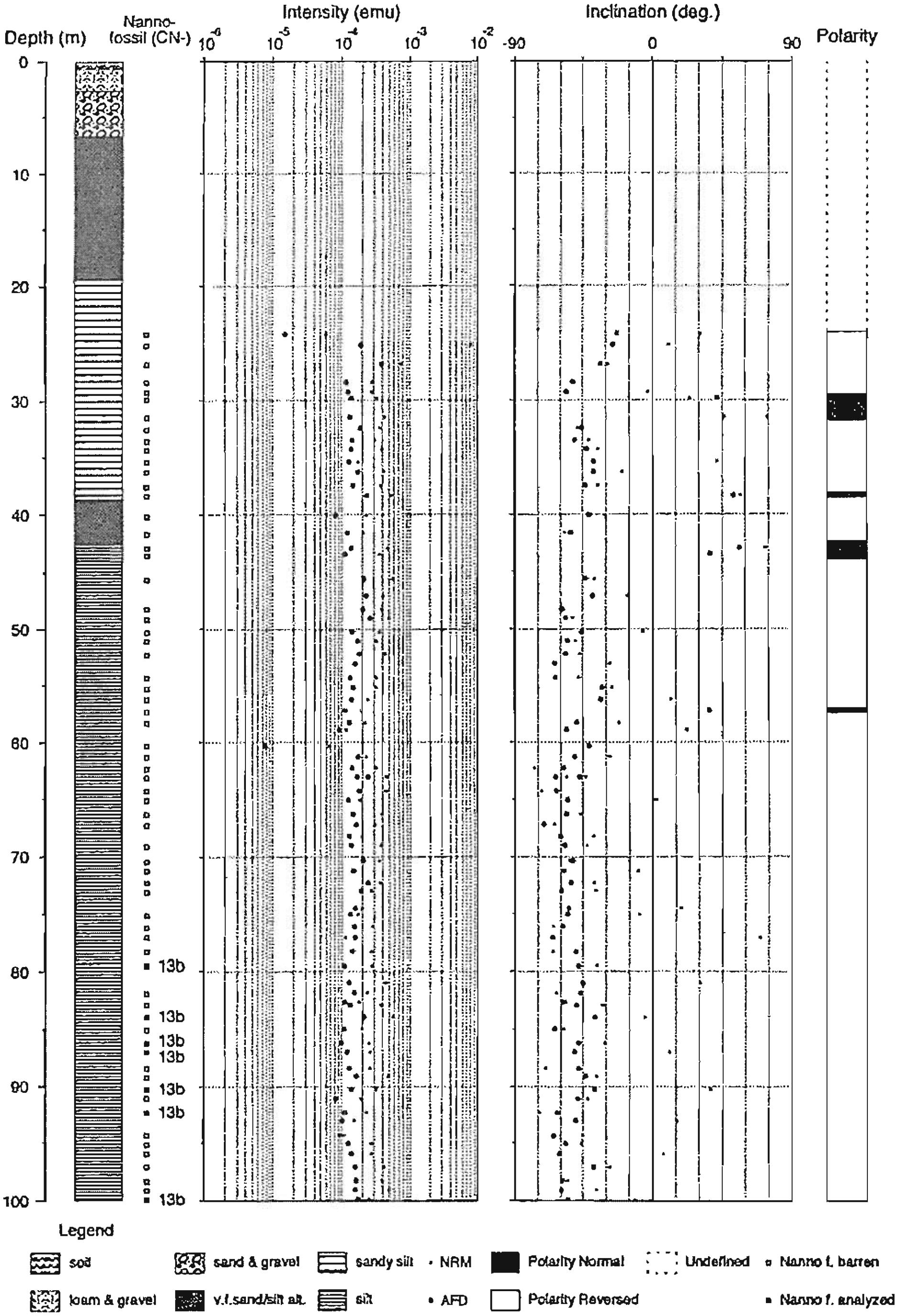

Figure 3: The results of paleomagnetic measurements

Nannofossil Analysis

Total 65 specimens were collected for the nannofossil analytical study. Calcareous nannofossils were detected from seven specimens collected from relatively deep part (79.55m,83.95m,86.27m,87.05m,90.30m, 92.35m and 99.95m in depth). A quantitative analysis could be done for four specimens (83.95m,87.05m, 90.30m and 99.95m in depth) among these specimens (Table 1).

All the specimens yield large *Gephyrocapsa oceanica*, *Gephyrocapsa caribbeanica*, *Pseudoemiliania lacunosa*, so the horizon below 79.55m can be correlated with CN13b to CN14a Zone (Okada and Bukry,1980).

The lowest specimen (99.95m) does not yield *Helicosphaera sellii* which extincted at 1.2Ma, then the age of starata is possibly younger than 1.2Ma. Furthermore the uppermost specimen (79.55m) yield much larage *Gephyrocapsa caribbeanica* which extincted at 1.1Ma (Matsuoka and Okada,1989), therefore the age of strata is probably older than 1.1Ma.

Magnetic Stratigraphy and Geochronology

Results of magnetic measurement and nannofossil analysis are compiled on Figure 3. It is clear that all horizons below 24m in depth can be correlated with the Matuyama Reversed Polarity Chron (before 0.73Ma). On the basis of the results of nannofossil zonation, the strata below 79.55m in depth correspond to the time between 1.1Ma to 1.2Ma. Three short normal polarity bands probably correlated with the Cobb Mountain Event.

References

Matuoka H. and Okada H.(1989) Mar.Micropaleontol.,14,97-118.
Okada H. and Bukry D.(1980) Mar.Micropaleontol.,5(3),321-325.

(submitted to The Quaternary Research)

RESULTS OF PALEOMAGNETIC MEASUREMENT AND FOSSIL POLLEN ANALYSIS OF THE SANTONODAI BOREHOLE CORE, YOKOHAMA CITY, JAPAN

Mitsuo YOSHIDA[1], Toshikazu INOUE[2] and Yaeko IGARASHI[3]

[1] Department of Resources and Environmental Geology, Geoscience Co.,Ltd., 2-1,Higashi-Ueno 6,Taito-ku,Tokyo 110,JAPAN (presently at Geoscience Laboratory, Geological Survey of Pakistan, c/o JICA, P.O.Box1772, Islamabad,PAKISTAN)

[2] Department of Resources and Environmental Geology, Geoscience Co.,Ltd., 2-1,Higashi-Ueno 6,Taito-ku,Tokyo 110,JAPAN

[3] Geological Laboratory, Geoscience Co.,Ltd., Kita-39,Nishi-3,Kita-ku, Sappro 001,JAPAN

The borehole site is located in the Santonodai Jomon Ruins on the Simosueyoshi Terrace which is one of the most typical Upper Pleistocene terrace in Japan (Figure 1). The core specimens collected from the borehole which consist of marine sediments of the Byobugaura and Shimosueyoshi Formation, and weathered volocanic ejecta of Kanto Loam Layers. This sequence may provide almost continuous geological information of the area during the Late Pleistocene time. We attempted to get its paleomagnetic polarity stratigraphy and palynostratigraphy. The paleomagnetic measurement was carried out by Yoshida and Inoue and the fossil pollen analysis was carried out by Igarashi.

Paleomagnetic Measurements

Total 57 specimens were sampled from the cores. Paleomagnetic samples were put in nonmagnetic poli-carbonate cubic capsules 2.5cm on a side ($10cm^3$). These samples were mainly collected from semi-consolidated fine sediments such as silt, fine sand and loam. Intensities of natural remanent magnetizations indicate from 10^{-4} to 10^{-3} emu which can be measured by a spinner magnetometer (Natsuhara SSM85).

We selected four pilot samples (5.83m,10.10m,10.51m and 22.33m in depth) for progressive alternating field demagnetization (AFD) experiments. The results are shown on Figure 2. In the AFD experiment, remanences of the pilot samples decayed toward origin after small randomly oriented components were removed at low inductions of less than 15mT. Therefore we chosed 15mT AFD as the demagnetization condition for estimating charcteristic components of the samples.

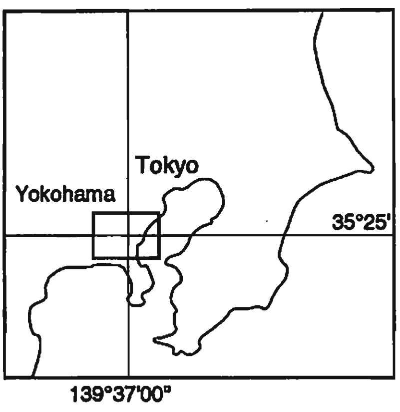

Figure 1. Locality Map of the Santonodai borehole site.

Results of Fossil Pollen Analysis

The fossil pollen assemblages obtained from this core were divided into four pollen zones IV to I in ascending order (Figure 3). The characteristic of each zone is rich Pinaceae and *Alnus* in I, rich *Fagus* and *Alnus* in II, rich *Cryptomeria* and *Alnus* in III and rich Pinaceae and *Alnus* in IV. The stratotype section of Shimosueyoshi Formation in Yokohama area was divided into two parts; the Upper and Lower part, with fossil pollen and plant. The Lower part shows a transgression stage which is characterized by warm elements like *Lagarstroemia*. On the contrary, the Upper part shows a regression stage including rich *Cryptomeria* and *Alnus* (Tsuji and Minaki,1985). The II zone of this borehole core could be correlated with the Upper part of Shimosueyoshi Formation.

Polarity Stratigraphy and Chronology

The continuous change of inclination and intensity of the characteristic magnetizations is graphically displayed on Figure 4. It is clear that a reversed polarity zone can be observed from 9.85m to 10.42m in depth represented by continuous seven specimens. The other part are magnetized normally.

On the basis of the geological observations of core specimens, the thick pumice layer of 6.5m to 7.0m in depth can be correlated with the maker bed TP ("Tokyo Pumice") which is dated 49,000yr by fission track method (Machida and Suzuki,1971). Marker beds YP and OP ("Orange Pumice", 66,000yr; Machida and Suzuki,1971) are also obseved in the section (Figure 4).

The result of fossil pollen analysis indicates that the sediments in the borehole below 16.40m in depth can be correlated with the upper part of the Shimosueyoshi Formation. The age of the uppermost Shimosueyoshi Formation is estimated approx. 100,000yr (Oka,1991).

The short reversed polarity zone detected from 9.85m to 10.42m in depth probably corresponds to a short event of reversed polarity in Brunhes Normal Polarity Chron, which is dated between 49,000yr and 66,000yr.

References

Tsuji S. and Minaki M.(1985) Jap.Jour.Ecol.,35,133-137.

Machida H. and Suzuki M.(1971) Kagaku (Science),41,263-370.

Oka S.(1991) Bull.Geol.Surv.Jap.,46,531-651.

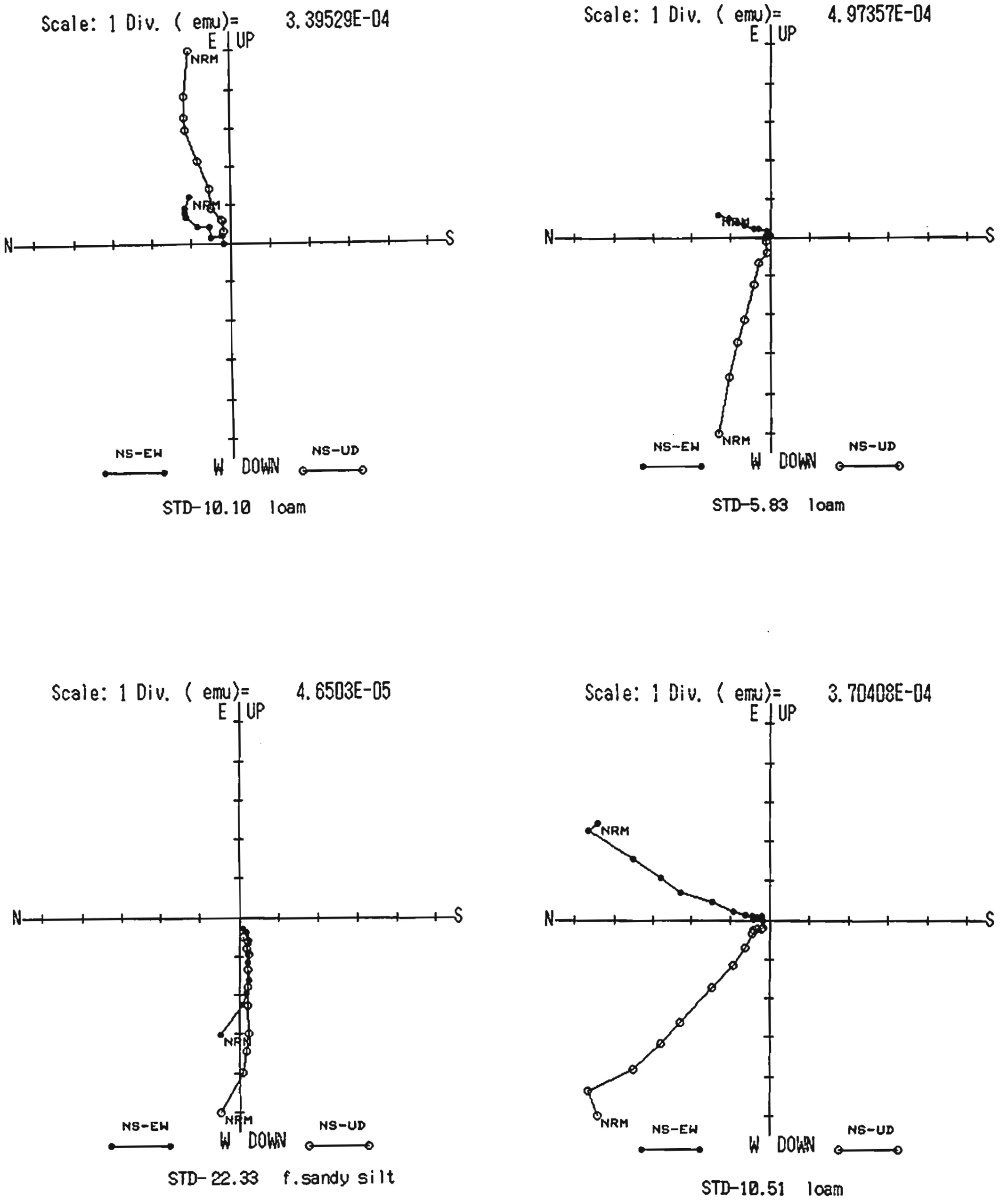

Figure 2: Vector orthogonal plots of progressive alternating field demagnetization analysis.

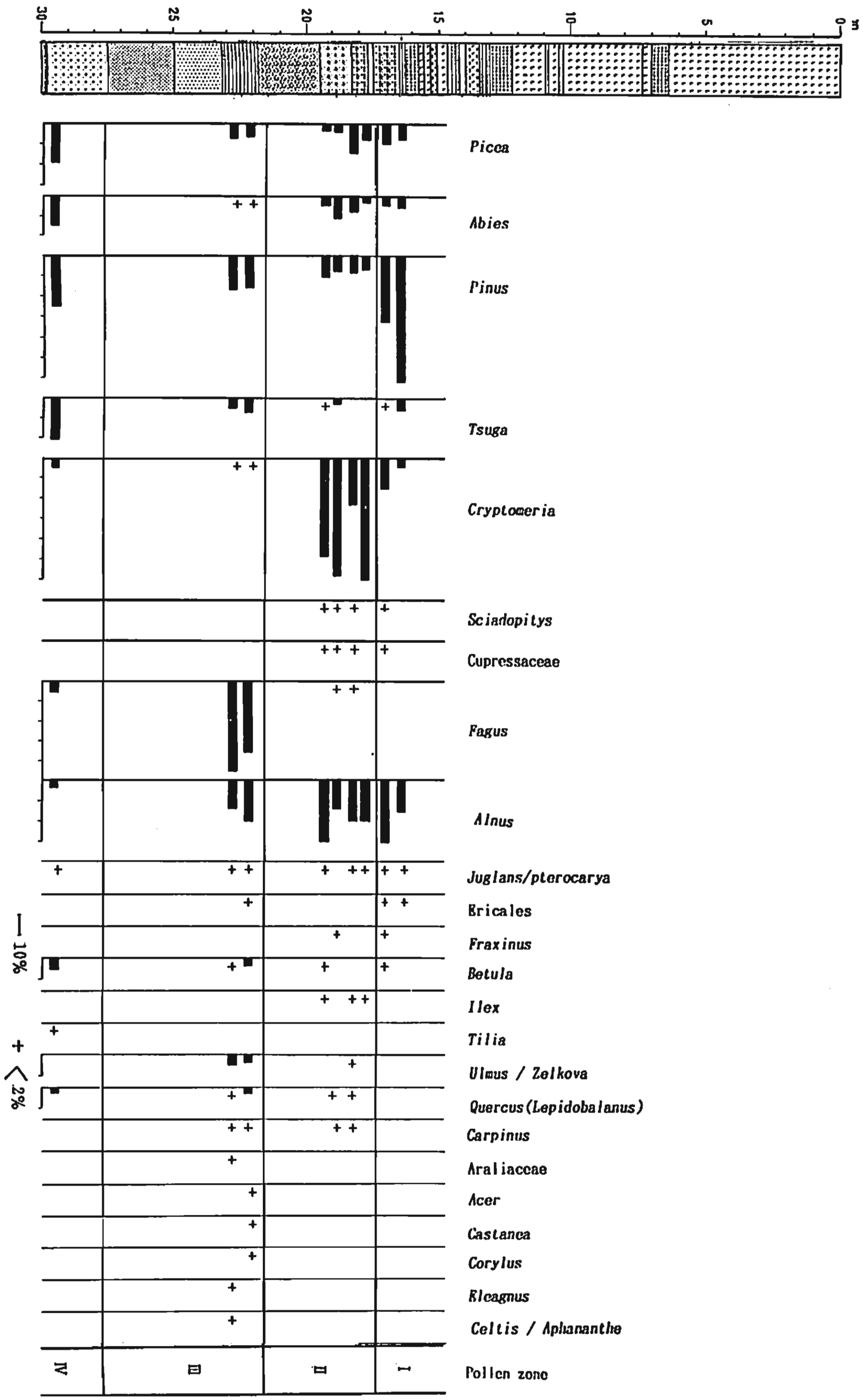

Figure 3: Result of fossil pollen analysis (analyzed by Igarashi).

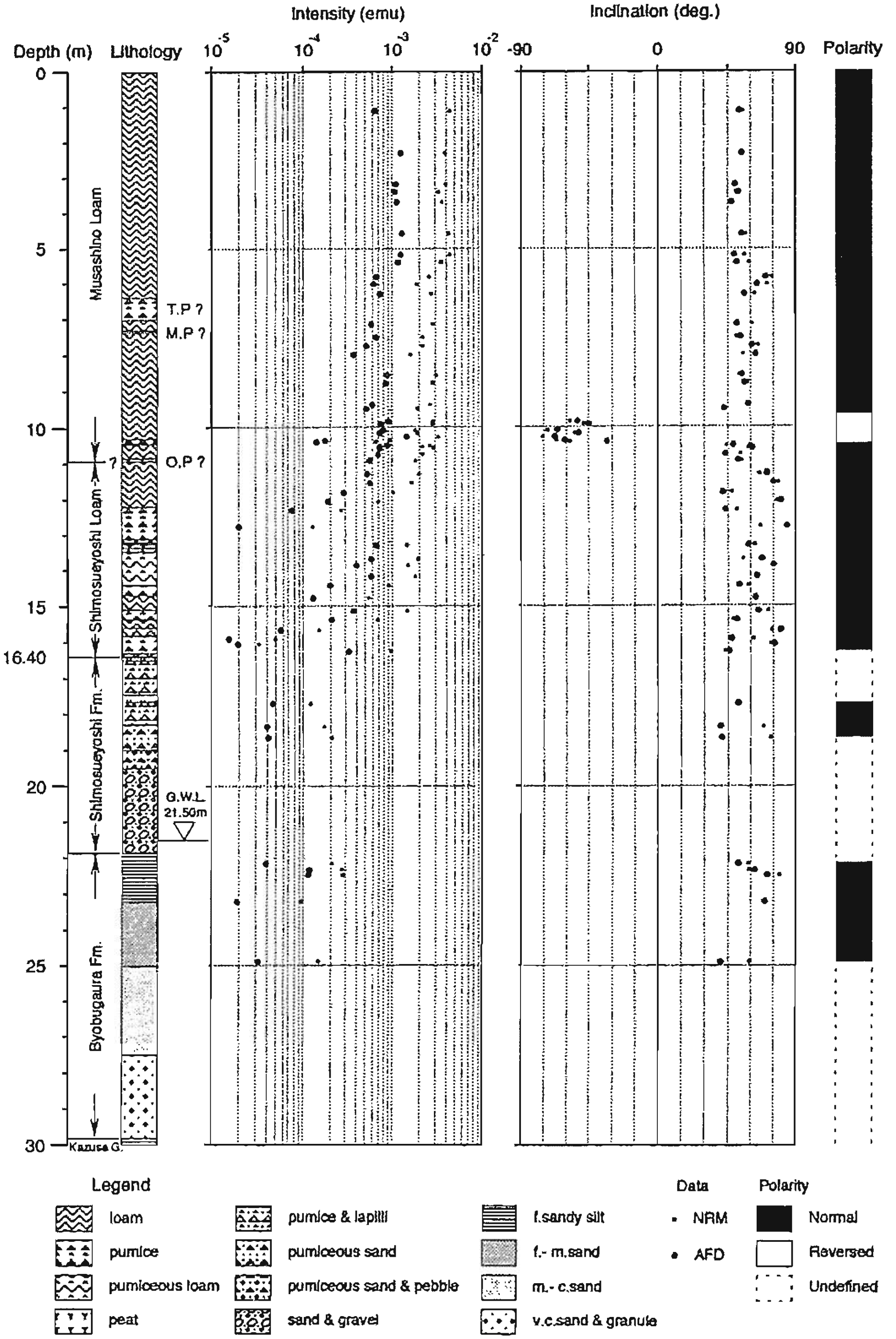

Figure 4: Change of inclination and intensity of remanent magnetization

REGULARITY AND CAUSES OF GEOMAGNETIC REVERSALS

Miho SEKI and Yozo HAMANO
Geophysical Institute, University of Tokyo,
Yayoi 2-11-16, Bunkyoku, Tokyo 113

§ 1 § Introduction

Geomagnetic reversals are generally considered to be a poisson process in which the reversal frequency gradually changes with time (McFadden, 1984). But, if you make histograms of the reversal intervals by taking a narrow range of each histogram column, you see many peaks. These peaks may be spurious but may also indicate that the geomagnetic reversals has a tendency to occur at several particular intervals.

In this paper we attempted to prove with various statistical methods that these peaks in the histogram of reversal intervals really exist and that the geomagnetic reversal sequence is not generated by a simple poisson process.

§ 2 § Data Analysis

2.1) Histogram

In making a histogram, there is always an arbitrariness in how to take the range of each histogram column. If we take the range too wide the peaks will be smoothed out, whereas many spurious peaks appear if we take the range too small compared to the number of data. In addition to that, if we have only a few data as in our case, the reliability of each histogram column will become unequal. The situation is obvious when you have only 20 data samples and want to make a histogram with about 10 columns. It makes a big difference in the reliability if a column has only 1 or 2 data samples.

To get rid of such problems we worked out a new method of making histogram. The following is the steps to create the histogram.

1) Make the accumulation curve of reversal intervals (Fig.1).
2) Divide the data points not by an equal interval range but by an equal number of data points so that the reliability of the height of each column is equal.
3) Take the gradients of a straight line fitted to the accumulation curve within each section as the height of each histogram column, since the growth rate of data number in each section of the accumulation curve represents the number of data points in each histogram column.

In this way we created histograms for several ranges of age using 40 reversal intervals in each histogram (Fig.2). We didn't take equal time span for each histogram for the same reason as in making histograms; the reliability of histogram depends on the data number. For the calculation we used the reversal records (0-164 Ma, 296 reversals) compiled by Cox (1982).

Most of the histograms in Fig.2

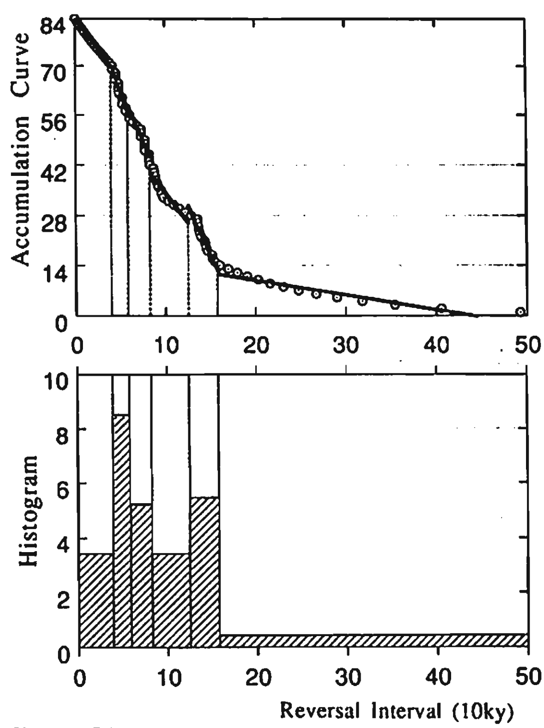

Fig.1 Diagram to show the process of making histogram by the present method. The upper figure is the accumulation curve divided into sections with equal (14) data number. The below is the histogram where the height of each column is obtained from the gradients of the straightline fitted to the accumulation curve in each sections.

Fig.2 Histogram of the polarity length at several age spans.
Each age span contains 40 reversals.

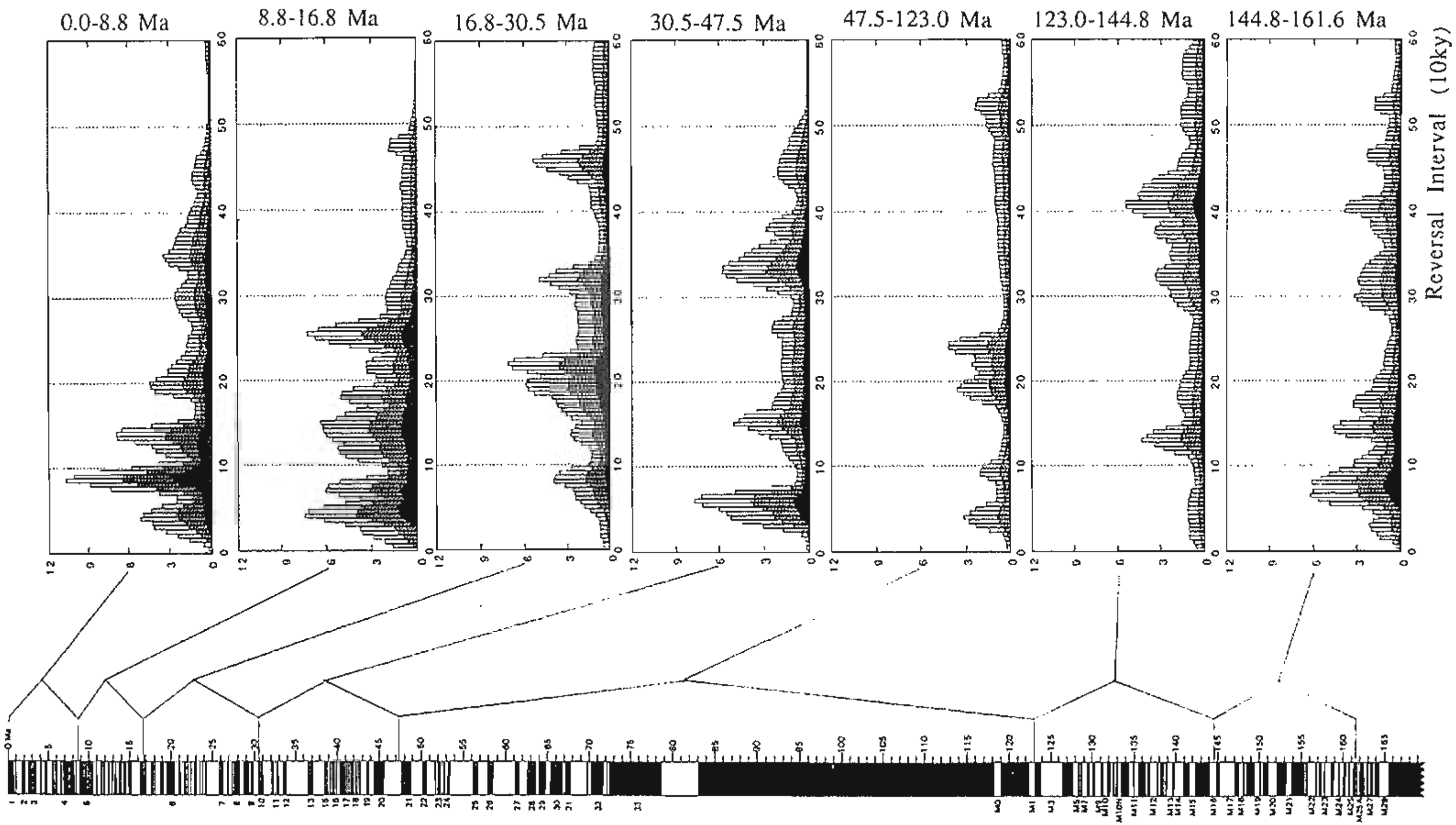

show several peaks, although the height of the peaks differ with age. This suggests that the reversal had a tendency to reverse at such particular intervals whereas a poisson process wouldn't have such a tendency, because in definition, the process has a time-independent constant possibility to reverse. Looking closer we also see that such particular peaks like 0.05, 0.08, 0.13 Ma observed in an age range of 0.0-8.8 Ma appear again in 144.8-161.6 Ma even though they are of completely different age. This also suggests a possibility that the reversal sequence is not a product of a simple poisson process, because a poisson process wouldn't have such a reproducibility.

2.2) Bootstrap Method

We created the histograms of reversal intervals. Now, to know the confidence interval of these peaks we used the bootstrap method (Fisher, 1990). The bootstrap method is a statistical tool to find a point estimate and its confidence interval when only a few data points are available as in the present case.

The geomagnetic reversal sequence is one and only process since the birth of the earth and, further, we can use only 40 reversal intervals for each histogram. (We don't use more because the reversal frequency changes with time, i.e., the statistical characteristics of the reversal sequence is not stable for a larger time span). With these limited data, we can't make use of conventional statistical methods which obtains a point estimate and its confidence interval from averaging a large number of data. Hence, the bootstrap method is really effective in our case. The process of the method can be decomposed into the following several steps.

1) Draw a random sample of same size as the original data set, i.e. 40 reversals, from the data set allowing duplicate samples.

2) Make histogram of the sampled data set with our new method.

3) Keep the height of each histogram column in memory.

4) Repeat stage 1) - 3) n times. It is better to take a large number for n. We took 2000 as " n " because the point estimate and its confidence interval converge within about this limit.

5) Calculate the mean value of each column from the data stored at step 3) to get the averaged histogram.

6) Sort the values in each column into an increasing order and for a $100(1-\alpha)\%$ confidence interval take the $\mathrm{int}(n\alpha)^{th}$ of the sorted values as the lower limit, the $(n-\mathrm{int}(n\alpha)+1)^{th}$ as the upper limit. In the present case we calculated the 95% confidence interval(α=0.05). So, we took the 100^{th} and the 1901^{th} as the lower and upper limit.

This method assumes that the unknown parent distribution of the data set can be approximated by the available few samples. With this concept we draw a random sample from the original data set as in stage 1) and suppose that it is also an independent data set of the unknown parent distribution.

The advantage of this method is that we need only few data to estimate the nature of the unknown parent distribution and that we can get the confidence interval of the estimate without assuming some kind of distribution functions such as the normal distribution.

Considering the 95% confidence interval of each histogram column in Fig.2, we realize that the two neighboring peaks are in most cases statistically distinguishable. This result is favorable for the assumption that these peaks really exists.

2.3) Theoretical histogram of poisson process

As the geomagnetic reversal is generally considered to be a poisson process, we made a histogram of poisson process by using the present method for comparison.

We simulated poisson process with 40 reversals and made the histogram of it. We repeated this operation by a large number of times, 2000 in our case to compare with the histogram of the bootstrapped real reversal data, and averaged each histogram column at the end. The 95% confidence interval of this

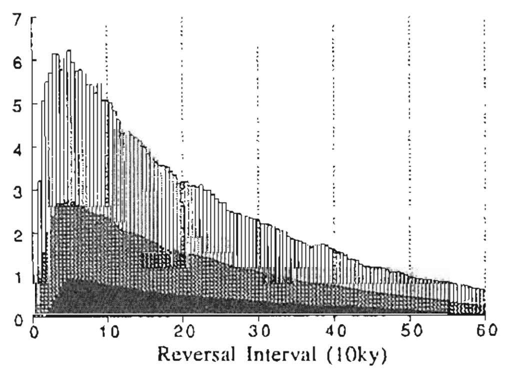

Fig.3 Histogram of the poisson process with a mean reversal frequency of 40 rev. per 10 Ma.

histogram was calculated as in the bootstrap method.

For comparison of the histogram obtained from a poisson process with that of the real reversals, we refer to the histogram of a poisson process having the same reversal frequency as the real process. But, as the histograms of poisson processes don't differ much having different reversal frequency, we present only one of the histograms with a reversal frequency 40 rev. per 10 Ma (Fig.3). We see that the average histogram doesn't have any significant peaks in contrast to the real reversal sequence at any age span.

2.4) Correlation of real reversal and poisson process with theorëtical poisson process histogram

In 2.3) we compared the histograms for the real reversal sequence and poisson processes. But, considering that the former is made by the bootstrap method with only few data available and the latter averaged with 2000 simulated poisson processes, it is not clear whether they can be compared equivalently. When picking out only one poisson process with 40 reversals and making histogram with the bootstrap method, this may also result in a histogram having several peaks. The histogram created in the last section has a gentle slope with no appreciable peak, which may be attributed to the averaging effect. Hence, the real reversal still has a chance to be a product of the poisson process. Therefore, we calculated the correlation coefficient of histograms between real reversal and theoretical poisson process obtained in 2.3) to compare with the correlation coefficient of histograms between each of the 2000 poisson processes simulated in 2.3) and theoretical poisson process.

Again we used the bootstrap method for the real reversals, i.e., we used the histograms obtained in 2.2) stage 2). For poisson processes we used the histograms created in 2.3) each time. The mean correlation coefficient with it's 95% confidence interval is shown for each ranges of age in Fig.4. In comparing the coefficients we used the poisson process having almost the same reversal frequency as the real reversal of each age range.

In Fig.4 we see that the difference between the correlation coefficients from the real reversals and those from the poisson processes is statistically significant, which indicates that it is improbable that the real reversal process is generated from a simple poisson process with 95% confidence level.

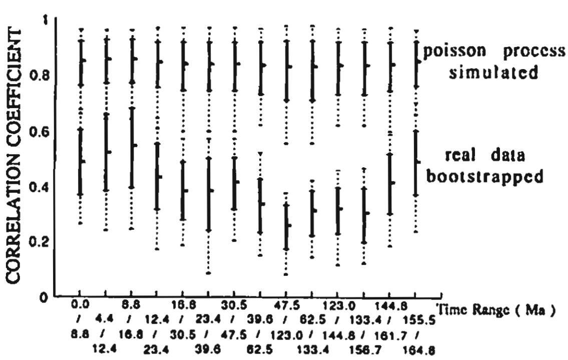

Fig.4 Correlation coefficient between the histograms
•) the real reversal sequence
vs.an averaged poisson process
•) single poisson processes
vs. an averaged poisson process

§ 3 § Discussion

So far we proved that the geomagnetic reversal sequence is not a simple product of poisson process with 95% confidence level. In addition to this, from the peaks in the histogram (Fig.2) it has a tendency to reverse at several special intervals like 0.05, 0.08, 0.13 Ma in 0.0-8.8 Ma age period, which is also apparent in 144.8-161.6 Ma, when the reversal frequency is almost the same.

Reversal process can be either of internal or external origin. But, the above regularity indicates that it may be of external origin triggering the reversals with some regularity. Of course, reversal process of internal origin cannot be excluded. But no observation of the earth's core having the variation with these time scales is available and it seems also inappropriate to explain the large temporal variation of reversal frequency with only one system in the core. Hence, we think of an external trigger which caused the geomagnetic reversals. As a new model of external origin, we assume that the fluctuation of the earth's rotation speed triggers the geomagnetic reversals. It is not inappropriate to assume that the rotational speed varies with a time scale of 0.01-0.10 Ma, because the sea-level change, which causes the change of the earth's moment of inertia, have such periods.

Although the variation of the rotational speed for this period is not directly available, the see level change resulting from the variation of glaciers can be observed from the $\delta^{18}O$ variation (Imbrie, 1982). As this $\delta^{18}O$ variation is explained by the so-called " Milankovitch cycles ", astronomical calculations can extend the variation to the past.

The variation of the earth's inertial moment, inferred from the $\delta^{18}O$ curve, is related with the fluctuation of the earth's rotation speed when no external force are exerted. Based on this assumption, we differentiate the $\delta^{18}O$ curve to get the curve of the earth's rotational speed variation and take the absolute value to represent its fluctuation. We assume that the fluctuation of the rotation speed disturb the geomagnetic field and increases the possibility of the reversals. We also suppose that the acceleration and slowdown of the earth's rotation both disturb the fluid flow in the outer core and, hence the earth's magnetic field.

Supposing that the variation curve obtained in this way represents the time variation of the reversal probability, we simulated the reversals and made histograms (Fig.5). It can be observed that the histogram obtained from the present model simulation of the reversals processes designates similar characteristic as the real reversals, in which several peaks are clearly observed having similar peaks.

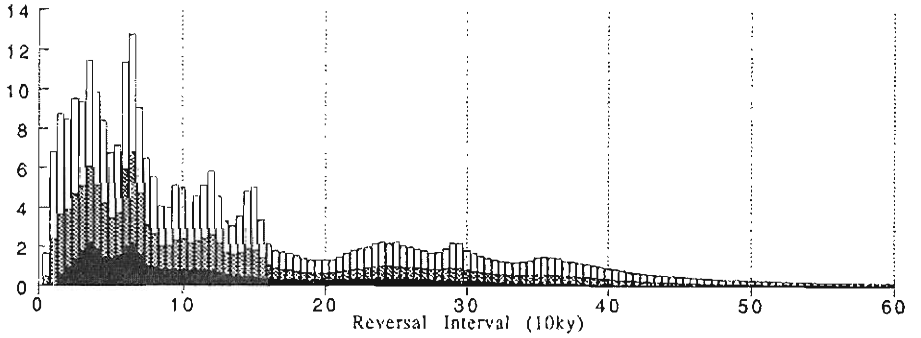

Fig.5 Histogram of the simulated reversal based on the present model with reversal frequency of 50 rev. per 10 Ma.

§ 6 § Summary

We created histograms of the geomagnetic reversal sequence with a fairly objective way and confirmed that the histograms show several peaks at any age span. Using the bootstrap method we estimated the 95% confidence interval of these peaks. Comparing these histograms with a theoretical histogram of poisson process obtained by simulating the poisson process many times, we conclude that the peaks are statistically significant. Calculation and comparison of the correlation coefficient of the real reversals and each poisson process with theoretical histogram of poisson process also confirm that the real reversal sequence can hardly be generated by a single poisson process with 95% confidence level.

Finally we simulated the geomagnetic reversing process by a model, in which the fluctuation of the earth's rotation speed triggers the reversals and proved that well-regulated external trigger can generate reversals having similar characteristics as the geomagnetic reversal. The result of the simulation designate several peaks in the histograms observed in that of the geomagnetic reversal sequence.

References

Cox, A.V. (1982) in " A geologic time scale "
Eds. Harland et al., Cambridge Univ. Press, London, 63-84
Fisher, N.I. and P. Hall (1990) Geophys. J. Int., 101, 305-313
Imbrie, J. et al. (1982) in " Milankovitch and Climate "
Eds. A.L. Berger et al., D. Reidel Publishing Company, Part 1, 269-305
McFadden, P.L. (1984) J. Geophys. Res., 89, 3363-3372

ARCHEOMAGNETIC DATA IN TOHOKU AREA

Tadashi NISHITANI

Institute of Applied Earth Sciences, Mining College,
Akita University, Akita 010, Japan

Archeomagnetic data were collected intensively in the south western Japan and age estimation is possible using those data of inclination and declination (Hirooka, 1971, Maenaka, 1990). However few archeomagnetic data were reported in Tohoku area in Japan. In order to estimate precise age of a remain or a kiln site in Tohoku area a large number of archeomagnetic data are necessary. The main object of this report is to show a set of archeomagnetic data, inclination and declination, in Tohoku area.

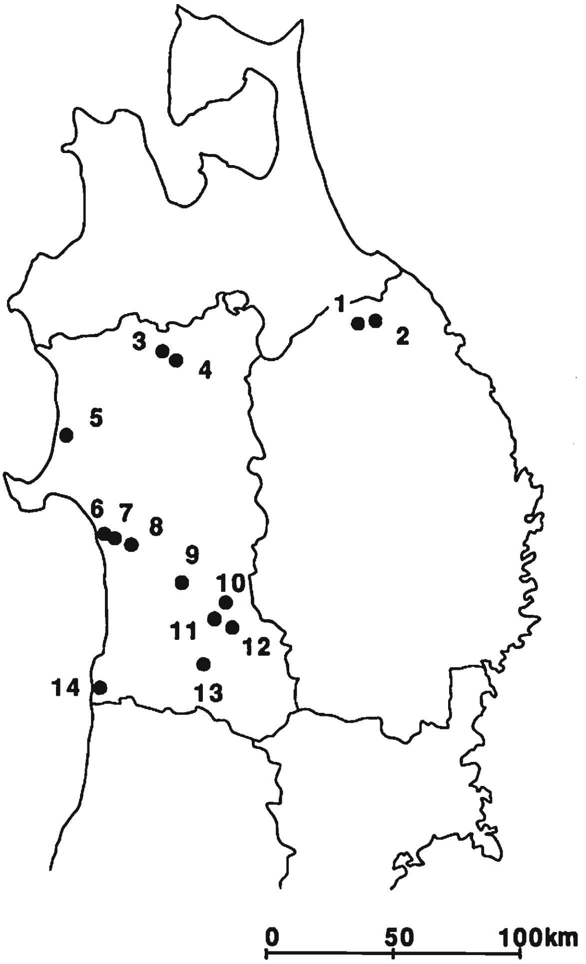

Fig.1 Location map of sampling sites. Each site is represented by a number.

1. Tamagawa tetsuzan A and B kiln sites,
2. Aosawa kiln site,
3. Oodateno remains,
4. Suwadai-C remains,
5. Kamokodai remains,
6. Akita-Jyo remains,
7. Sakanoue-F remains,
8. Shimozutsumi-C remains,
9. Hiyamagoshi kiln site,
10. Goshidate kiln site,
11. Takewara remains,
12. Tomigasawa A, B and C kiln sites, Tomigasawa-A remains, and Takuboshita remains,
13. Nanakubo remains,
14. Kamikumanosawa remains.

About 1,300 samples were collected from sixty seven kiln sites or baked earth in Tohoku area and archeomagnetic investigation was performed. Figure 1 shows the location map of sampling sites. Archeological age distributes from 15,000 B.C. to Edo period (1868 A.D).

After alternating field demagnetization mean inclinations and declinations were calculated. Table 1 shows the results of archeomagnetic investigation and their archeological ages in Tohoku area. In this table the declination angle refers to the magnetic north in Akita city. In the present stage it is difficult to create a new variation curve of geomagnetic field direction as a function of age in Tohoku area.

Results obtained from this work offer the basic data for the reference curve of geomagnetic field vector in Tohoku area and a correct reference curve will be provided in the future.

References

Hirooka, K.(1971) *Mem. Fac. Sci. Kyoto Univ. Ser. Geol. Mineral.*, **38**, 167.

Maenaka, K.(1990) *Rock Mag. Paleogeophys.*, **17**, 21.

Table 1 Results of archeomagnetic investigations and their archeological ages.

Site	No. of samples	Dec.	Inc.	k	α_{95}	archeological age
Kamokodai remains						
SN81	26	-0.948	58.62	140.80	2.40	about 15000 B.C.
Kamikumanosawa remains						
SN-20	7	14.58	67.77	188.27	4.41	last part of the Middle Jyomon period (about 4000 B.C.)
SN-15	8	29.27	41.46	5.78	25.22	about 4000 B.C.
SI-14	10	17.22	56.88	116.34	4.50	about 4000 B.C.
SI-18	7	0.53	55.47	104.89	5.92	about 4000 B.C.
SI-03	4	-3.77	62.45	270.06	5.60	about 4000 B.C.
SI-40	2	6.90	49.80	14.90	70.11	about 4000 B.C.
SI-12	9	10.89	56.68	128.34	4.56	about 4000 B.C.
SI-01	15	-6.46	42.44	191.69	2.77	last part of the Last Jyomon period to Yayoi period (about 2300 B.C)
Suwadai-C remains						
SZ-75	4	32.94	21.96	10.63	29.55	Last Jyomon period
SZ-48	5	40.06	54.53	112.90	7.23	Last Jyomon period
SI-76	4	16.03	31.67	11.57	28.22	last part of the Last Jyomon period
SI-61-1	6	-10.76	-27.58	2.20	60.00	early Yayoi period

Table 1 (continued)

Site	No. of samples	Dec.	Inc.	k	α_{95}	archeological age
SI-61-2	3	-60.81	43.03	1.36	-	early Yayoi period
SI-60-1	4	-6.60	35.93	117.97	8.49	early Yayoi period
SI-60-2	4	-15.87	32.24	10.06	30.48	early Yayoi period
SI-34	3	-6.74	52.87	51.41	17.37	early Yayoi period
SI-28	3	17.85	46.83	8.64	44.91	early Yayoi period
SI-18	2	13.24	43.24	257.25	15.64	Heian (about 10th c.)
Sakanoue-F remains						
SI-07-1	40	61.90	67.26	1.54	30.50	Yayoi period
SI-07-2	20	22.69	15.89	3.43	20.82	Yayoi period
Oodateno remains						
SI-15	7	-12.36	54.16	147.85	4.98	Heian
SI-06	19	5.68	49.21	105.93	3.27	Heian
SI-14	4	2.89	52.12	373.14	4.76	Heian
SI-15'	5	5.50	60.50	54.11	10.49	Heian
SI-04	14	3.95	54.40	213.75	2.72	Heian
SI-04'	5	12.63	51.52	21.04	17.06	Heian
SI-03	6	6.25	50.37	260.06	4.16	Heian
SI-01	7	1.03	55.41	24.52	12.43	Heian
SI-13	3	30.22	54.00	24.30	25.56	Heian
SI-07	6	21.11	53.26	92.35	7.00	Heian
SI-08	7	11.71	50.31	292.17	3.53	Heian
SI-05	10	12.81	53.04	57.22	6.44	Heian
SI-17	3	-16.25	49.86	65.12	15.40	Heian
Akita-Jyo remains						
SI1020	15	2.49	50.79	73.89	4.48	Heian (last part of 9th c.)
SI1022	5	0.93	54.27	256.63	4.79	Heian (last part of 9th c.)
SI1007	2	10.83	56.83	875.55	8.45	Heian (last part of 9th c.)
SI1014	10	-	-	-	-	Heian (last part of 9th c.)
Shimozutsumi-C remains						
SI-28	9	-7.06	49.54	347.37	2.77	Heian
ST-01	3	18.02	74.35	7.08	50.27	Heian
SI-15	4	-1.21	42.29	8.36	33.80	Heian
SI-10	9	-7.51	50.97	140.81	4.35	Heian
SI-12	5	-2.27	49.45	238.24	4.97	Heian
SI-13	5	-22.63	49.34	36.02	12.92	Heian

Table 1 (continued)

Site	No. of samples	Dec.	Inc.	k	α_{95}	archeological age
Goshidate kiln site						
kiln site	11	-0.84	49.86	228.07	3.03	Heian
Takewara remains						
SJ-20	10	25.97	30.27	15.32	12.75	Heian (middle 8th – last 9th c.)
Tomigasawa-A remains						
Hira gama (SK02)	21	-0.17	57.47	197.90	2.27	Heian (9th c.– 10th c.)
Hearth (SI01)	23	-2.01	57.29	142.50	2.54	Heian (9th c.– 10th c.)
Tomigasawa-A kiln site						
Sueki gama (SJ01)	56	-8.48	53.90	154.00	1.54	Heian (early 9th c.)
Hira gama (SJ04)	25	-3.41	55.62	171.48	2.22	Heian (early 9th c.)
Tomigasawa-B kiln site						
Sueki gama (SJ101)	63	-2.89	54.32	197.98	1.27	Heian (early 9th c.)
Tomigasawa-C kiln site						
Sueki gama (SJ201)	26	-4.87	54.88	72.03	3.36	Heian (early 9th c.)
Takuboshita remains						
Sueki gama (SJ301)	41	-4.28	61.25	160.08	1.77	Heian (early 9th c.)
Sueki gama (SJ302)	22	-11.20	67.21	78.79	3.51	Heian (early 9th c.)
Sueki gama (SJ303)	28	-2.85	57.64	158.36	2.17	Heian (early 9th c.)
Hearth (SI305)	14	-2.12	53.86	197.88	2.83	Heian (early 9th c.)
Hira gama (SJ327)	23	-3.84	49.44	342.13	1.64	Heian (early 9th c.)
Hearth (SI338)	27	-2.48	55.26	208.57	1.93	Heian (early 9th c.)
Nanakubo remains						
Hajiki gama (SJ01)	10	-2.33	51.89	145.06	4.02	Heian (last 10th c.)
Sueki gama (SJ02)	46	3.36	55.42	213.38	1.44	Heian (last 9th - early 10th c.)
Sueki gama (SJ03)	36	-8.67	54.00	456.33	1.12	Heian (last 9th - early 10th c.)
Hiyamagoshi kiln site						
Nobori gama	30	13.36	58.67	66.85	3.24	Kamakura (early 13th c.)
Tamagawa tetsuzan-A kiln site						
TG-03	5	8.46	47.69	152.63	6.21	Edo period
TG-02	5	14.18	48.64	115.55	7.28	Edo period
Tamagawa tetsuzan-B kiln site						
TG-01	8	3.84	52.63	92.10	4.04	Edo period
Aosawa kiln site						
AS-01	9	7.37	51.87	52.78	7.15	Edo period
AS-02	7	9.86	56.00	141.62	5.09	Edo period

TIME-AVERAGED PALEOMAGNETIC FIELD FROM SEDIMENT CORES IN THE CENTRAL EQUATORIAL PACIFIC

Toshitsugu YAMAZAKI

Geological Survey of Japan, Higashi, Tsukuba, Ibaraki 305, Japan

Introduction

It is well known that the first order description of the time-averaged geomagnetic field is the geocentric axial dipole field (represented by the Gauss coefficient g_1^0 in the spherical harmonic analysis). However, the evidences for existence of small, but important, second-order terms, in particular an axial quadrupole (g_2^0) component, have been accumulated (Wilson and Ade-Hall, 1970; Merrill and McElhinny, 1977, 1983; Coupland and Van der Voo, 1980; Livermore et al., 1983). Recently Schneider and Kent (1988, 1990) examined Pliocene and Pleistocene paleomagnetic data of deep-sea sediment cores from the world oceans, and concluded that long-term non-dipole components are dominantly axially symmetric and that the amplitude of the axial quadrupole (g_2^0) varies with polarity (g_2^0/g_1^0=0.026 for normal; 0.046 for reverse) but not for the axial octupole (g_3^0) (g_3^0/g_1^0=-0.029 for normal; -0.021 for reverse).

It is useful to express deviations of the direction of paleomagnetic field from that of the geocentric axial dipole field as inclination anomalies (Cox, 1975). The inclination anomaly (ΔI) is defined as the difference between observed inclination (Io) and the expected inclination from the geocentric axial dipole field for a site latitude (θ):

$$\Delta I = Io - \tan^{-1}(2\tan\theta)$$

The sign of the reversed polarity (both observed and dipole inclinations) are inverted to give normal polarity equivalents. Schneider and Kent (1988) showed that at equatorial latitudes the average inclination anomaly during the Brunhes chron is -2.37°±0.50°, and that of the Matuyama chron (except for periods of normal polarity subchrons such as the Jaramillo) is -4.30°±0.71°.

A paleomagnetic study was performed on sediment cores collected at closely spaced 20 sites (Table 1) in the central equatorial Pacific (GH82-4 area). The cores were composed mainly of siliceous clay or siliceous ooze. Here I will interpret the paleomagnetic data on the viewpoints of the time-averaged magnetic field.

Paleomagnetic measurements

Cores were split into halves on board soon after the recovery, and samples for paleomagnetic measurements were taken continuously with plastic cubic cases of about 7 cm^3 each. Measurements of the remanent magnetization were done after the cruise in 1982 using an SCT's cryogenic magnetometer. Several pilot samples were chosen from each core, and stepwise alternating-field (AF) demagnetization experiments were carried out to investigate the stability of the remanent magnetization. It is revealed that most samples have been little affected by secondary magnetizations (Fig. 1). Based on the results of the progressive AF demagnetization experiments, the peak field of the routine AF demagnetization was chosen, and the rest of the samples were demagnetized by that field.

The direction and intensity of the remanent magnetization after the AF demagnetization and interpretation of the polarity of Core P343 are shown in Fig. 2 for an example. Because the cores were not oriented horizontally, the declination is relative. Although sampling sites are close to the equator, the polarity of the remanent magnetization could be recognized from inclinations. The inclination expected for these sites (less than 2° in latitude) from the hypothetical geocentric axial dipole field is shallower than ±4°. However, observed inclinations were usually several degrees deeper than the prediction (Fig. 2), as discussed later.

Table 1 Positions of cores from GH82-4 area and inclination anomalies during the Brunhes and Matuyama chrons.

Core	Latitude (S)	Longitude (W)	Depth (m)	Brunhes (N)				Matuyama (R)			
				n	*Io*	*ΔI*	σ	n	*Io*	*ΔI*	σ
P336	0°53.63'	166°25.77'	5434								
P337	1°32.97'	167°36.36'	5667	63	-6.3	-3.2	5.8	26	-12.4	-9.3	6.8
P338	1°47.70'	168°03.61'	5537	7	-12.3	-8.7	5.2				
P339	1°40.52'	166°44.32'	5403								
P340	1°52.67'	166°53.31'	5687	82	-1.8	2.0	5.7	32	-9.2	-5.4	6.3
P341	1°00.05'	166°24.68'	5377	30	-10.5	-8.5	5.9	9	-3.7	-1.7	8.8
P342	0°49.18'	166°08.68'	5174	15	-10.9	-9.3	5.2	32	-4.7	-3.1	3.9
P343	1°54.65'	167°27.55'	5791	97	-12.9	-9.1	5.7	18	-9.2	-5.4	4.9
P344	1°43.48'	167°21.77'	5791	75	-5.3	-1.9	5.8	32	-1.8	1.6	5.9
P345	1°22.65'	166°56.40'	5648	33	-10.8	-8.0	13.6				
P346	1°11.87'	166°55.25'	5323	39	-5.1	-2.7	7.0	18	-5.7	-3.3	9.6
P347	1°14.37'	166°37.33'	5169	31	-3.3	-0.8	7.3	12	-8.8	-6.3	6.4
P348	1°10.83'	166°41.65'	5292								
P349	1°03.94'	166°23.94'	5309	26	-7.5	-5.4	11.0	12	-13.8	-11.7	10.2
P350	0°45.17'	166°04.76'	5219	49	-4.9	-3.4	5.0				
P351	1°10.01'	166°05.35'	5382								
P352	0°59.05'	166°04.70'	5517	37	-6.3	-4.3	4.0	31	-5.6	-3.6	3.6
P353	0°49.07'	166°14.03'	5249	21	-8.3	-6.7	4.4	32	-2.1	-0.5	4.6
P354	1°06.33'	166°08.23'	5353	14	-11.4	-9.2	5.3	39	-6.6	-4.4	4.1
P355	0°50.34'	166°09.43'	5164	13	-6.8	-5.1	7.0	43	1.5	3.2	6.3

n : number of samples.
Io : average observed inclination (the sign of the reversed polarity was inverted).
ΔI : inclination anomaly.
σ : standard deviation of the observed inclination.

Magnetostratigraphy revealed that some cores have continuous sedimentation, and the ages of the bottom of the cores are 1 to 3.5 Ma. The average sedimentation rate of these cores during the Quaternary ranges from 2 to 9 m/m.y. Other cores have hiatuses of various durations. Hiatus formation seems to have been intensified in the early Pleistocene.

Time-averaged magnetic field

The average inclination anomalies within the Brunhes and Matuyama chrons were calculated for each core (Table 1). The data within polarity transitions and periods of normal polarity in the Matuyama chron (the Jaramillo and Olduvai subchrons) are excluded. The mean inclination anomaly during the Brunhes chron obtained from 16 cores is -5.3° (±3.4°; 1σ), and that for the

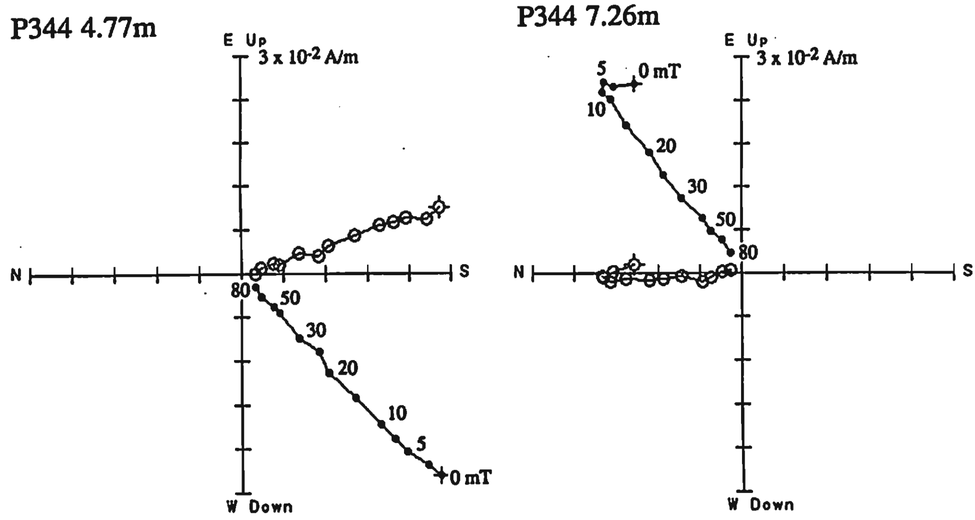

Fig. 1 Orthogonal plots of progressive alternating-field demagnetization data. Solid and open circles represent projections of vector endpoints on the horizontal and vertical plane, respectively. Horizontal components are relative.

Matuyama chron is -3.8° (±4.1°) for 13 cores. It is estimated that the Brunhes chron was sampled evenly because most cores used are reached to the Brunhes/Matuyama boundary, but the the data of the Matuyama chron were biased toward the later part of the period. Here simple arithmetic averages were employed. The simple averaging of inclination-only data causes a systematic bias toward shallower inclination compared with the estimation based on more sophisticated methods such as a maximum likelihood technique of McFadden and Reid (1982). However, the bias is negligibly small, an order of 0.1°, in the equatorial latitudes. Non-vertical penetration of a corer, which is usually within a few degrees (Seyb et al., 1977), may have occurred, and this probably caused the scatter of the mean inclination anomalies among cores.

Correction for the movement of the Pacific plate was not applied. Based on the model AM1-2 of Minster and Jordan (1978), the effect of the plate motion to the inclination anomalies is about 0.5° for the age of 1 Ma. It is thus considered that the inclination anomalies in Table VII-1 are a little (~0.2°) overestimated for the Brunhes chron, and a little (~0.5°) underestimated for the Matuyama chron.

As a result the inclination anomalies recorded in the sediment cores from the GH82-4 area agree with the analysis by Schneider and Kent (1988). Although included in the range of the error, the mean inclination anomaly of the Brunhes chron in the GH82-4 area may be a little larger than that of the global analysis. This suggest a possible contribution of non-zonal components, but more data are needed to test this possibility.

References

Coupland, D.H. and R. Van der Voo (1980) *J. Geophys. Res.*, 85, 3529.
Cox, A (1975) *Rev. Geophys. Space Phys.*, 13, 35.
Livermore, R.A., F.J. Vine, and A.G. Smith (1983) *Geophys. J. R. astr. Soc.*, 73, 153.
McFadden, P.L. and A.B. Reid (1982) *Geophys. J. R. astr. Soc.*, 69, 307.
Merrill, R.T. and M.W. McElhinny (1977) *Rev. Geophys. Space Phys.*, 15, 309.
Merrill, R.T. and M.W. McElhinny (1983) The earth's magnetic field. (Academic Press, London), 401.
Minster, J.B. and T.H. Jordan (1978) *J. Geophys. Res.*, 83, 5331.
Schneider, D.A. and D.V. Kent (1988) *Science*, 242, 252.
Schneider, D.A. and D.V. Kent (1990) *Rev. Geophys.*, 28, 71.

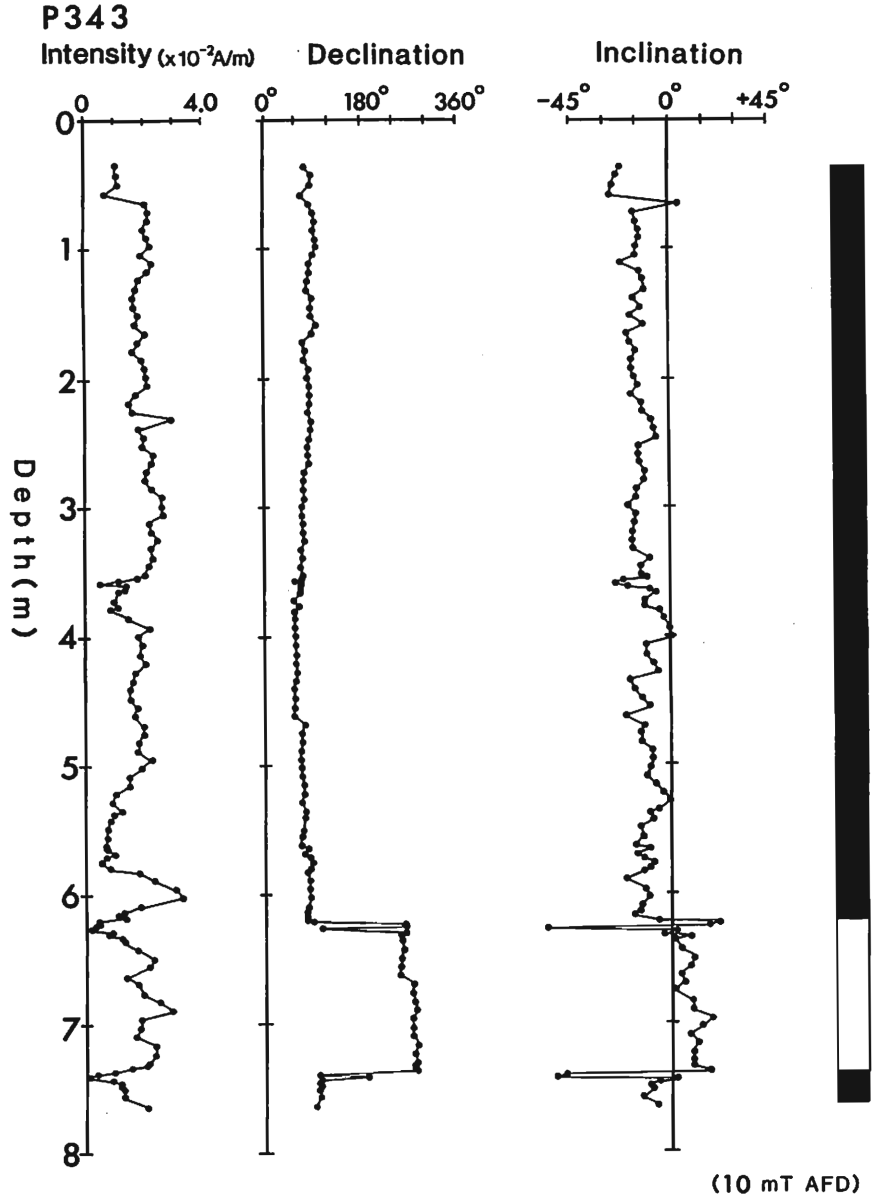

Fig. 2 Remanent magnetization of Core P343 after partial alternating-field demagnetization of 10mT. Declination is relative. Interpretation of magnetic polarity is shown on right column (solid represents normal, open reverse).

Seyb, S.M., S.R. Hammond, and T. Gilliard (1977) *Deep-Sea Res.*, 24, 943.
Wilson, R.L. and J.M. Ade-Hall (1970) *In* Runcorn, S.K. (ed.), Palaeogrophysics, (Academic Press, London), 307.

(In press in Cruise Rept. Geol. Surv. Japan No.22)

GEOMAGNETIC PALEOSECULAR VARIATION IN EASTER ISLAND, THE SOUTHEAST PACIFIC

Masako MIKI*1, Satoru YAMAGUCHI*2, Jun-ichi MATSUDA*3, Keisuke NAGAO**, Hiroo INOKUCHI*, Nobuhiro ISEZAKI*4 and Katsumi Yaskawa*

* Faculty of Science, Kobe University, Kobe 657, Japan
**Institute for study of the Earth's Interior, Okayama University, Tottori 682-02, Japan.

The geomagnetic secular variation in the Pacific is characterized by the anomalously low value of the angular dispersion for the last few million years. This phenomenon is believed to be due to the Pacific dipole window (e.q. Doell and Cox, 1971; McWilliams et al., 1982). The low value was observed from the paleomagnetic data of Hawaii and other small islands in the central Pacific. Easter Island is in the southeast pacific. We made a paleomagnetic and geochronological study in Easter Island in an attempt to determine the southeastward distribution of the Pacific dipole window.

Easter island (27.1°S, 109.2°W) is a part of the seamount chain generated by a hot spot during the last 10 m.y. in the Nazca plate (Herron, 1972). The island consists of three volcanoes; Poike, Rano Kau and Terevaka. We corrected more than 250 samples from 45 sites of lava flows of the three volcanoes.

K-Ar whole rock dating was attempted on thirteen sites. The reliable age data were obtained from six sites on RanoKau volcano. They distribute between 0.1 Ma and 0.7 Ma. The upper limits of the ages were obtained from seven sites on Terevaka and Poike volcano. The ages are less than 0.3 Ma. The potassium rates in these lavas are too small to determine the absolute ages.

More than two cylindric specimens of 2.5 cm high and 2.5 cm diameter were obtained from each block sample. Natural remanent magnetization (NRMs) were measured using a spinner magnetometer. The stability of the magnetization was examined through progressive demagnetization experiments of both alternative field and thermal techniques. The principal component analysis of Kirschvink (1980) was used to calculate the best -fit demagnetization lines for linear demagnetization trajectories.

Present addresses
1. Faculty of Science, Kyoto University, Kyoto 606, Japan.
2. College of Liberal Arts, Kobe University, Kobe 657, Japan.
3. Faculty of Science, Osaka University, Osaka 560, Japan.
4. Faculty of Science, Chiba University, Chiba 260, Japan.

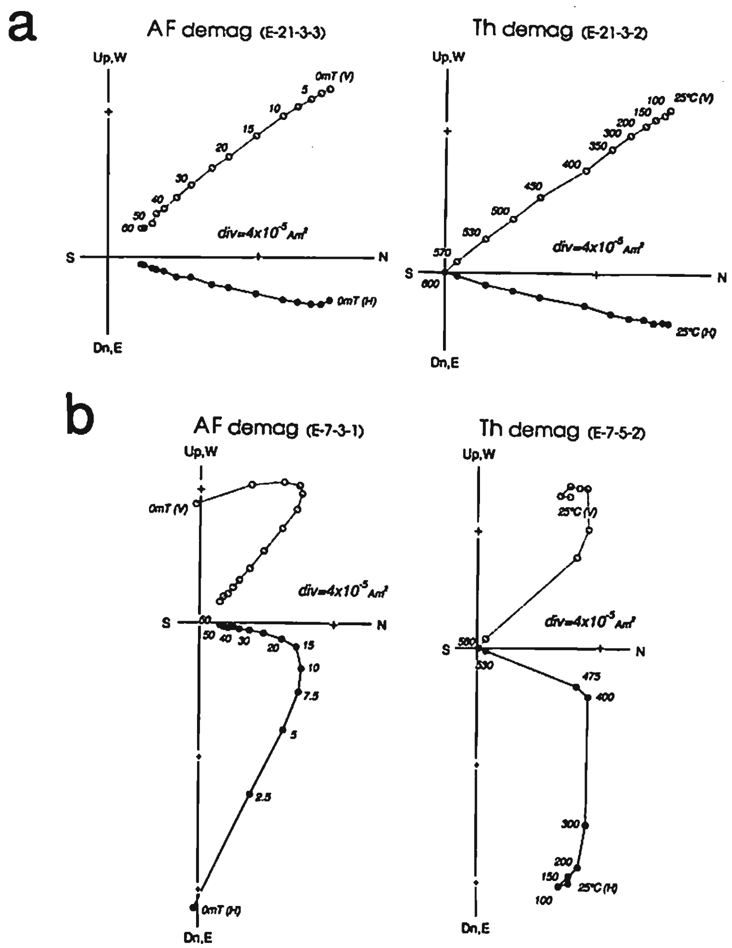

Fig.1. Examples for vector plots of progressive Thermal and AF demagnetization. Open (Solid) Circles are on the vertical (horizontal) plane. a:Single component type. b:Two component type.

The stable magnetic component was obtained from almost all samples. The component is identified as a linear segment toward the origin on both alternating field and thermal demagnetization paths.
More than half of the samples have unicomponent magnetization. Unblocking temperature of the component is about 600°C, indicating the magnetic charier of titanium poor magnetite. The directions of stable magnetic component in individual samples were determined using more than four points on the alternative field demagnetization path.

Reliable paleomagnetic directions were obtained from 8 sites of Poike, 6 sites of RanoKau and 20 sites of Terevaka volcanoes. All of the directions have normal polarity. There is no significant difference among the paleomagnetic directions of three volcanoes. The mean direction of all 34 sites is D=0.2° and I=-44.0° with the radius of the 95 % confidence circle of 3.6°.

The activities of the three volcanoes on Easter Island appears to have occurred during Brunhes polarity chron because of the young K-Ar ages and the normal polarity of paleomagnetic directions.

The time span of the samples is probably long enough to discuss the geomagnetic secular variation. RanoKau volcano appears to have formed during last 0.7 m.y. according to the obtained K-Ar ages. Although our data dose not indicate the time span of the Terevaka and Poike volcanoes, we estimate it to be a few times of 10^{-5} years from the geological view points.

The VGP position was calculated from the paleomagnetic direction of each site. The mean VGP position is 89.2°N and 239.1°E with a 95 % confidence value of 3.8°. The geographical pole is contained within the 95 % confidence limit circle.

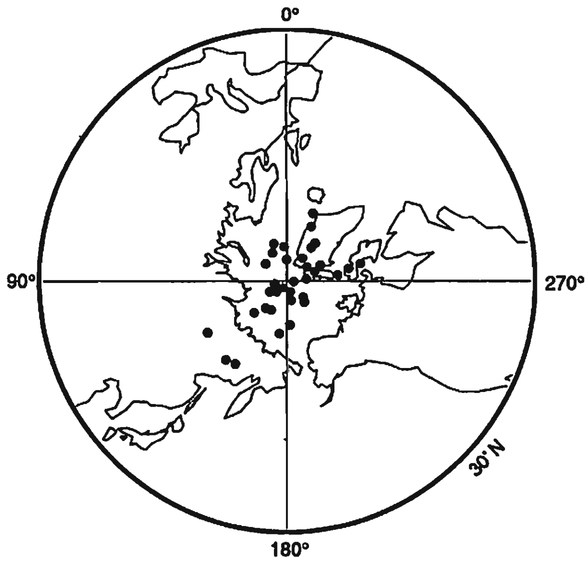

Fig.2. VGP positions for Easter Island lava flows. The stereographic projection.

The angular dispersion value of Easter Island was calculated from the VGPs for 34 sites after McElhinny and Merrill (1975). The value is 11.8° with an upper limit of 14.1° and a lower limit of 9.8°.

The calculated value in this study is fairly lower than the value in preliminary study (Miki et al., 1988). The large value in the preliminary results is probably due to the insufficient treatment of the demagnetization path. The characteristic magnetic component in each specimen was determined by a blanket demagnetization at a single step without any line fitting method.

The angular dispersion value in Easter Island is significantly lower than the values predicted by the theoretical secular variation models; e.g., Model C (Cox,1962), Model D (Cox, 1970) and Model F (Mcfadden and McElhinny, 1984). This is probably due to the anomalously low secular variation in Easter Island. The pacific dipole window appears to exist also in the southeast Pacific.

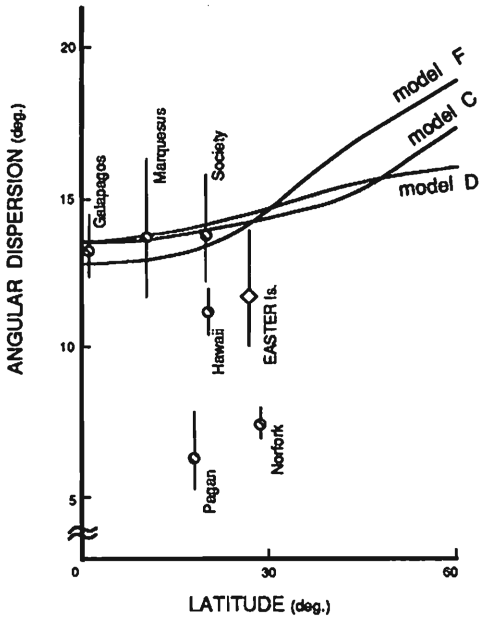

Fig.3. VGP angular dispersion in the Pacific and the models of angular dispersion vs. latitude: Garapagos (doell and Cox, 1972), Hiva-Oa (katao et al., 1988), Society (Duncan, 1975), Pagan (U.S.-Japan P.C.P.M., 1975), Hawaii (McWilliams et al., 1982), Model C (Cox, 1962), Model D (Cox, 1970), Model F (McFadden and McElhinny, 1984). The square indicates the angular dispersion value for Easter Island in this study.

References

Cox, A. (1962) J.Geomag. Geoelectr., 13, 101.

Cox, A. (1970) Geophys. J. R. Astr. Soc., 20, 253.

Doell, R.R. and A. Cox (1971), Science, 171, 248.

Doell, R.R. and A. Cox (1972), In: The Nature of the Solid Earth (eds E.C. Robertson, McGraw-Hill, NewYork), 245.

Duncan, R.A. (1975) Geophys. J.R.Astr. Soc., 41,245.

Herron, E.A. (1972) Geol. Soc.Amer. Bull., 83, 1671.

Katao, H., et al.(1988), J.Geomag. Geoerectr., 40,703.

Kirschvink, J.L.(1980), Geophys. J.R.Astr.Soc., 62,699.

McElhinny, M.W. and R.T.Merrill(1975) Rev. Geophys.Space Phys., 13,687.

McFadden,P.L. and M.W.McElhinny (1984) Geophys.J.R.Astr. Soc.,78, 809.

McWilliams, M.O., R.T.Holcomb and D.E.Champion (1982) Phill. Trans.R. Soc. Lond. A., 306, 211.

Miki M. H.Inokuchi, J.Matsuda, S.Yamagnuchi, N.Isezaki and K.Yaskawa (1988) Rock. Magn. Paleogeophys., 15, 25.

U.S.-Japan paleomagnetic Cooperation Program in Micronesia (1975) J.Geomag. Geoelectr., 28, 57.

GEOMAGNETIC SECULAR VARIATION CURVE RECORDED IN THE SEDIMENT FROM BEPPU BAY, KYUSHU, JAPAN

Masao OHNO[1], Yozo HAMANO[2], Makoto OKAMURA[3], and Kunihiko SHIMAZAKI[1]

1 Earthquake Research Institute, University of Tokyo, Tokyo 113, Japan
2 Geophysical Institute, University of Tokyo, Tokyo 113, Japan
3 Department of Geology, Kochi University, Kochi 780, Japan

1. Introduction

Beppu Bay (34.4N, 131.6E) is located in the north-eastern part of Kyushu in Southwest Japan. In 1988 and 1989, a few tens of cores were collected by using a piston corer of Columbia University type. Most of the cores are 10 to 15 m long and the longest one is as long as about 18 m. The corer is an aluminum pipe, of which the inner diameter and the thickness are 80 mm and 5 mm, respectively. Eight cores from six sites were paleomagnetically analyzed.

The sediment mainly consists of olive gray clay, which is composed of fecal pellet, but also contains a tephra layer (Kikai-Akahoya volcanic ash, 6,300 yr b.p.), which is one of the best known key beds in Southwest Japan. From the depth of this tephra layer, the average sedimentation rate is estimated as about 2 mm/year, which is large enough that we can expect a high resolution of time in our analysis. In addition the core is long enough to recover data for about 10,000 years.

2. Paleomagnetic study of the sediment

After recovered from the sea bottom, the core samples were stored unopened in the aluminum pipes until right before the measurement. They are divided into two D-shaped sections, and cubic-like samples about 10 cc each were taken every 3 to 5 cm for the paleomagnetic study. The remanent magnetization of these cubic samples were measured using 2-G SQUID magnetometers at Kochi University, and at Tokyo Institute of Technology. Initial susceptibility was measured using a Bartington susceptibility meter.

The NRM intensity was 2 to 4 $\times 10^{-6}$ (Am^2/kg) in average. For some pilot samples, about one sample in every one meter, progressive AF demagnetizing experiments were applied. A typical example is shown in Fig. 1. The left figure shows the demagnetizing curve. The MDF (Median Destructive Field) was 150 to 200 (Oe) at any horizons in the sediment. The right figure shows the orthogonal projections. The open circles denote horizontal projections and the open squares denote vertical projections. As demonstrated in this figure, after small secondary components are demagnetized at AF demagnetization level of 50 (Oe), the primary component which goes straight towards the origin of the plot is obtained at most horizons in the sediment. The results of some samples of the deeper part of the

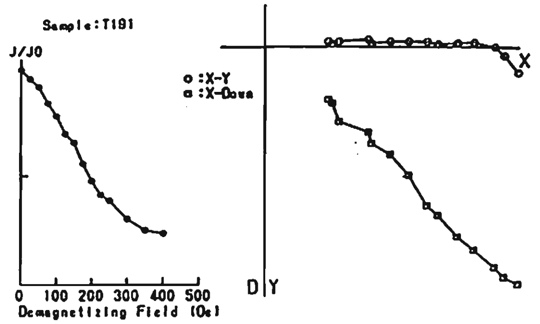

Fig. 1. A typical example of the stepwise AF demagnetization. The left figure shows the demagnetizing curve and the right figure shows the Zijderveld plot. The squares denote the vertical projection and circles denote the horizontal projection.

sediment show a little larger fluctuation compared with the upper part of the sediment. This is probably due to that the sediment contains volcanic ash layers.

Considering these results, the demagnetizing field of 50 to 150 (Oe) was applied for other samples, and doubtful results were rejected. The results from all cores were averaged to obtain one reliable curve after detrending and converting to a common depth scale.

First, the artifact trends were removed in the inclination and the declination curves, which probably originate from the rotation and the inclination of the corer in penetrating the sea bottom. The estimated rotation of the corer did not exceed 5 degrees per one meter, which is considered to be too small to affect the remanent magnetization of the sediment. The correction applied to the inclination curves did not exceed 2 degrees except for that at Site-U89, which amounted to 4 degrees.

Next, by using the correlated characteristic layers among the cores, the depth of each core was converted to a common reference depth. We chose the depth at Site-U as reference because the radiocarbon dating of organic materials is made from the sediment of Site-U88. The correlation was determined mainly by the magnetic susceptibility measurement. The characteristic variations in the NRM intensity and the results of the study by Yamaguchi (1991), who determined the correlation of the cores precisely by analyzing the contents of the sediment, were also used. Fig. 2 shows the inclination and the declination curves of the remanent magnetization after these corrections are made. We could not recover the declination curve for Site-U88 because we failed to recover the relative azimuth of sub-cores when the long core was divided into sub-cores. It is noticeable that the characteristic variations of each core are coherent.

We stacked all these results and averaged them to get one reliable curve. In Fig. 3, Bayesian spline regression was applied after Ishiguro and Arahata (1982). The advantage of this method is that the degree of smoothing is determined objectively by ABIC (A Bayesian Information Criterion). Instead, this method has the disadvantage that we cannot estimate the confidence band of the calculated results. Therefore in order to estimate the confidence band, we calculated "running vector mean" of the directional data. That is, the mean direction and the angular radius of 95% confidence based on Fisher distribution (Fisher, 1953) were calculated from the data which lie within a

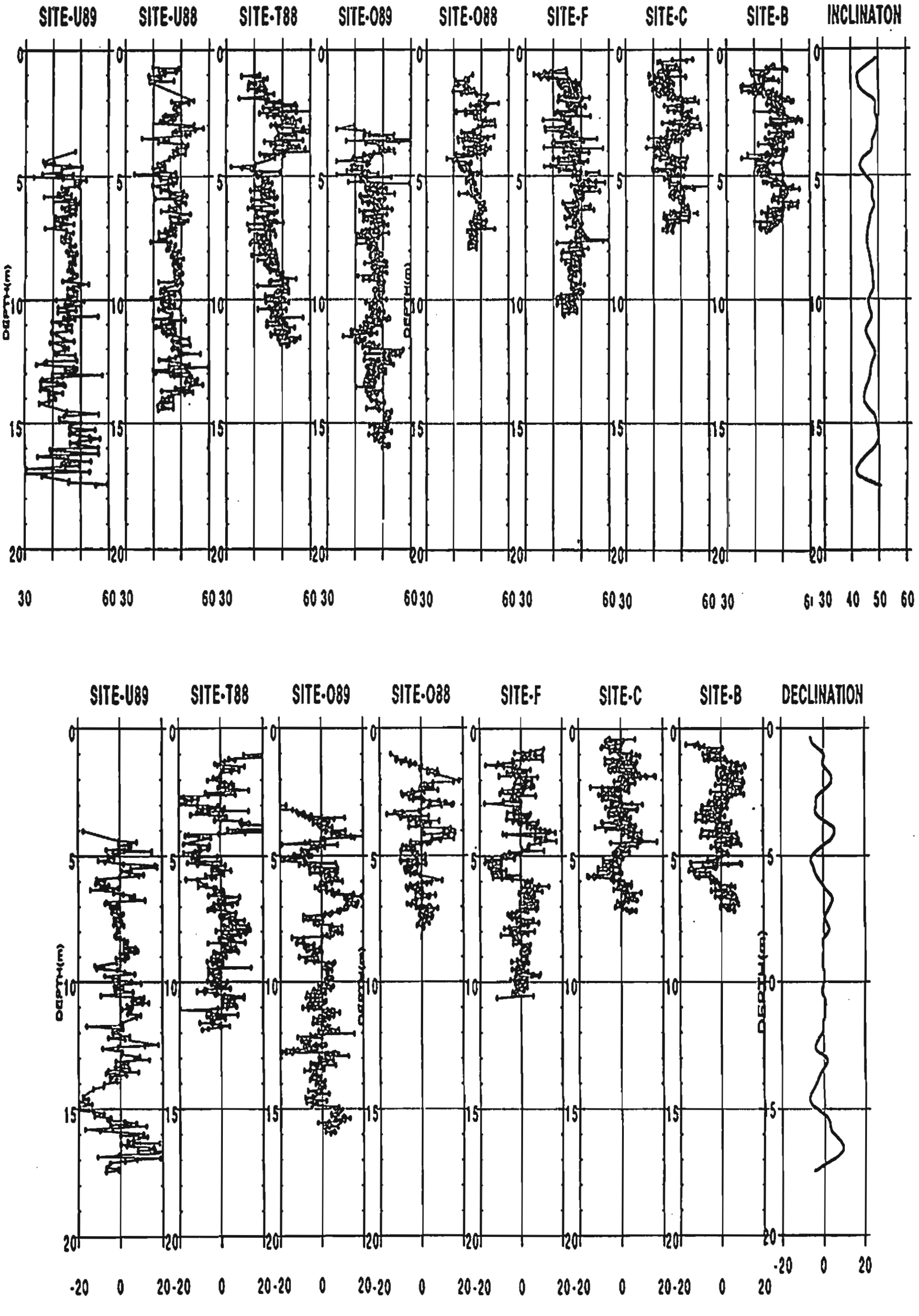

Fig. 2. Variation in the inclination (upper figures) and the declination (lower figures) of the remanent magnetization after AF cleaning and conversion to the depth at Site-U. The rightmost figures show the results of averaging.

depth of 20 cm above and below the median horizons. This depth interval was chosen to make the smoothness of the results of this method similar to those of the Bayesian spline. In Fig. 4, 95 percent confidence limit is calculated from the results of seven cores except for Site-U88, because this method needs both inclination and declination values.

3. Results and discussion

The secular variation curves obtained from the sediment do not necessarily represent the actual variations because of the smoothing effect resulted from the acquisition process of the remanent magnetization of sediment (Hamano ,1980). Due to the gradual acquisition of the remanence, the geomagnetic field variation recorded in the sediment becomes an integrated function of the ambient field change. Therefore the recorded variation is a smoothed one of the actual variation. We attempted to correct this smoothing effect by comparing the result with the archaeomagnetic data. By the archaeomagnetic studies, the secular variation for the past 2,000 years is studied well in West Japan (Maenaka, 1990). In Fig. 3, the characteristic variations in both inclination and declination show remarkable similarity to the archaeomagnetic data, but the amplitude of these variations from Beppu

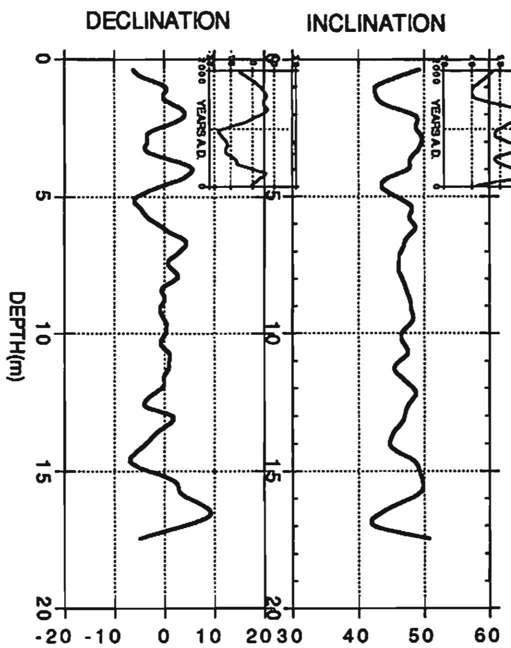

Fig. 3. Time variation in the inclination and the declination obtained from the sediment and those obtained by the archaeomagnetic study by Maenaka (1990). The thick lines show the result of averaging using Bayesian spline regression. The small figures show the results by the archaeomagnetic study for the past 2000 years.

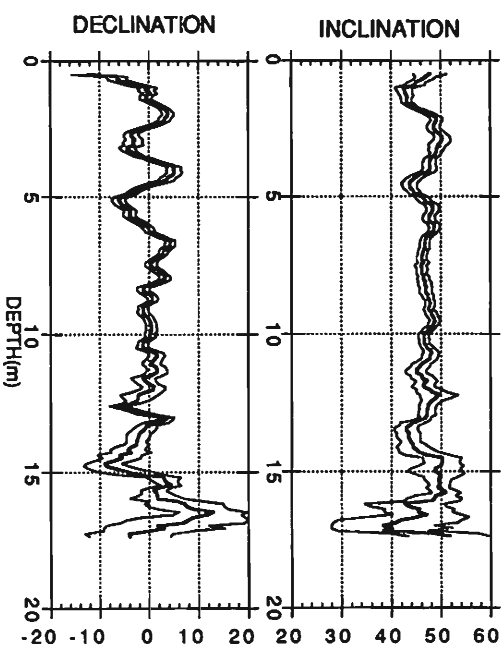

Fig. 4. Results of averaging of the inclination and the declination curves from 7 cores by "running vector mean". The thin lines give the 95% confidence limit.

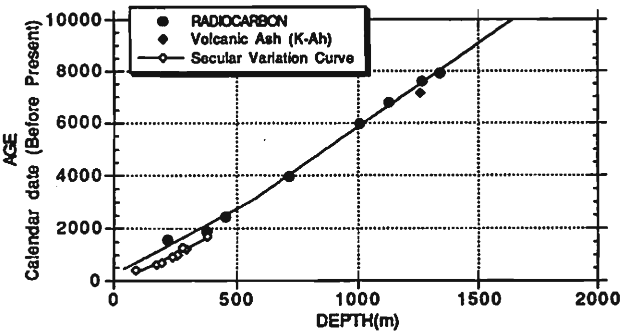

Fig. 5. Relationship between the age and the depth of the sediment. The solid circles denote the results of the radiocarbon measurement. The solid diamond denotes the Kikai-Akahoya volcanic ash. The open diamonds denote the comparison of the characteristic peaks in the inclination and the declination curves with the archaeomagnetic results. All ages are represented in calendar date.

Bay are about half of those in the archaeomagnetic study. This is considered to be due to the smoothing effect during the depositional acquisition process of remanence.

In order to reconstruct the true variation in the geomagnetic field, "deconvolution" was applied to the inclination and the declination curves. The convolution function r(z) was defined as

$$r(z)=A\cdot\exp(-Az) \qquad (A=\ln 0.5/Zhf)$$

after Hyodo (1984). The term Zhf, which is defined as the half fixing depth, is a characteristic depth at which half of the magnetization is acquired. This "deconvolution" was carried out with this parameter Zhf taken as 40, 60 and 80 cm. Bayesian spline regression, which was modified to include the convolution function, was used again. When Zhf is taken as 60 cm, the results showed good consistency with the archaeomagnetic data.

Next these data were converted into time series. Nakamura (personal communication, 1991) determined eight radiocarbon ages for organic materials (shell, gastropod and echinoid) from the sediment of Site-U88 using the AMS (Accelerator Mass Spectrometer) at Dating and Materials Research Center, Nagoya University. In Fig. 5 the solid circles show the results of the radiocarbon measurements which were converted to calendar date after Clark (1975) and Stuiver et al. (1991). The solid diamond shows the radiocarbon age of Kikai-Akahoya volcanic ash layer which is also converted to calendar date. And the open diamonds give the results of the comparison between the results of Beppu Bay and the archaeomagnetic study. The data points correspond to the characteristic peaks in the declination and the inclination curves. The abscissa shows the depth of the sediment corresponding to the characteristic peaks. The ordinate show the date of the corresponding peaks of the curves obtained from the archaeomagnetic study. And the lines show the linear regression to them. In Fig. 5, the radiocarbon ages of the sediment from Beppu Bay differ by 450 years from the ages determined by the comparison between the paleomagnetic results, although the slope of both results show good consistency. Thus we used the age 450 years younger than the radiocarbon age. Part of this offset is considered to be the time difference between sedimentation and the onset of acquiring remanent magnetization. And the rest of the offset is attributed to the error of the radiocarbon age (Hedges, 1983).

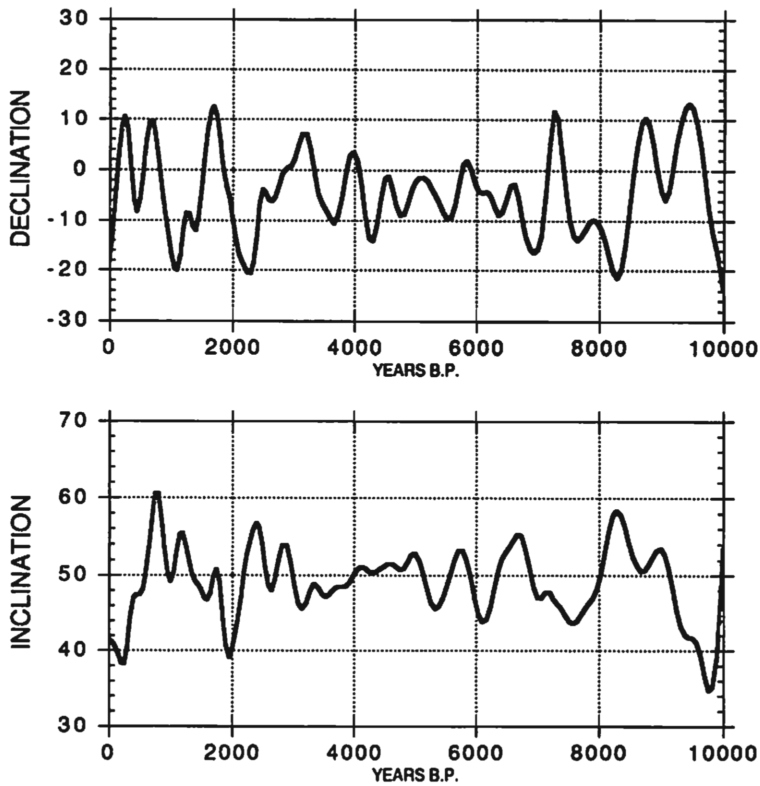

Fig. 6. Time variation in the declination and the inclination of the geomagnetic field at Beppu Bay.

By converting the depth to calendar date, we finally obtained the paleomagnetic secular variation curves of inclination and declination (Fig. 6). The "relative" declination values were thus converted to the "absolute" declination values by using the archaeomagnetic results. The following characteristic features of the secular variation curves can be pointed out based on the results in this study. In Fig. 4, variations with various period are recognized, such as about 2,000, 1,500, 1,000, 700 and 500 years, both in the inclination and the declination curves. The large amplitude variation from ca. 10,000 B.P. to ca. 8,000 B.P. has a long period of about 2,000 years, in contrast, the small amplitude variations from ca. 6,000 B.P. to ca. 4,000 B.P. have short wavelength of about 500 to 700 years. In the inclination curve, it is remarkable that the amplitude is very small from ca. 5,000 B.P. to ca. 3,000 B.P. In the declination curve, the amplitude is smaller between ca. 7,000 B.P. and ca. 4,000 B.P. than the other time intervals. After this quiet period, the amplitude became large again ca. 4,000 B.P. in the declination curve, and ca. 3,000 B.P. in the inclination curve.

References

Clark,R.M. (1975) Antiquity 49, 251
Fisher,R.A. (1953) Proc. Roy. Soc. London, A217, 295.
Hamano,Y. (1980) Earth Planet. Sci. Lett., 51, 221.
Hedges,R.E.M. (1983) in Geomagnetism of baked clays and resent sediments, K.M.Creer, P.Tucholka, and C.E.Barton (eds.), Elsevier, New York.
Hyodo,M. (1984) J. Geomag. Geoelectr., 36, 45.
Ishiguro,M., and E.Arahata (1982) Proc. Inst. Statst. Math., 30, 29.
Maenaka,K. (1990) Rock mag. Paleogeophys., 17, 21.
Stuiver,M., T.F.Braziunas, B.Becker, and B.Kromer (1991) Quaternary Res., 35, 1.
Yamaguchi,C. (1991) MS thesis, Kochi Univ., Kochi.

PALEOSEISMICITY DEDUCED FROM PALEOMAGNETISM OF STALAGMITES (SPELEOTHEMS) COLLECTED FROM AKIYOSHI PLATEAU, JAPAN

Hayao MORINAGA(1), Takafumi YONEZAWA(2), Yoshinori KAWAMURA(2), Yasuhisa ADACHI(3), Yuyan LIU(4), Tadashi KURAMOTO(5), Hiroo INOKUCHI(2), Hiroya GOTO(6), and Katsumi YASKAWA(2)

1. Faculty of Science, Himeji Institute of Technology, 2167 Shosha, Himeji 671-22, Japan
2. Faculty of Science, Kobe University, 1-1 Rokkodai-cho, Nada, Kobe 657, Japan
3. The Graduate School of Science and Technology, Kobe University, 1-1 Rokkodai-cho, Nada, Kobe 657, Japan
4. China University of Geoscience, Yujia Hill, Wuhan 430074, People's Republic of China
5. The Akiyoshidai Museum of Natural History, Shuho-cho, Yamaguchi 754-05, Japan
6. College of Liberal Arts and Sciences, KObe University, 1-2-1 Turukabuto, Nada, Kobe 657, Japan

Many large-scale collapsed rock blocks and speleothems are observed in several limestone caves distributed in Akiyoshi Plateau, Yamaguchi, Japan. The collapse events may have been caused by the past strong seismic activity. Several speleothems, especially stalagmites, which started to grow after collapse events, are observed on collapsed rock blocks. If such stalagmites can be dated, it is possible to estimate the minimum origin times of the past collapse events, that is the seismic events. Although ages of speleothems have been determined by U/Th or 14-C dating method (Postpischl et al., 1991), we report the paleomagnetic method (Morinaga et al., 1988) here.

Three stalagmite samples were collected from Yurino-no-ana and Komori-ana caves in Akiyoshi Plateau; one is called YLI from Yurino-no-ana cave and two are called KMR1 and KMR2 from Komori-ana cave. Core samples 2.5 cm in diameter were drilled along the growth axes of the collected stalagmites, and then were sliced into thin disc specimens of about 2.0 to 3.5 mm thickness for magnetic measurement. Three core samples; YLI, KMR1 and KMR2 are about 12, 7, and 4 cm long, from which 51, 24 and 15 disc specimens were separated, respectively. Their remanent magnetization were measured using a cryogenic magnetometer. Progressive alternating-field demagnetization (AFD) method were used to test their magnetic stability and to eliminate a viscous component. Steps of the progressive AFD were 3, 6, 9, 12, 15, 20, 25, 30, 35, 40, and 45 mT for all the specimens.

Characteristic directions were separated by principal component analysis (PCA). Several specimens have weak and unstable remanences (less than 10E-9 Amm) and show no significant characteristic direction; 2 and 2 specimens from KMR1 and KMR2, respectively. The characteristic directions separated by PCA are shown every stalagmite in Figure 1. Horizontal axes correspond distance from the sample surface (left side is more recent) and vertical ones show values of declination (upper) and inclination (lower). Some specimens having fairly weak intensity, which are located near the surface, show relatively unstable behavior during the progressive AFD for two sample from Komori-ana cave. Characteristic directions of such specimens are relatively scattered. Therefore, the direction curves (three point moving averages) of the outer portion do not have so high reliability and so significant meaning. Three sets of the direction curves, however, show similar variation pattern to each other but the beginnings of three records are different from each other. From this appearance of direction curves, the following two conclusions are

demonstrated;
(1) The directional (both declination and inclination) records can be correlated with each other among three stalagmites. This suggests that these records indicate the paleomagnetic secular variation (PSV), although the reliability is not so high.
(2) Supposing that all the stalagmites immediately started to grow after the collapse of the corresponding rock blocks, difference of the beginning of the records indicate that the corresponding tectonic events have different origin times from each other.

In order to estimate beginning times of three stalagmites' growth, we compared the direction curve from KMR1, from which the longest record was obtained, with a paleosecular variation curve from sediments in West Japan (M. Hyodo, Kobe Univ., personal Communication). After several trials of comparison and judgment, the correlation shown in Figure 2 was regarded to be the best. According to this correlation, it is concluded that the KMR1 stalagmite started to grow at about 6,000 years BP. Assuming a constant growth rate for the KMR1 stalagmite and on the basis of this correlation, it is suggested that the other two stalagmites; KMR2 and YL1 started to grow at about 2,500 and 2,000 years BP, respectively. These three ages (6,000, 2,500 and 2,000 years BP.) and one previously estimated age of 4,500 years BP using the same method (Morinaga et al., 1988) correspond to origin times of collapse events, which may have been caused by strong earthquakes, occurred around Akiyoshi Plateau in the past. More paleomagnetic datings of stalagmites on collapsed rock blocks and speleothems can clarify the frequency and the periodicity of the past seismic activities in Akiyoshi Plateau.

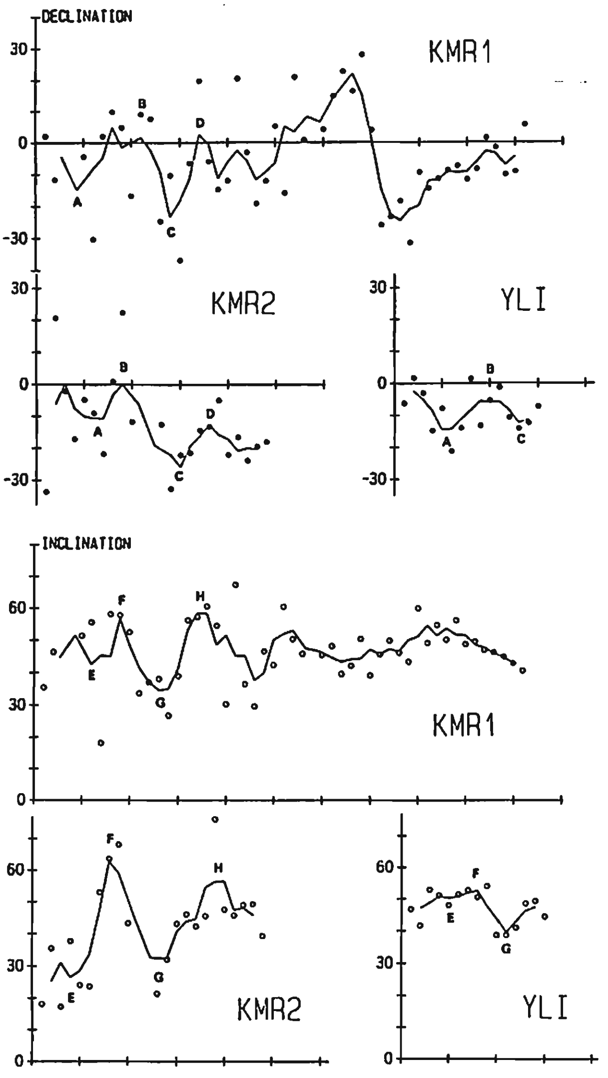

Figure 1 Paleomagnetic results of three stalagmites; KMR1, KMR2 and YL1. Closed (open) Circles show declination (inclination) values obtained by PCA. Three-point moving averages are also shown (curves). Alphabets indicate corresponding positions among three records.

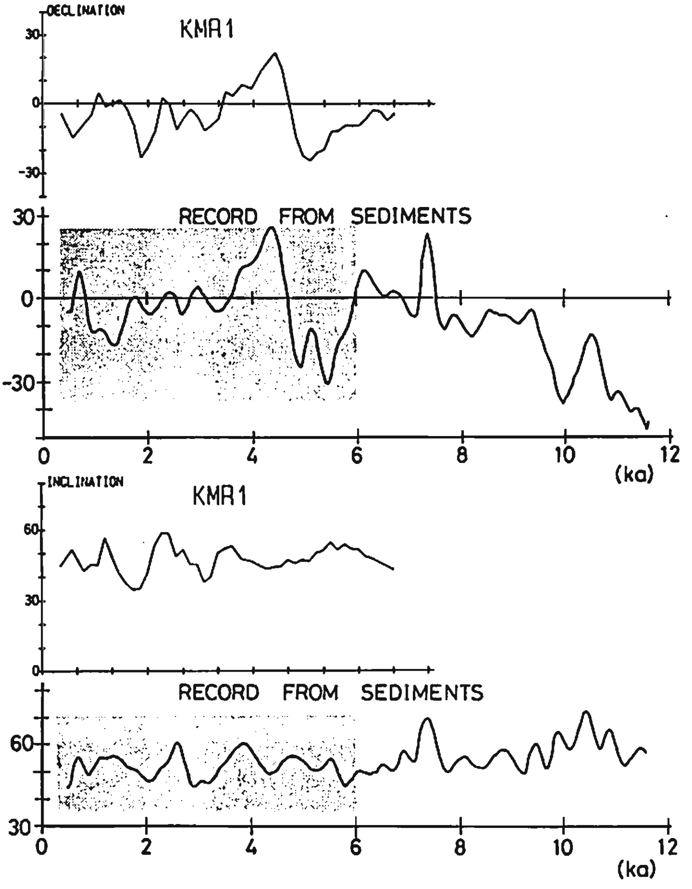

Figure 2 The best correlation between direction curves from the KMR1 stalagmite and from sediments (M. Hyodo, Kobe University, personal communication). Numerics on horizontal axes of the record from sediments are ages in years BP. Shaded zones in the records from sediments show the corresponding part to the KMR1 record.

References

Morinaga, H., I. Horie, H. Murayama, Y. Liu, T. Kuramoto, and K. Yaskawa (1988) Rock Mag. Paleogeophys., 15, 15.

Postpischl, D., S. Agostini, P. Forti, and Y. Quinif (1991) Tectonophys., 193, 33.

(To be submitted to J. Geomag. Geoelectr.)

THE EARTH'S MAGNETIC FIELD FOR THE PAST 10,000 YEARS

Masao OHNO[1] and Yozo HAMANO[2]

1 Earthquake Research Institute, University of Tokyo, Tokyo 113, Japan
2 Geophysical Institute, University of Tokyo, Tokyo 113, Japan

1. Introduction

The study of the geomagnetic secular variation is a first step towards clarification of the generating process of the geomagnetic field that is taking place in the Earth's core. In this paper, we examined the secular variation curves obtained from the paleomagnetic studies of unconsolidated sediments around the world in comparison with the archaeomagnetic secular variation curves, and prepared a data set of the secular variation for the past 10,000 years. With this data set, the global features of the geomagnetic field were investigated.

2. Secular variation curves in the world

First, we compiled the archaeomagnetic studies, and a data set of secular variation from 11 locations (triangles in Fig. 1) for the past 1500 years were prepared. The data were taken from Brynjolfsson (1957), Tarling (1989), Thellier (1981), Kovacheva (1980), Zagniy (1981a; 1981b), Wei et.al. (1983), Maenaka (1990), Sakai and Hirooka (1986), Nagata et al. (1963), Kono (1969), Sasajima and Maenaka (1966), Ohno (1988), Barton (1983), Holcomb (1986), DuBois (1989), Sternberg (1989) and Wolfman (1984). In all, 24 elements of the geomagnetic field (11 for inclination, 10 for declination and 3 for intensity) were available. For Australia, the secular variation curve obtained by combining the paleomagnetic and the archaeomagnetic data was used. From this data set, the Gauss coefficients up to degree 2 were calculated for every 100 years between 450 and 1550 A.D. using the spherical harmonic expansion.

Secondly, available secular variation curves from sediments were examined considering the sedimentation rate and the stability of the remanent magnetization. The time lags and the offsets in the inclination and the declination curves, which are considered to originate in the depositional acquisition process of remanent magnetization and/or in the coring process, were corrected in comparison with the model field calculated from the above obtained Gauss coefficients. After all, paleomagnetic secular variation curves from nine locations (circles in Fig. 1) were obtained. The data were taken from Turner and Thompson (1982), Morner and Sylwan (1989), Thompson et.al. (1985), Ohno (1991), Barton (1983), Verosub et.al. (1986), Creer and Tucholka (1982), King et.al. (1983) and Creer et.al. (1983). Very long archaeomagnetic results from Bulgaria and Ukraine were added to them in the succeeding analysis. Fig. 3 gives the time interval spanned by each data.

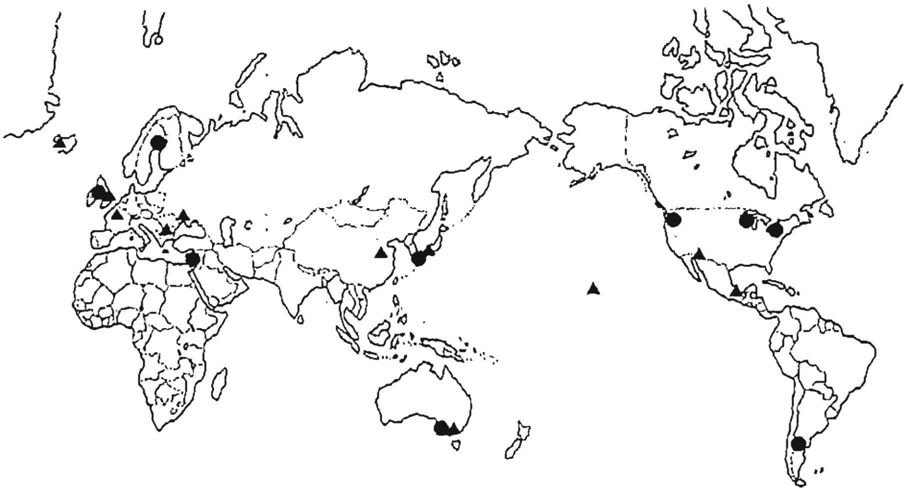

Fig. 1. Locality of the data point of the archaeomagnetic study (triangles) and the study from sediment (circles).

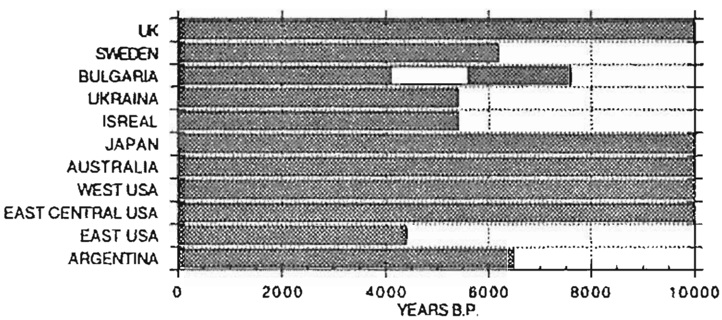

Fig. 2. Time interval spanned by each study.

3. Time variation in the Geomagnetic Pole position

There is a fairly general agreement that the mean VGP is a good approximation to the Geomagnetic Pole position (Cox and Doell, 1960; Barbetti, 1977). Champion (1980) and Merrill and McElhinny (1983) inferred the Geomagnetic Pole position for the past 2000 years by the mean VGP from the archaeomagnetic data. In the same manner, we inferred the Geomagnetic Pole position for the past 10,000 years from the above obtained data set. Fig. 3 and Fig. 4 show the results. It is noteworthy that the results of this study for the past 1500 years show good agreement with the result by Merrill and McElhinny (1983), in spite of the difference of the distribution of the data points between them.

The following features can be pointed out. The distribution of the Geomagnetic Pole for the past 10,000 years has, as a whole, an elliptic shape which is elongated to the direction of about 45 and 225 degrees in the longitude. And the period that the Geomagnetic Pole stayed in the eastern hemisphere was longer than in the western hemisphere. During the period between ca. 7000 B.P. (Before Present; years before 1950 A.D.) and ca. 4000 B.P., the Geomagnetic Pole stayed near the geographical pole and never came

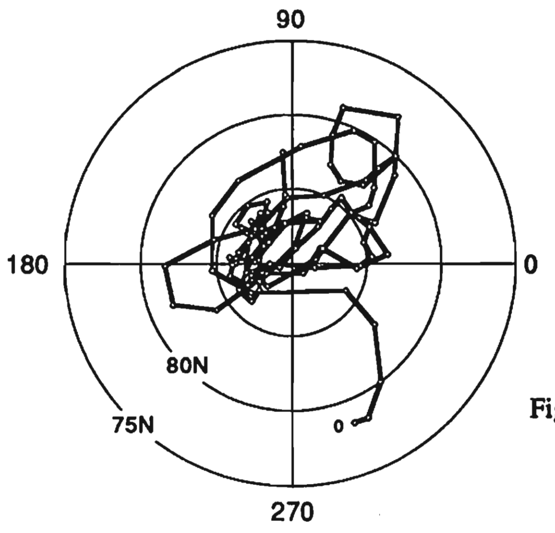

Fig. 3. North Geomagnetic Pole position for the past 10,000 years which are plotted every 100-year interval.

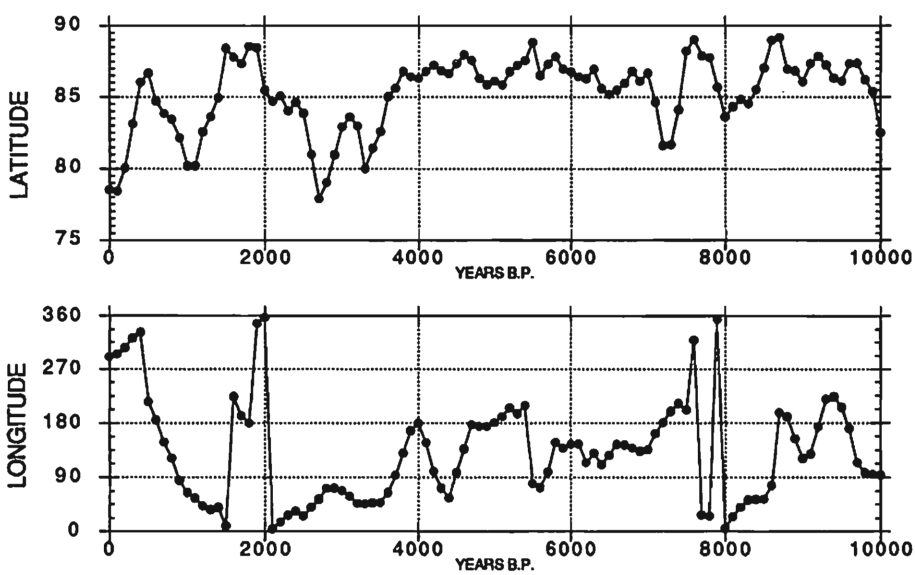

Fig. 4. Time variation in the latitude and the longitude of the north Geomagnetic Pole.

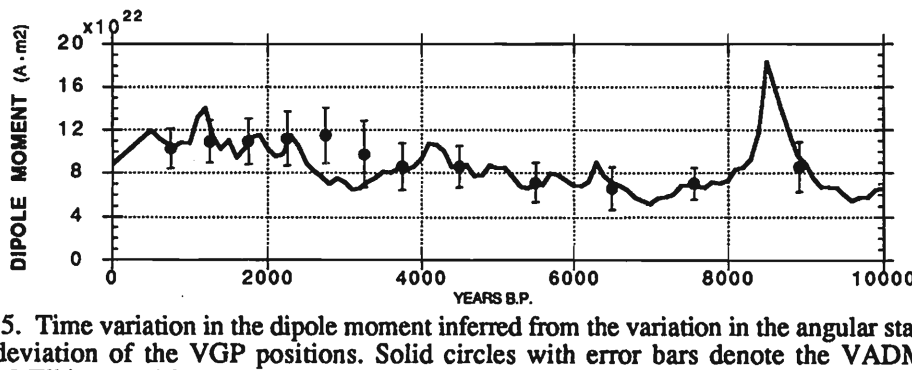

Fig. 5. Time variation in the dipole moment inferred from the variation in the angular standard deviation of the VGP positions. Solid circles with error bars denote the VADMs by McElhinny and Senanayake (1982).

out of the circle of 85 degrees of north latitude. In contrast to this inactive period, it moved to the outside of the circle of 80 degrees of north latitude before and after this period. It is noticeable that the period in which the Geomagnetic Pole moved westward was longer than that of eastward prior to ca. 2000 B.P., which can be seen in the time variation in the longitude.

4. Time variation in the dipole moment

In this chapter, we will discuss further the property of the VGP positions, and from the analysis of the dispersion of the VGP positions, we will infer the variation in the dipole moment. The VGP positions calculated from each data point disperse around the Geomagnetic Pole, due to the non-dipole components of the geomagnetic field. The angular standard deviation is defined as a measure of the degree of the dispersion (Merrill and McElhinny, 1983). It is obvious that the angular standard deviation is zero if the non-dipole field is zero all over the sphere. And as the non-dipole to dipole ratio becomes larger, the angular standard deviation becomes larger. We examined the relationship between the angular standard deviation and the non-dipole to dipole ratio in the recent geomagnetic field, and confirmed that the tangent of the angular standard deviation is a good approximation to the non-dipole to dipole ratio.

Now that we have obtained the continuous time variation in the non-dipole to dipole ratio, and on the other hand, the dipole moment (VADM) averaged over 500- to 1000-year-interval was obtained by McElhinny and Senanayake (1982). We compared these two results and noticed the similarity in the long period variation in the VADM and in the cotangent of the angular standard deviation. After this relationship, we introduced a model in which the variation in the total non-dipole field is proportional to the variation in the dipole moment, and calculated the "continuous" time variation in the dipole moment.

In Fig. 5, the calculated dipole moment and the VADMs are compared. The coincidence between them is remarkable. Furthermore the details of the variations are clear in the result of this study. A most remarkable feature is the steep peaks around 8500 B.P., around 4200 B.P., and around 1200 B.P. Several paleointensity studies from lava flows report high field intensity in the periods above, for example, Tanaka (1990), Salis et. al., (1989) and Schweitzer and Soffel (1980). In the results of these studies, during the periods when high paleointensity values are reported, low paleointensity values are also reported. Considering the result of this study, the coexistence of both high and low values is interpreted that the periods of the high field intensity were very short. That is to say, the paleointensity studies of lava flows cannot distinguish the short periods of high intensity from the periods of low intensity before and after, because they can only give the information of the geomagnetic field at one moment and the precision of dating is not sufficient. In contrast, in this study, the time variation in the dipole moment was obtained continuously, which revealed the precise variation clearly.

5. Spherical harmonic analysis

In order to investigate further the characteristics of the geomagnetic field, we calculated the Gauss coefficients up to degree 2 for the past 6000 years (Fig. 6). Because only directional data of the geomagnetic field were available, the relative Gauss coefficients were calculated. It is remarkable that the term h_2^1 changed largely in correspondence with the movement of the Geomagnetic Pole from 4000 B.P. to 2000 B.P.

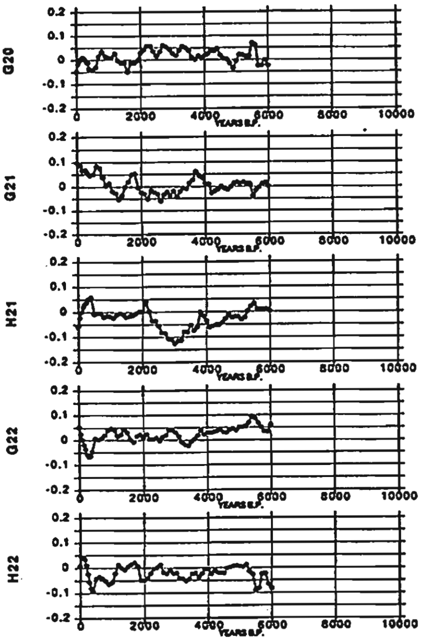

Fig. 6. Time variation in the Gauss coefficients of the order 2 which are normalized by the dipole moment.

6. Discussion

Movement of the Geomagnetic Pole position was active, changing its latitude to about 80 degree, around 8000 B.P. However its activity decreases with time. During the period between 7000 and 4000 B.P., the range of the movement was limited within 5 degrees. After ca. 4000 B.P., the movement was very active again, fluctuating over 10 degrees. It is interesting to note that the time when the dipole activity changed correspond to that of the maximum intensity. After the time of the maximum intensity, the movement of the pole position became active.

REFERENCES

Barbetti,M. (1977) Earth Planet. Sci. Lett., 36, 207.

Barton,C.E. (1983) Section 4.6 of Geomagnetism of baked clays and resent sediments, K.M.Creer, P.Tucholka, and C.E.Barton (eds.), Elsevier, New York.

Brynjolfsson,A. (1957) Adv. in Phys., 6, 247.

Champion,D.E. (1980) Rept. Open file series US Geol. Surv., 314, 80.

Cox,A., and R.R.Doell (1960) Geol. Soc. Amer. Bull., 71, 645.

Creer,K.M., D.A.Valencio, A.M.Sinito, P.Tucholka, and J.F.A.Vilas (1983) Geophys. J. R. astr. Soc., 74, 199.

Creer,K.M., and P.Tucholka (1982) Can. J. Earth Sci., 19, 1106.

DuBois,R.L. (1989) Phys. Earth Planet. Int., 56,18.

Holcomb,R., D.Champion, and M.McWilliams (1986) Geol. Soc. Am. Bull., 97, 829.

King,J.W., S.K.Banerjee, J.Marvin, and S.Lund (1983) Palaeogeog. Palaeocl. Palaeoecol., 42, 167.

Kono,M. (1969) D. Sc. thesis, Univ. of Tokyo, Tokyo.

Kovacheva,M. (1980) Geophys. J. R. astr. Soc., 61, 57.

Maenaka,K. (1990) Rock mag. Paleogeophys., 17, 21.

McElhinny,M.W., and W.E.Senanayake (1982) J. Geomag. Geoelectr., 34, 39.
Merrill,R.T., and M.W.McElhinny (1983) The Earth's magnetic field, Academic Press, London.
Morner,N.A., and C.A.Sylwan (1989) In: F.J.Lowes et. al. (eds.), Geomagnetism and paleomagnetism, Kluwer Academic Publishers, the Netherlands.
Nagata,T., Y.Arai, and K.Momose (1963) J. Geophys. Res., 68, 5277.
Ohno,M. (1988) MS thesis, Univ. of Tokyo, Tokyo.
Ohno,M. (1991) D. Sc. thesis, Univ. of Tokyo, Tokyo.
Sakai,H., and K.Hirooka (1986) J. Geomag. Geoelectr., 38, 1323.
Salis,J.S., N.Bonhommet, and S.Levi (1989) J. Goephys. Res., 94, 15771.
Sasajima,S., and K.Maenaka (1966) Mem., Fac. Sci. Kyoto Univ. Ser. Geol. & Min., 33, 53.
Schweizer,C., and H.C.Zoffell (1980) J. Geophys., 47, 57.
Sternberg,R.S. (1989) Phys. Earth Planet. Int., 56,1.
Tanaka,H. (1990) J. Geophys. Res., 95, 17517.
Tarling,D.H. (1989) In: F.J.Lowes et. al. (eds.), Geomagnetism and paleomagnetism, Kluwer Academic Publishers, the Netherlands.
Thellier,E. (1981) Phys. Earth Plant. Int., 24, 89.
Thompson.R, G.M.Turner, M.Stiller and A.Kaufman (1985) Quaternary Res., 23, 175.
Turner,G.M., and R.Thompson (1982) Geophys. J. R. astr. Soc., 70, 789.
Verosub,K.L., P.J.Mehriger,Jr., P.Waterstraat (1986) J. Geophys. Res., 91, 3609.
Wei,Q.Y., T.C.Li, G.Y.Cao, W.S.Chang, S.P.Wang, and S.F.Wei (1983) Section 3.11 of Geomagnetism of baked clays and resent sediments, K.M.Creer, P.Tucholka, and C.E.Barton (eds.), Elsevier, New York.
Wolfman,D. (1984) In: M.B.Schiffer (Editor), Advances in archaeological method and theory, 7.
Yukutake,T. (1987) Heinrich-Herz Int., 21.
Zagniy,G.F. (1981a) Geophys. J., 3, 741.
Zagniy,G.F. (1981b) Geofiz Zh. 3(5) Naukova dumka, Kiev.

PALEOMAGNETIC EVIDENCE FOR POST-LATE MIOCENE INTRA-ARC ROTATION OF SOUTH KYUSHU, JAPAN

Kazuto KODAMA and Kenji NAKAYAMA

Department of Geology, Kochi University, Kochi 780, Japan

A paleomagnetic study was carried out on the Late Miocene Uchiumigawa Group exposed in southeast Kyushu (Fig. 1). Biostratigraphic study (Takehi, 1978) suggests that the age of the group ranges from earliest Late Miocene to late Late Miocene (10 to 6 Ma). With progressive thermal demagnetizations for a total of 215 specimens collected at 19 sites, characteristic magnetization components with higher unblocking temperatures were isolated for 88 specimens from 17 sites. The other 71 specimens displayed demagnetization great circle trajectories that were used to estimate stable endpoints. Reliable site-mean directions were obtained for 17 sites; 14 of these were of reversed polarity and three at the intervening horizons were of antipodal normal polarity. All these paleomagnetic directions deviate significantly westward (Fig. 2). The tilt-corrected, overall formation-mean direction is D = 322.0°, I = 48.6° with α_{95} = 6.0°. This is statistically indistinguishable from the mean direction of D = 331.2°, I = 41.3° with α_{95} = 9.9° for the Middle Miocene deposits in Tanegashima Island of the northern Ryukyu arc (Kodama et al., 1991). The common mean direction become D = 333.2°, I = 45.1° with α_{95} = 4.9°. This indicates that both south Kyushu and the northernmost Ryukyu arc have experienced 27° ± 6° of counter-clockwise rotation with respect to the Eurasian continent after the latest Miocene, or during the last 6 Ma.

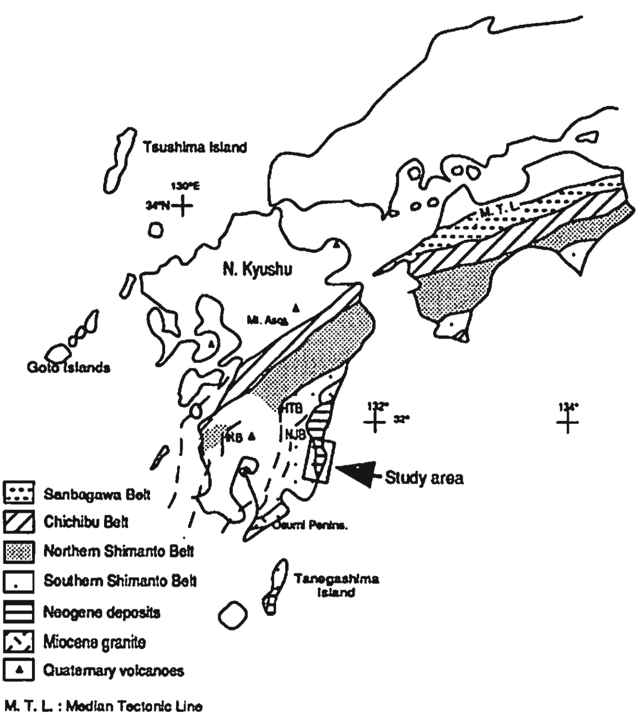

Fig. 1 General geology south of the Median Tectonic Line in Kyushu and Shikoku Islands. Study area, indicated by an arrow, is located in the south of Miyazaki Prefecture.

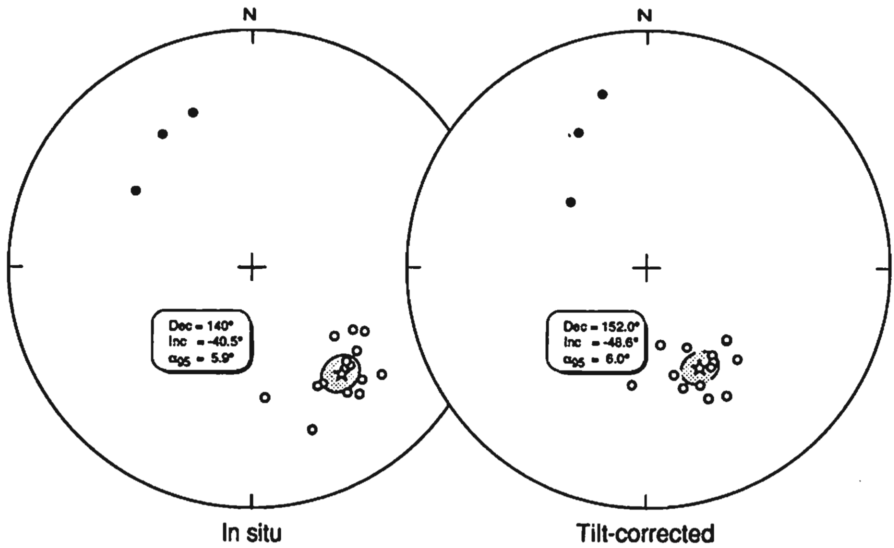

Fig. 2 Site-mean directions and overall mean directions for formations with normal or reversed polarity, in geographic (left) and stratigraphic (right) coordinates. Solid symbols are equal-area projections on the lower hemisphere, and open and dashed ones on the upper hemisphere. Circles denote site-mean directions, and stars and shaded ovals indicate formation-mean directions and the 95% errors as in attached boxes.

This intra-arc rotation yielded a cusp-form bend of the pre-Miocene strata in southwest Kyushu (Fig. 1). This result opposes a previous model which interprets the bend as a consequence of the Middle Miocene clockwise rotation of southwest Japan (e.g., Murata, 1987). An extensional tectonic regime has been predominant for central Kyushu from at least 5 Ma to the present (e.g., Kamata, 1989). It is thus unlikely that either the collision or the buoyant subduction of the Kyushu-Palau ridge produced this intra-arc deformation, as seen in the central Honshu-Izu arc collision area. Since the back-arc spreading is only at an incipient rifting stage behind the northern Ryukyu arc (Sibuet et al., 1987), the conventional model which ties arc rotation to back-arc basin formation (e.g., Otofuji et al., 1985) cannot fully account for the rotation of south Kyushu. We propose that widespread crustal stretching prior to the back-arc opening is able to cause an arc rotate.

Reference

Kamata, H., *Bull. Volcanol.*, **51**, 315-332, 1989.
Kodama, K., T. Ozawa, K. Inoue, Y. Mayeda, and T. Takeuchi, *J. Geomag. Geoelectr.*, **43**, 1991.
Murata, A., *J. Geol. Soc. Japan*, **93**, 91-105, 1987.
Otofuji, Y., T. Matsuda, and S. Nohda, *Nature*, **317**, 603-604, 1985.
Sibuet, J.-C., J. Letouzey, F. Barrier, J. Charvet, J.-P. Foucher, T. W. C. Hilde, M. Kimura, L.-Y. Chiao, B. Marsset, C. Muller, and J.-F Stephan, *J. Geophys. Res.*, **92**, 14041-14063, 1987.
Takehi, N., *Grad. thesis* , Inst. Geol. Paleont. Tohoku Univ., 1978.

(Submitted to *Tectonics*)

PALEOMAGNETISM OF THE UETSU AND THE TSUGAWA REGIONS, NORTHEAST JAPAN: IMPLICATIONS FOR NORTHEAST JAPAN TECTONICS DURING THE JAPAN SEA FORMATION

Hiroshi MOMOSE*, Masayuki TORII* and Atsushi YAMAJI**

*Department of Geology & Mineralogy, Kyoto 606-01, Japan

**Department of Earth Sciences, College of General Education,
Tohoku University, Sendai 980, Japan

Early to middle Miocene formations are exposed in the Uetsu and the Tsugawa regions overlying pre-Neogene sequences (Yamaji, 1989; Yamaji, 1990; The Agency of Resources and Energy, 1982; Research group for Tsugawa Green Tuff, 1979). Paleomagnetic samples were collected from 71 sites of the Neogene formations. Both alternating field and thermal demagnetization experiments show paleomagnetic directions from 35 sites to be stable and essentially free from secondary overprintings. The mean directions from 35 sites display mixed pattern of declination; clockwise and counter-clockwise deflections relative to the expected mid-Tertiary direction (Fig. 1). Our data are generally consistent with the previous work of Otofuji et al. (1985).

These results may be basically explained by combining the counter-clockwise rotation of two blocks (ca. 50 km x 50 km) and clockwise rotated domains (ca. 10 km x 10 km) placed in the dextral sheared zone between the blocks (Fig. 2). To understand complicated tectonics, we suggest two models of Northeast Japan tectonics which is related to the Japan Sea formation. Tectonic settings in the Hokkaido, Southwest Japan and west kyushu archipelagoes are based on previous works (Jolivet and Miyashita, 1985; Otofuji and Matsuda, 1987; Ishikawa et al., 1989; Ishikawa and Tagami, 1991).

The first model is that the counter-clockwise rotations are caused by sinistral shear motion of Northeast Japan along the Japan Sea coastal area . The clockwise rotated domains may be ubiquitously observed between the counter-clockwise rotated blocks which were activated during the opening of the Japan Basin (Fig. 3a). In this model, the Itoigawa-Shizuoka Tectonic Line (ISTL) is assumed to be the southern extent of the sinistral sheared zone.

The second model is that whole Northeast Japan rotated counter-clockwise as a coherent tectonic block and the clockwise rotated small domains were formed by the dextral shear motion along a southern boundary of the block (Fig. 3b). The boundary is assumed to be the Tanakura Tectonic Line (TTL) in this model. We believe that both of these models are realistic tectonics for Northeast Japan which is considered to be occurred during the Japan Sea formation.

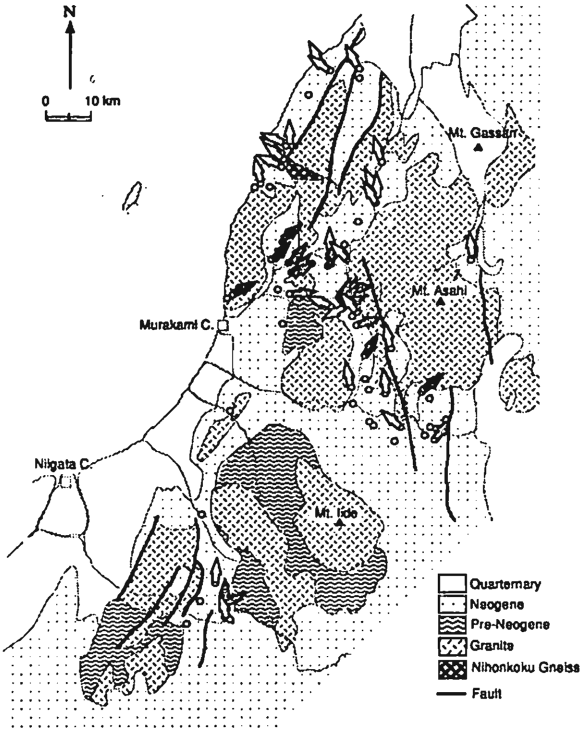

Fig. 1. Directions of the primary remanence.
Open and solid circles represent sampling sites of the present study and that of Otofuji et al. (1985), respectively. Remanent directions of negative inclinations are converted by 180°. Open and hatched arrows represent negative and positive declination, respectively.

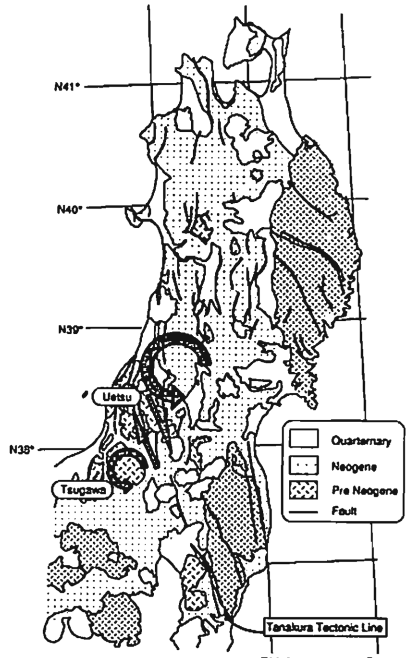

Fig. 2 Geological map of Northeast Japan.
Arrows represent rotation and shear motion infurred from paleomagnetic directions.

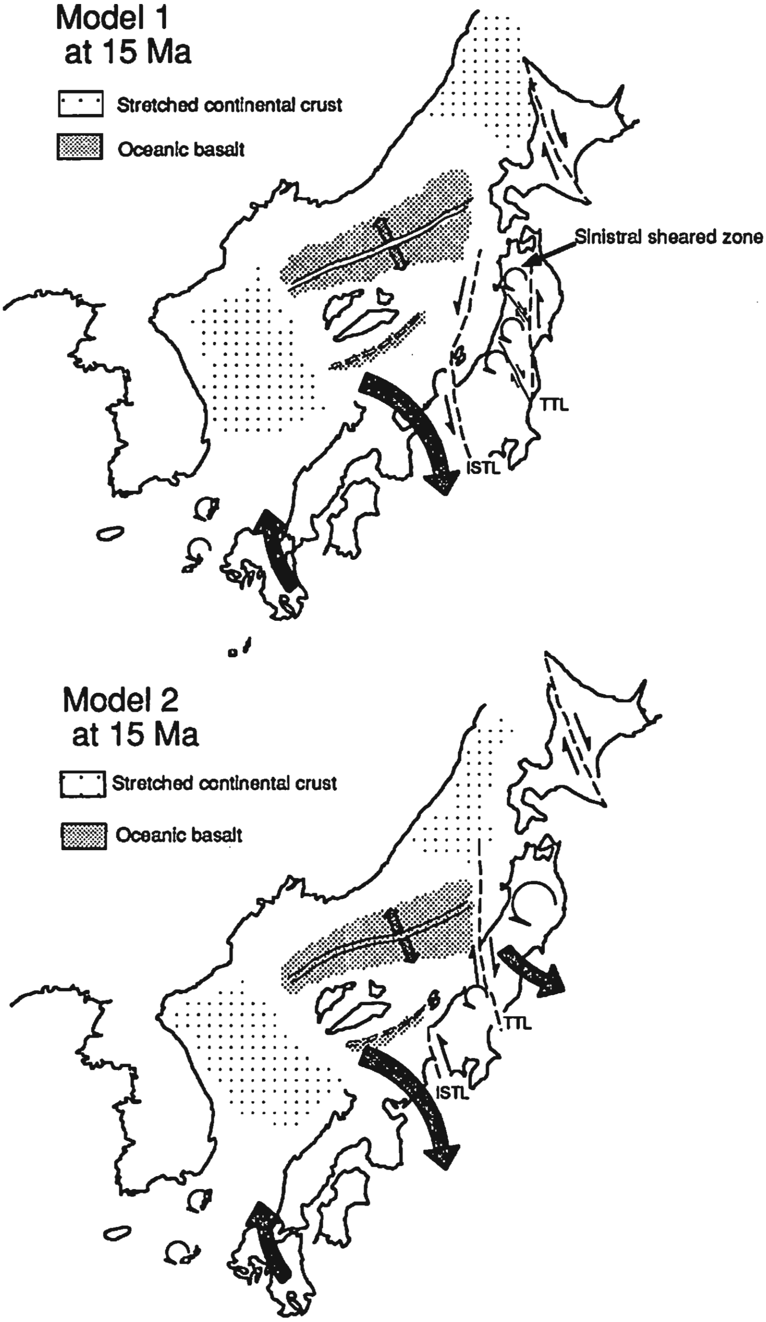

Fig. 3 (a) Sinistral shear model (above).

(b) Whole rotation model (below).

References

Ishikawa, N., M. Torii and N. Koga (1989) *J. Geomag. Geoelectr.*, **41**, 797.
Ishikawa, N. and T. Tagami (1991) *J. Geomag. Geoelectr.*, **43**, 229.
Jolivet, L. and S. Miyashita (1985) *Tectonics*, **4**, 289.
Otofuji, Y., T. Matsuda, and S. Nohda (1985) *Earth Planet. Sci. Lett.*, **75**, 265.
Otofuji, Y. and T. Matsuda (1987) *Earth Planet.. Sci. Lett.*, **85**, 259.
Research group for Tsugawa Green Tuff (1979) *Mem. Geol. Soc. Japan*, **16**, 1.
The Agency of Resources and Energy (1982) Research Report of the Uetsu Region (1), 164.
Yamaji, A. (1989) *Mem. Geol. Soc., Japan*, **32**, 305.
Yamaji, A. (1990) *Tectonics*, **9**, 365.

PALEOMAGNETIC STUDY OF CRETACEOUS ROCKS FROM CENTRAL YUNNAN OF THE YANGTZE BLOCK, CHINA

Shoubu FUNAHARA*†, Nobukazu NISHIWAKI*, Fumiyuki MURATA*, Yo-ichiro OTOFUJI* and Yi Zhao WANG**

* Department of Earth Sciences, Faculty of Science, Kobe University, Kobe 657, Japan
** Yunnan Bureau of Geology and Mineral Resources, Kunmin, China

More than 200 samples were collected at 30 sites from the Cretaceous Matoushan and Puchanghe formations around the city of Chuxiong (25°N, 101.5°E) in the Ynunnan province. Twenty four sites have characteristic directions with high temperature component above 350°C. Paleomagnetic directions from 21 sites of the Cretaceous formations reveal clockwise deflection in declination, and the tilt-corrected mean direction is Dec=46.4°, Inc=38.6°, and α_{95}=11.3° (Fig. 1). These 21 sites pass the reversal test and pass the fold test, with k_2/k_1 ratios of 3.0 at the 99 percent confidence level.

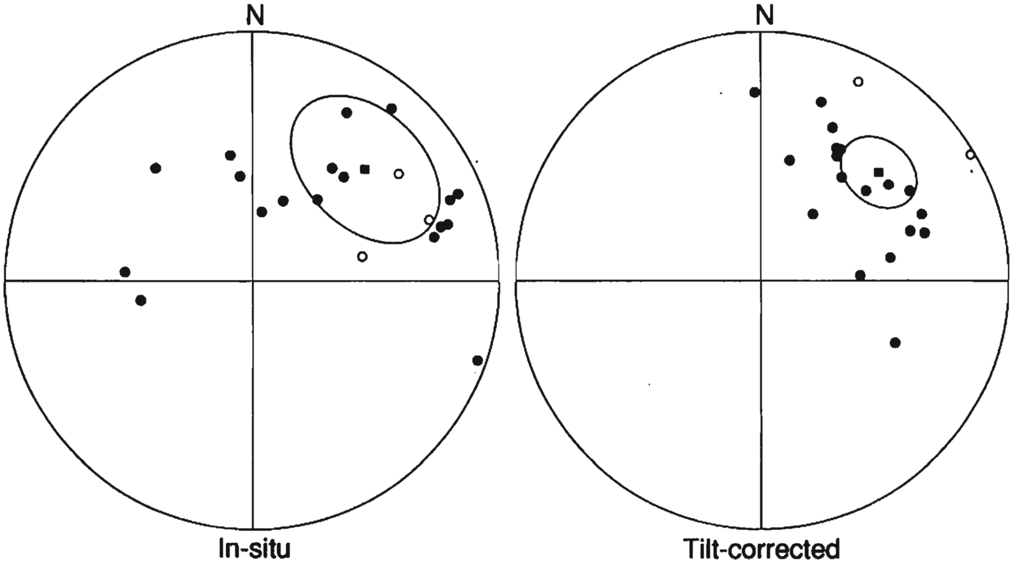

Fig. 1. Site-mean characteristic directions for the 21 sites (circles) and their mean direction (square) together with 95 % confidence circle for the Cretaceous formations at Chuxiong before and after application of the tilt correction. For a better visual impression, the reversed directions have been inverted through origin. Projections are equal area, filled and open symbols refer to the lower and the upper hemispheres respectively.

Comparison with paleomagnetic data from other areas indicates that the Chuxiong area was rotated clockwise through 27° with respect to the eastern part of the Yangtze block whereas it was subjected to more than 46° clockwise rotation with respect to the neighboring blocks of the Lhasa Terrane and western Sichuan since the Cretaceous time. The clockwise rotation of Chuxiong is a reflection of rotational motion of the large region including the southeastern Qiangtang Terrane, western Yangtze block and the Jinsha suture - Red River fault. This large regional rotation is ascribed to the deformation due to collision of India rather than the local deformation due to left-lateral strike slip faults along the Red River fault. Paleomagnetic data and tectonic features suggest that the rotational motion occurred in the early phase of the continental collision, and folding followed in the central Yunnan province.

† He has been a victim of snow avalanche at the camp 3 of the Mt. Meylixueshan (6740m) in the Yunnan Province on January 3, 1991

(to be submitted to Earth Planet. Sci. Lett.)

REGIONAL TECTONIC IMPLICATIONS FROM PALEOMAGNETISM OF THE D/C BOUNDARY SECTION IN GUILIN, SOUTH CHINA

Hayao MORINAGA(1), Akira MATSUNAGA(2), Yasuhisa ADACHI(3), Hiroo INOKUCHI(2), Yuyan LIU(4), Weiran YANG(4), Hiroya GOTO(5), and Katsumi YASKAWA(2)

1 Faculty of Science, Himeji Institute of Technology, 2167 Shosha, Himeji 671-22, Japan
2 Faculty of Science, Kobe University, 1-1 Rokkodai-cho, Nada, Kobe 657, Japan
3 The Graduate School of Science and Technology, Kobe University, 1-1 Rokkodai-cho, Nada, Kobe 657, Japan
4 China University of Geoscience, Yujia Hill, Wuhan 430074, People's Republic of China
5 College of Liberal Arts and Science, Kobe University, 1-1 Rokkodai-cho, Nada, Kobe 657, Japan

Stratigraphic section including Devonian-Carboniferous (D/C) boundary, which is located at Nanbiancun in Guilin, Guangxi, China, is designated to the international standard one. This section is classified into 26 beds named to 49 to 67 and 68a to 68g from the lower bed (total thickness is about 5 m here). All the beds are slightly tilted and are divided by a clear bedding and are thought to have a comformable relationship to each other. Most of beds are composed mainly of muddy limestones and the rest five beds (51, 53, 58, 60 and 65) are classified as thin shale beds of a few centimeters thickness. The D/C boundary is defined as an alternation of fossils from *praesulcata* to *sulcata* and was placed between bed 55 and bed 56 (Gong et al., 1989). However, because *Siphonodella sulcata* fossils were newly identified in bed 53, it is demonstrated that the D/C boundary in this section is placed between bed 52 and bed 53 (Gong et al., 1989).

In order to establish magnetostratigraphy of this section, we collected fifty-four hand samples of muddy limestones from beds 50 to 68d in a locality several ten meters away from the standard section (Fig.1). The rest beds except for 8 beds of 58 to 65 represented clear

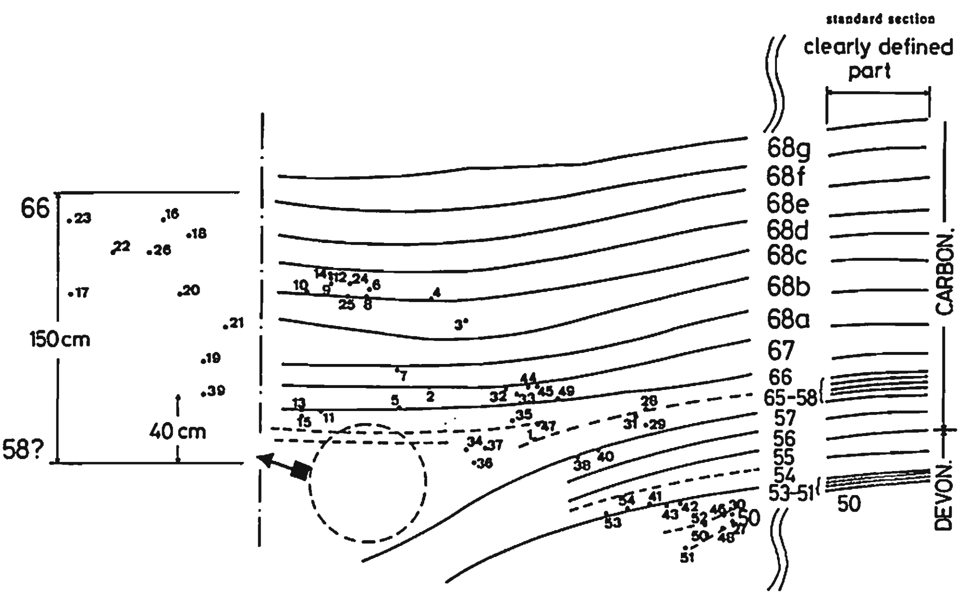

Figure 1 Sampling locality and positions in the D/C boundary section at Nanbiancun in Guilin, China.

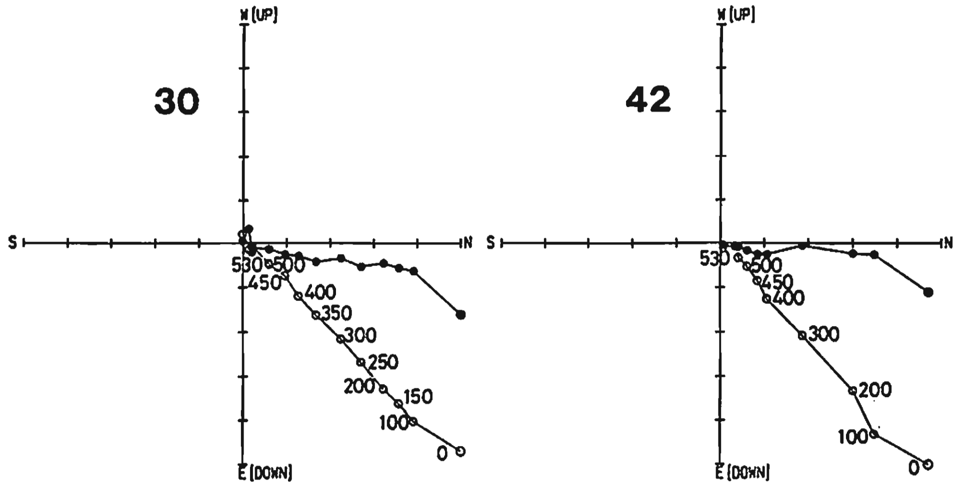

Figure 2 Typical examples of progressive thermal demagnetization treatment of investigated samples. Numbers adjacent to circles denote demagnetizing temperature in °C.

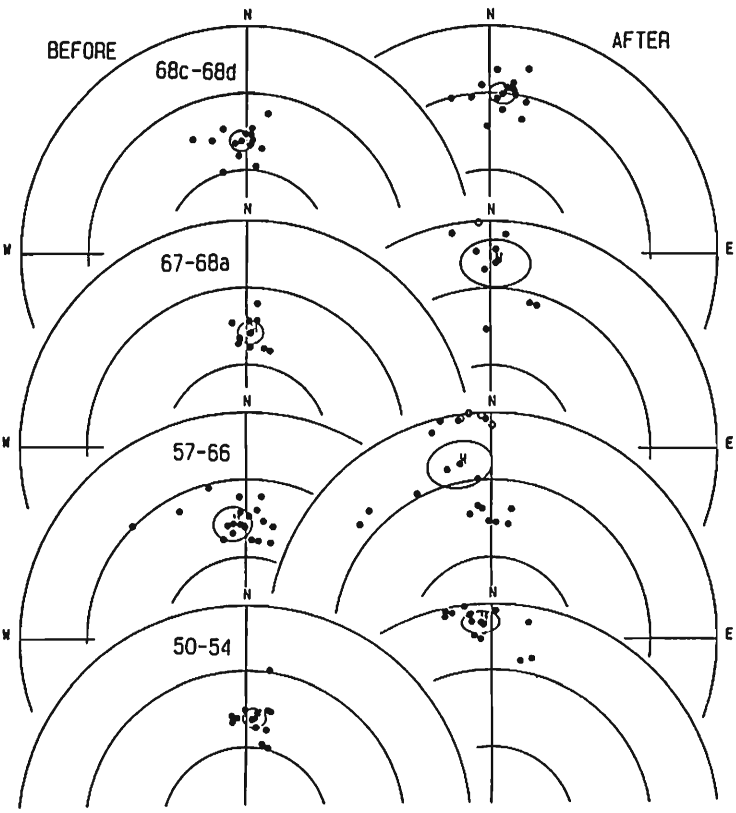

Figure 3 Characteristic directions for specimens of four groups (left; *in situ* directions, right; tilt-corrected directions).

beddings in the sampling locality. Although these 8 beds are classified by their bedding at the standard section, they could not divided into any unit in the sampling locality. Total thickness of them is only 20 cm at the standard section. On the other hand, in the sampling locality it is about 150 cm, showing great difference from the standard section (Fig.1).

Magnetic measurements of cored specimens 2.5 cm in diameter and 2.5 cm long were carried out using a cryogenic magnetometer. Magnetic stability test was investigated by progressive thermal demagnetization treatment for all specimens. All the specimens have a scanty viscous component and a single stable component. The viscous component can be eliminated with thermal treatment less than 100 °C. The single stable component could be recognized in the demagnetizing temperature steps from 100 to 530 °C (Fig.2). Characteristic directions of all the specimens were separated by a principal component analysis (PCA) by Kirschvink (1980).

All the specimens were classified to four groups on the basis of accumulation of beds where they were sampled; 50 to 54, 57 to 66, 67-68a, and 68c to 68d, except for a portion whose beddings were unclear in beds 58 to 66 (enclosed with a circle in Fig.1).

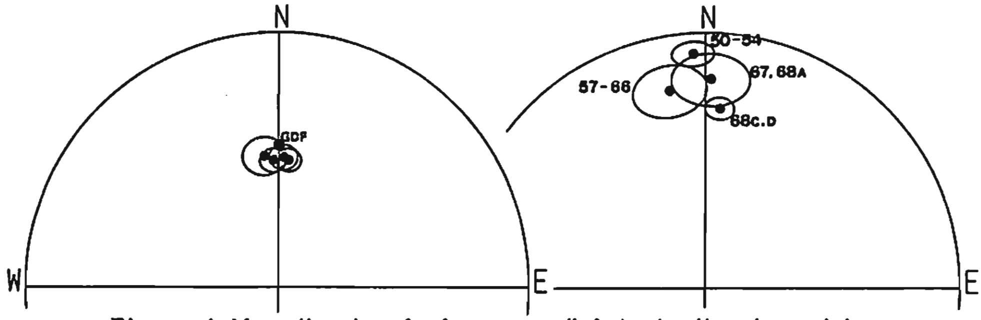

Figure 4 Mean directions for four groups (left; *in situ* directions, right; tilt-corrected directions): GDF; direction of geocentric dipole field.

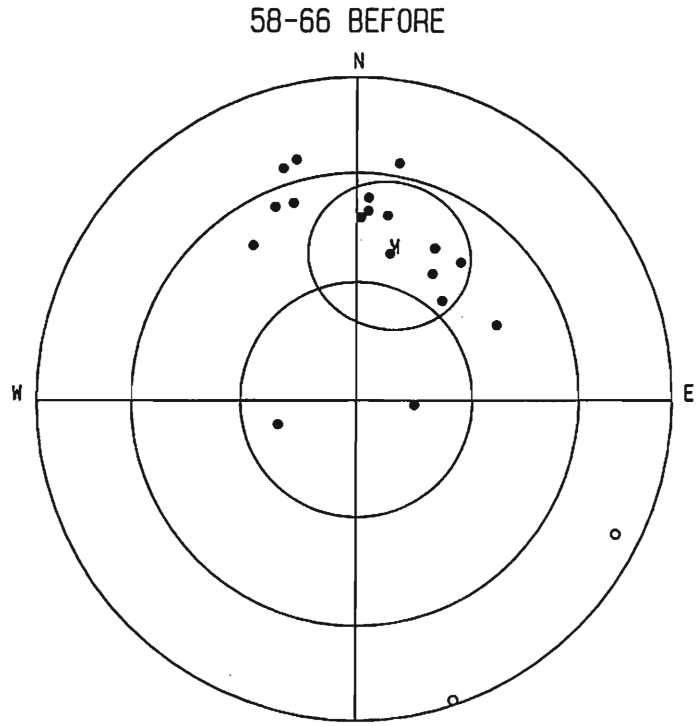

Figure 5 *In situ* characteristic directions and the mean for samples from an unclear bedding portion.

Characteristic directions and their means of these four groups are shown in Fig.3 (left; *in situ* directions, right; tilt-corrected directions). These *in situ* means are equal but tilt-corrected ones are rather scattered to each other as shown in Fig.4 (left; *in situ* means, right; tilt-corrected means). In addition, the *in situ* means closely agree with direction of geocentric dipole field (GDF). These observations lead a conclusion that the remanent magnetizations of all the samples from this locality were secondarily acquired after a slightly tilting event and quite recently.

As the surrounding limestones have a secondary magnetization overprinting a primary component perfectly, limestones from the portion characterized by unclear beddings (enclosed with a circle in Fig.1) must also have acquired a secondary magnetization. However, characteristic directions for samples from this portion are fairly scattered unlike the other groups and the mean also differs from both the other means and the GDF direction (Fig.5). These differences can be explained by regional tectonic deformation after a slightly tilting event and quite recently. Fig.6 summarizes tectonic history after sedimentation in the vicinity of this standard section.

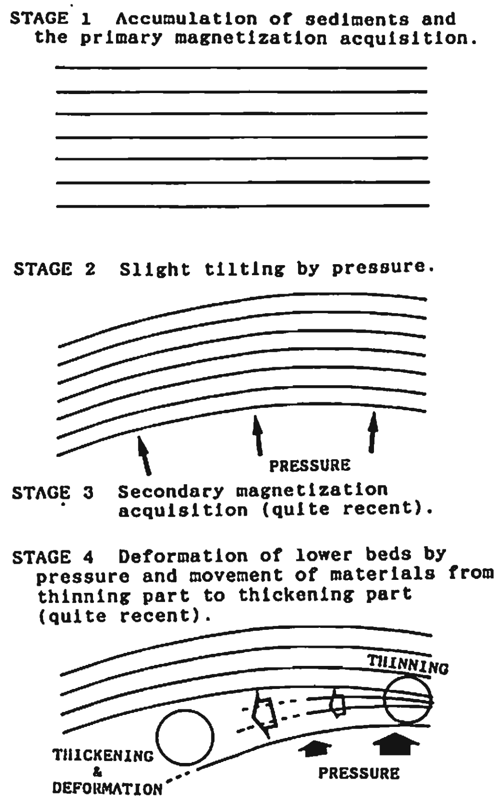

Figure 6 Regional tectonic history deduced from the the paleomagnetism.

References

Gong, X., H. Huang, J. Huang, M. Zhang, and Q. Huang (1989) *Carsologia Sinica*, **8**, 85 (Chinese with English abstract).

Kirschvink, J.L. (1980) *Geophys. J. R. astr. Soc.*, 62, 699.

PALEOMAGNETIC ESTIMATE OF EMPLACEMENT MECHANISMS OF DEEP BASALTIC VOLCANICLASTIC ROCKS IN THE SUMISU RIFT, IZU-BONIN ARC

Masato KOYAMA,[1] Stanley M. CISOWSKI,[2] and James B. GILL[3]

[1] Faculty of Education, Shizuoka University, 836 Oya, Shizuoka 422, Japan.
[2] Department of Geological Sciences, University of California at Santa Barbara, Santa Barbara, CA 93106, U.S.A.
[3] Department of Earth Sciences, University of California at Santa Cruz, Santa Cruz, CA 95064, U.S.A.

A paleomagnetic study was made on the highly vesiculated basaltic tuff breccia (the basaltic mousse) drilled by Ocean Drilling Program Leg 126 from the Izu-Bonin backarc, Sumisu Rift, to estimate the mode of its emplacement. Thirty four 10-cm^3 minicore samples were collected from almost all the horizons of the basaltic mousse. Stepwise thermal and alternating-field demagnetization experiments show that the natural remanent magnetization of many samples is mainly composed of a single stable component. Although remanence inclinations are not expected to be disturbed by rotary drilling, the measured inclinations of remanence show a random directional distribution as a whole (Fig. 1). The remanence inclinations, however, show directional consistency on a smaller scale (Fig. 2). High-density sampling and measurements from a limited interval of drilled cores, and the measurement of small disks cut from a single minicore sample show that there is directional consistency over several centimeters. Strong and stable remanent magnetization, the existence of remanence direction consistency, and the fresh lithology of the samples suggest the thermal origin of remanence. Combining the paleomagnetic results with other geological, petrographic, and paleontological characters (Gill et al., 1990; Taylor, Fujioka, et al., 1990), the basaltic mousse can be interpreted as a subaqueous explosion breccia produced by deep-sea pyroclastic fountaining.

Figure 1. Histogram showing the directional distribution of remanence inclination of the basaltic mousse samples. Lithic clast content (clast% by volume) of each sample is shown by patterns.

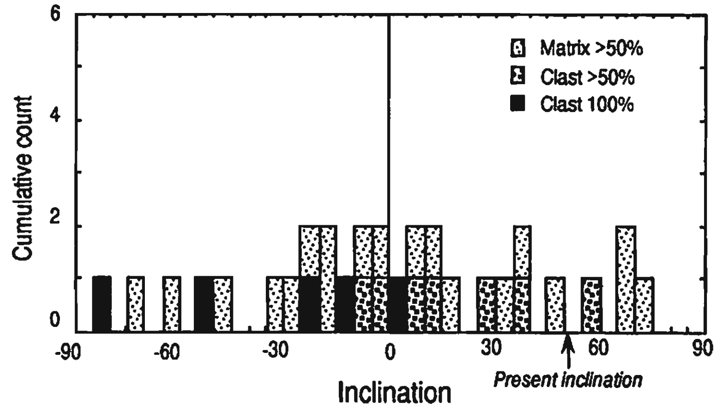

Figure 2. Equal area projection showing remanence directions of small disk specimens taken from the selected minicore samples. Disks from the same minicore are circled with a solid line. Solid and open circles are on lower and upper hemispheres, respectively.

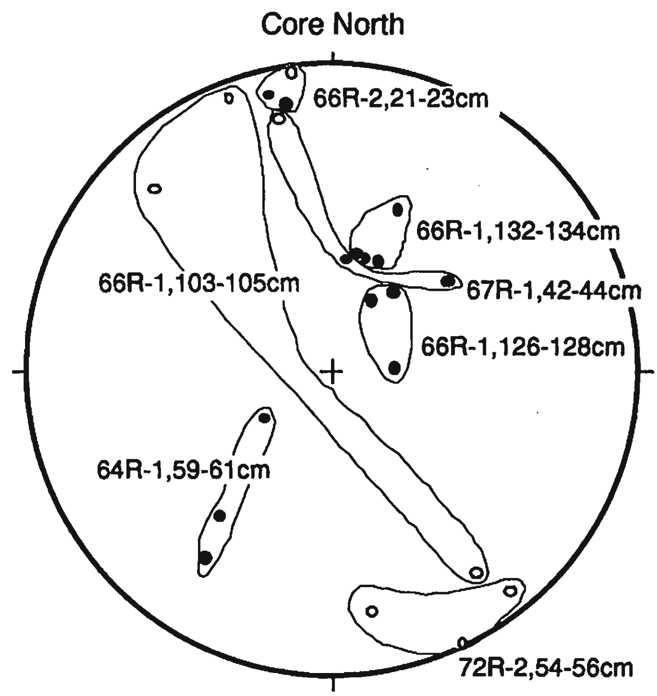

References

Gill, J. B., Torssander, P. Lapierre, H., Taylor, R., Kaiho, K., Koyama, M., Kusakabe, M., Aitchison, J., Cisowski, S., Dadey, K., Fujioka, K., Klaus, A., Lovell, M., Marsaglia, K., Pezard, P., Taylor, B., and Tazaki, K. (1990). *Science*, **248**, 1214-1217.

Taylor, B., Fujioka, K., et al. (1990). *Proc. ODP, Init. Rept.*, **126**, (Ocean Drilling Program, College Station, TX).

(In press in *Proc. ODP, Sci. Results*)

PALEOMAGNETIC AND Ar^{40}/Ar^{39} DATING STUDIES OF THE MAWSON CHARNOCKITE AND SOME ROCKS FROM THE CHRISTENSEN COAST

Minoru FUNAKI[1] *and Kazuo SAITO*[2]

1: National Institute of Polar Research, 9-10 Kaga 1-chome, Itabashi-ku, Tokyo 173, Japan
2: Yamagata University, Faculty of Sciences, Yamagata 990, Japan

1. Introduction

The Christensen Coast locates between Queen Maud Land and Wilkes Land divided by the Lambert Glacier in East Antarctica. This area consists of high-grade metamorphic rocks of Proterozoic to Archaean crust (Sheraton and Black, 1984). A total of 444 paleomagnetic samples were collected from 27 sites of Mawson Station area (Mawson Station, Rumdoodle Peak and Painted Hill), Scullin Monolith, Larsemann Hills and Vestfold Hills (Fig. 1). The samples consist of charnockite, biotite gneiss, pyroxene gneiss, granitic gneiss, tanalite, pegmatite and dolerite.

A pilot paleomagnetic study was reported for dolerite dyke rocks (1,000 Ma) from Vestfold Hills (Embleton and Arriens, 1973). The NRM direction was decided to be inclination (I)=−42.5°, declination (D)=107.5° with confidence of 95% probability (α_{95})=11°. Virtual geomagnetic pole (VGP) position located at I=17°S, D=13°E where is quite similar to the Cambro-Ordovician VGP positions from East Antarctica.

2. Experimental results

2-1 AF and thermal demagnetization of NRM

Representative 3 samples from every site were demagnetized by alternating field (AF) up to 50 mT with 5mT intervals, as shown in Fig. 2. The NRM of Mawson charnockite (intensity $5.05 \times 10^{-6} Am^2/kg$) demagnetized clearly; reversed NRM (downward) inclination appeared after the demagnetization more than 25mT, even if the original NRM inclinations were normal polarity (Fig. 2(a)). The NRM ($4.2 \times 10^{-7} Am^2/kg$) of granitic gneiss from Scullin Monolith was relatively stable between 25 to 40 mT, although it showed zigzag variation throughout the AF demagnetization (Fig. 2(b)). The NRM ($5.53 \times 10^{-7} Am^2/kg$) of the biotite gneiss from Larsemann Hills was demagnetized smoothly up to 30 mT, then small zigzag variations appeared. This NRM was the most stable among the samples used in this study as shown in Fig.2(c).

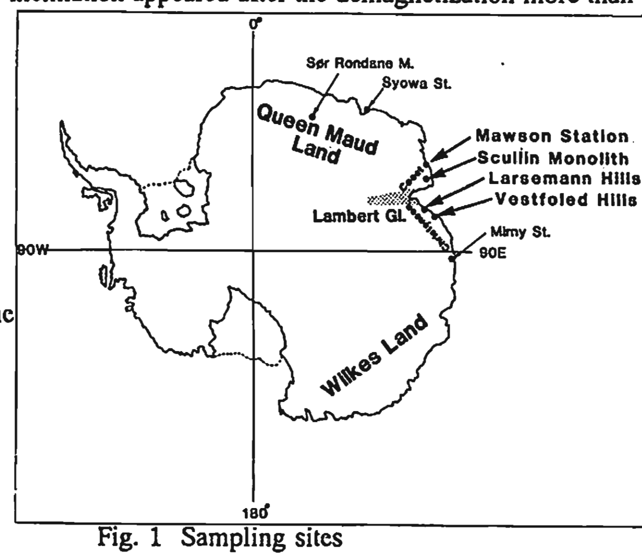

Fig. 1 Sampling sites

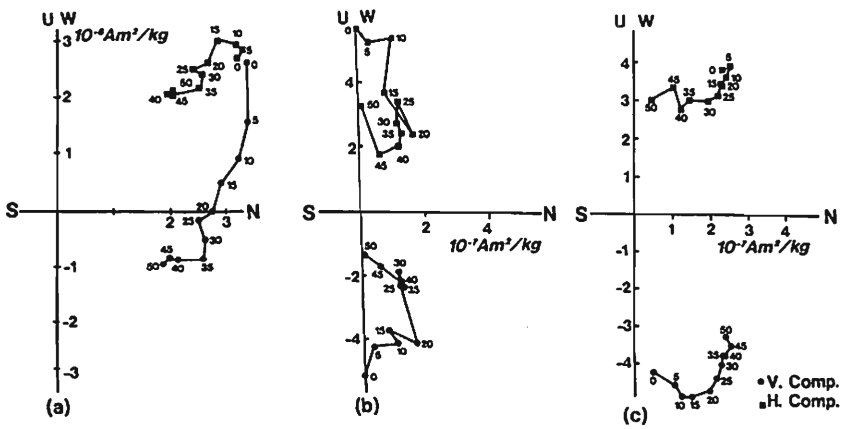

Fig. 2 AF demagnetization curves, (a): Mawson charnockite, (b): granitic gneiss from Scullin Monolith, (c): biotite gneiss from Larsemann Hills.

However, the samples of other gneiss, dolerite dyke and pegmatite dyke rocks from Mawson Station area, Scullin Monolith, Larsemann Hills and Vestfold Hills were quite unstable against AF demagnetization.

Other 3 representative samples from every rock type were demagnetized thermally in air from room temperature to 600°C or 630°C with interval of 50°C as shown in Fig. 3. The demagnetization curve of Mawson charnockite showed zigzag variation of the NRM intensity up to 550°C but the intensity decreased steeply from 500° to 550°C. The NRM direction of this sample did not change drastically between 350° and 500°C. The NRM intensity of granitic gneiss from Scullin Monolith decreased smoothly between 280° and 580°C and the direction did not change largely between 230° and 480°C. The biotite gneiss from Larsemann Hills showed gradually decreased intensity curve from 230°C to 480°C and small directional variations from room temperature to 530°C. The abrupt increase of intensity from 580° to 630°C may be due to chemical alteration of the magnetic minerals during heat treatment. These 3 samples in Fig. 3 showed similar thermal demagnetization characteristics up to 400°C; the magnetization decreased up to about 130°C then increased up to about 300°C. These variations are explained overprint of the upward NRM component demagnetized before 350°C and the downward one survived up to about 500°C.

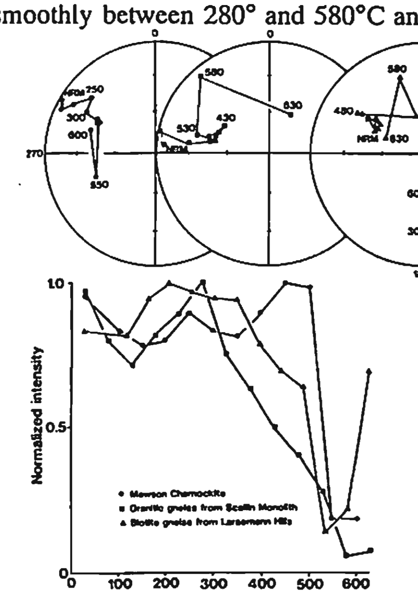

Fig. 3 Thermal demagnetization curves

3-2 NRM directions

The mean NRMs of the samples to have relatively hard NRM components against AF demagnetization were obtained for the original NRM and the NRM after AF demagnetization to 5, 10 and 15 mT. Subsequently the samples were thermally demagnetized at 380°, 450° and 500°C. A part of the results were listed in Table 1.

The original NRM direction of 88 samples of Mawson charnockite scattered widely. It clustered around I=13.3° and D=317.1° with α_{95}=9.0° and precision parameter (K)=5 by AF demagnetization to 10 mT. The best clustering was obtained as I=44.3° and D=315.0° with α_{95}=2.3°and K=44.

The original NRM of granitic gneiss from Scullin Monolith scattered around I=30.4° and D=271.5° with α_{95}=35.2°, although the number of samples was only 5. The clustering of NRM was not improved drastically by the AF demagnetization, but the best clustering appeared toward I=49.5° and D=273.4° with α_{95}=20.8° by thermal demagnetization to 380°C.

The NRM of biotite gneiss from Larsemann Hills made a cluster around I=68.1° and D=304.1° with α_{95}=13°, although the cluster was improved (α_{95}=11.2°) by the AF demagnetization to 10 mT. The best one also appeared by thermal demagnetization at 380°C as I=62.9° and D=295.5° with α_{95}=7.8°.

Table 1. Paleomagnetic results of the rocks from the Christensen Coast

SITE	MAWSON ST.	SCULLIN M.	LARSEMANN H.
Rock type	Charnockite	Granitic gn.	Biotite gn.
Demag	450°C	380°C	380°C
N	88	5	23
R	2.28×10^{-6}	1.64×10^{-7}	7.95×10^{-8}
I	44.3	49.5	62.9
D	315.0	273.4	295.5
K	44	15	16
α_{95}	2.3	20.8	7.8
LAT	9.3S	26.5S	32.8S
LON	22.9E	7.4W	27.8E

3-3 Thermomagnetic properties and microscopical observations

Thermomagnetic (Js–T) curves were obtained for the samples to have reliable NRM components by a vibrating sample magnetometer under 1.0 T of external magnetic field in 10^{-4}Pa atmospheric pressure from room temperature to 650°C. The Js–T curve of the first run cycle of Mawson charnockite was irreversible. The observed magnetization (Js) 0.129 Am^2/kg decreased gradually up to 400°C, then a magnetic hump appeared between 400° to 580°C in the heating curve. Clearly defined Curie point was identified at 580°C. In the cooling curve, the magnetization increased steeply from 580°C (Curie points) and the magnetization 0.325 Am^2/kg appeared at room temperature. In this sample, pyrrhotite grains less than 30μm in diameter were observed frequently by a microscope. Magnetite grains more than 50μ in diameter were also recognized, while the amount was smaller than that of the pyrrhotite grains. The 1st run Js–T curve of charnockite is explained by both magnetization change of pyrrhotite and magnetite; the Js of pyrrhotite decayed before 320°C; magnetite is newly formed from the oxidation of the pyrrhotite (hump of the Js–T curve). The Js–T curve of granitic gneiss (Js=0.0395 Am^2/kg) from Scullin Monolith showed reversible curves with the principal Curie point at 580°C and minor one at 235°C. Almost pure magnetite and titanomagnetite were inferred for the magnetic carrier mineral in the granitic gneiss. The Js–T behavior of biotite gneiss from Larsemann Hills (Js=0.0673

Am^2/kg) consisted with that of the granitic gneiss from Scullin Monolith, except the Curie point at 235°C; magnetite is a magnetic mineral in the sample.

4 Dating of Mawson charnockite

Dating of Mawson charnockite from Mawson Station was performed by K/Ar and $^{40}Ar/^{39}Ar$ methods. An age 475±15 Ma was decided by K/Ar dating, where K=5.28±0.06 %, $^{40}Ar=111.4\pm3.8\times10^{-6}$ cmSTP/g and air content=0.9%. The results indicated that the fraction of each temperature located on an isochron line as shown in Fig. 4. From this distribution, a ratio of $^{40}Ar/^{36}Ar$ in trapped Ar was obtained as 1222±52 and an isochron age was determined as 445±27 Ma. This ratio can explain that ^{40}Ar was accumulated in the parent substances (tanalite) of charnockite magma and the ^{40}Ar was caught in the charnockite during its crystallization.

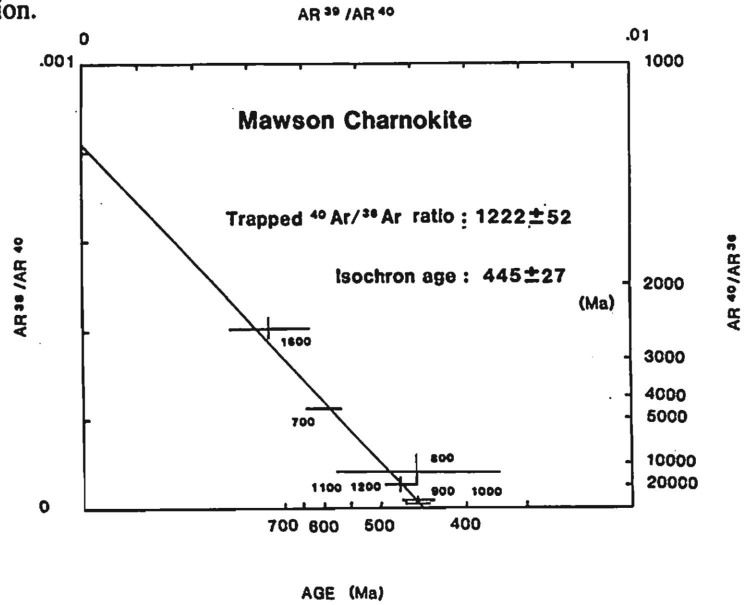

Fig. 4 Isochron age of Mawson charnockite

Almost same age of 444±18 Ma as taken from plateau age spectrum, where the ratio was given as 1222±52. As the ratio $^{40}Ar/^{36}Ar$ of the every fraction, except that of maximum and minimum temperatures, was sufficiently high, obtained ages were not so different if the ratio was given as 295.5 (ratio in present atmosphere). The apparent old age at 700°C fraction of the $^{40}Ar/^{39}Ar$ analysis would be owing to an artifact, such as redistribution of radiogenic ^{40}Ar or recoil effect during the neutron irradiation.

5. Discussion

The NRM carrier of Mawson charnockite is inferred to be ferrimagnetic pyrrhotite and magnetite. Usually the NRM of pyrrhotite can not be believed paleomagnetically due to its crystal anisotropy and unknown formation age. As the magnetic pyrrhotite is transformed easily into nonmagnetic one by heating less than 320°C, the NRM of original magnetite can be taken by thermal demagnetization higher than 320°C in temperature. The NRM resulting from newly formed magnetite from pyrrhotite during the thermal demagnetization may be negligibly weak, because the residual magnetic field in the thermal demagnetizer was less than 50nT. From these viewpoints, thermal demagnetization is the best demagnetization method to take reliable NRMs from these samples.

The NRM of the granitic rock from Scullin Monolith were not so stable as a whole against AF demagnetization, but the reversed NRM components was recorded in the samples and the reversed one was survived to more than 30 mT of sufficient high coercivity. The NRM carriers of magnetite and titanomagnetite with reversible Js–T curve do not have any magnetic problems such as pyrrhotite. It may be, therefore, that the reversed NRM component showed some meaningful paleomagnetical information when the samples were cooled down from the Curie point.

As the reversed NRM of biotite gneiss from Larsemann Hills was the most stable against AF demagnetization. Since the NRM carrier of magnetite and its Js–T characteristics were quite similar to the granitic gneiss from Scullin Monolith, the NRM can be believed paleomagnetically.

The clustering of NRM by the thermal demagnetization was better than that by the AF demagnetization for the rocks from Scullin Monolith and Larsemann Hills. The reason can not be focused in present, but there is a possibility of some magnetic noise resulting from FeOOH and/or pyrrhotite which were not identified by the Js–T analyses and microscopical observations because of too fine–grained and small amount.

The mean NRM directions, as listed in Table 1, are the most significant paleomagnetic data from each site from these viewpoints. The significant NRMs might be acquired after through the 580°C at the cooling stage of final metamorphism in the respective areas.

The $^{40}Ar/^{39}Ar$ age of Mawson charnockite 445±27Ma was younger than K/Ar age of 475±15 (this study) and 535 Ma (Ravich and Krylov, 1964). This is the reason why the K/Ar age indicates average age obtained by every fraction in the plateau age of the $^{40}Ar/^{39}Ar$ method. The geochronological consistency between isochron age (445±27 Ma) and plateau age (444±18 Ma) for the Mawson charnockite gives sufficient reliability of these ages. Recently $^{40}Ar/^{39}Ar$ ages were measured from Scullin Monolith (455 Ma) and Larsemann Hills (443 Ma) by Takigami (private communication). Early Paleozoic metamporphism

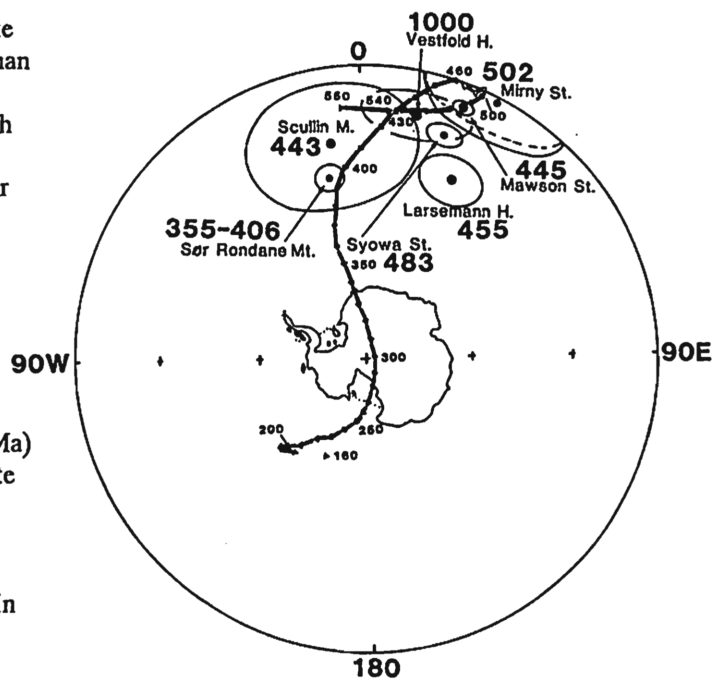

Fig. 5 Paleozoic VGP positons for East Antarctica and the APWP for Gondwana

related to the upper Pan–African mobile belt (600–450 Ma) was commonly observed in wide area between Enderby Land and Western Wilkes Land by dating K/Ar, $^{40}Ar/^{39}Ar$ and Rb/St methods, e.g. Lützow Holm Bay area (Shibata et al., 1985), Sør Rondane Mountains (Takigami and Funaki, 1991), Mawson charnockite (this study, Ravich and Krylov, 1964) and Mirny Station (McQueen et al., 1972). These similar ages in the Christensen Coast indicate that this area was metamorphosed and remagnetized almost simultaneously at early Paleozoic Period under the upper Pan–African mobile event.

The VGP positions were calculated from the mean NRM directions, as listed in Table 1. Figure 5 showed their positions with the α_{95} values and ages obtained from this study and previous works from Wilkes Land and Queen Maud Land. A statistically estimated apparent polar wander path (APWP) for Gondwana (Thompson and Clark, 1982) was also shown in this figure, where the reconstruction model of Smith and Hallam (1970) was adopted. The VGP position of granitic gneiss from Scullin Monolith is satisfied with the APWP at 443 Ma taking the confidence into consideration, although the confidence was very large as α_{95}=20.8°. That from Mawson charnockite did not fit the APWP in the figure. When the confidence of APWP around 445±27 Ma (α_{95}=8°) is considered, the VGP consists with APWP. However, the VGP of biotite gneiss from Larsemann Hills did not fit with the APWP under consideration of their α_{95} values. This disagreement is considered due to (a) tectonical displacement of Larsemann Hills, (b) effect of the magnetic anisotropy of biotite gneiss, (c) inconsistency between magnetization age and dating age by thermo–viscous remanent magnetization (d) non–dipole effect of the geomagnetic field,and (e) inaccuracy of the APWP for Antarctica, etc. It is difficult to decide which term is the most effective in present, but items (a) and (b) must be further considered in detail.

6. Conclusion

The VGP positions from Mawson charnockite, Scullin Monolith and Larsemann Hills were newly obtained. The first and second VGPs distributed around the APWP of Gondwana from Cambrian to Ordovician periods, but the last one did not fit to the APWP. Many kinds of gneiss acquired unstable NRM toward the present geomagnetic field direction. Geochronological ages were decided as 475±15 Ma (K/Ar), 445±27 Ma ($^{40}Ar/^{39}Ar$ isochron age) and 444±18 Ma ($^{40}Ar/^{39}Ar$ plateau age).

<u>References:</u>

Embleton, B.J.J. and Arriens, P.A. (1973), Geopys. J.R. astr. Soc., **33**, 239–245.

Fedorov, L.V., Grikurov, G.E., Kurinin, R.G. and Masolov, V.N. (1982), Antarctic geoscience, 931–936.

Funaki, M. and Wasilewski, P. (1986), Mem. Nat. Inst. Polar Res. Spec. Issue, 43, 37–47.

Hofmann, J. (1991), Geological Evolution of Antarctica. 107–112.

McQueen, D.M., Scharnberger, C.K., Scharon, L. and Halpern, M. (1972), Earth Planet.Sci. Lett., **16** 433–438.

Ravich, M.G. and Krylov, A. Ya (1964), Antarctic Geology. 579–589.

Sheraton J.W. (1982), Antarctic Geoscience. 489–497.

Shibata, K., Yanai, K. and Shiraishi, K. (1985), Mem. Nat Inst. Polar Res., Spec. Issue, 37, 164–171.

Smith, A.G. and Hallam, A. (1970), Nature, **225**, 139–144.

Takigame, Y. and Funaki M. (1991), Proc. NIPR Symp. Antarct. Geosci. 5, in press.

Thompson, R. and Clark, R.M. (1982), Earth Plan. Sci. Lett. 57, 152–157.

FORMATION OF THE VOLCANIC FRONT

Yoshitsugu FURUKAWA

Department of Geology and Mineralogy, Faculty of Science, Kyoto University, Kyoto 606-1, Japan

The volcanic front is the key feature for understanding the magmatic activities under arcs. It is well-known that depth of the subducting slab is about 100 km at the volcanic front for various arcs. Tatsumi (1986) proposed a formation mechanism of the volcanic front considering the constancy of the slab-depth under the volcanic front. In his model diapiric uprise of partially molten mantle materials due to the buoyancy of magma is assumed in order to form the volcanic front. However, it is pointed out that uprising velocity of diapirs is too slow to keep temperature of diapirs above solidus (e.g. Turcotte, 1981).

Ascending velocity of basalts has been estimated to be 0.01~1 m/s for alkali basalts (e.g. Spera, 1987). Considering the high ascending velocities, crack propagation is the plausible mechanism of magma upwelling. It is suggested that magma segregation from solid matrix due to its buoyancy is relatively fast compared with velocities of mantle convection (Mckenzie, 1984). Therefore, it is inferred that in partially molten mantle magma will segregate with relatively high velocities and then upwell by the crack propagation mechanism (e.g. Spence and Turcotte, 1985).

Crack propagation direction is controlled by stress field and tends to be parallel to the direction of the maximum principal stress (e.g. Shaw, 1980). Stress field caused by the induced flow in the wedge mantle under arcs is calculated with a two-dimensional variable viscosity model. In Fig. 1 estimated magma migration paths are plotted. In the wedge mantle it is considered that water is supplied from the subducting slab. The water reduces the solidus temperature and magma will be generated in the wedge mantle. Hatched area denotes partially melting mantle assuming the wet solidus temperature of 1000 °C.

This figure shows that magma migrating paths curve and diverge toward the wedge corner. Near the corner, magma bodies cannot accumulate and lose its buoyancy. Thus magma will solidify in the low-temperature wedge corner and cannot uprise to the surface. In contrast, magma will uprise easily in the back-arc side due to the upward propagation direction of magma-filled cracks and relatively high deviatoric stress. In this zone volcanic belt will be formed. Depth of the slab at the location of this change of propagation direction is about 100 km. Therefore, it is concluded that this change of propagation direction causes the volcanic front. Estimated seismic velocity structure under the Tohoku arc shows low velocity regions under the volcanic front (Hasegawa et al., 1991). Distribution of the low velocity is consistent with the zone of partial melting and network of magma-filled fissures in the mantle wedge estimated in this study.

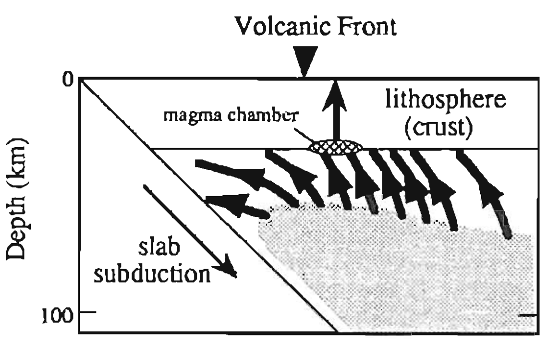

Fig. 1 Estimated propagation paths of magma-filled cracks (solid arrows) from the partially moltem mantle (hatched area) in the wedge mantle.

References

Hasegawa, A., D. Zhao, S. Hori, A. Yamamoto, S. Horiuchi (1991) Nature, 352, 683.
Mckenzie, D. (1984) J. Petrol., 25, 713.
Shaw, H.R. (1980) Physics of Magmatic Processes, Princeton University Press, 201.
Spence, D.A. and D.L. Turcotte (1985) J. Geophys. Res., 90, 575.
Spera, F.J. (1987) Mantle Metasomatism, Academic Press, 1
Tatsumi, Y. (1986) Geophys. Res. Lett., 13, 717.
Turcotte, D.L., (1981) J. Volcano. Geotherm. Res., 10, 267.

Geophysical Features of Japan Sea

Yukari NAKASA (1), Tetsuzo SENO (2), T.W.C.HILDE (3) and Hajimu KINOSHITA (2)

(1) Department of Earth Sciences, Chiba University, Chiba City, Chiba 260
(2) Earthquake Research Institute, Univ.Tokyo, Bunkyo-ku, Tokyo 113
(3) Geodynamics Research Institute, Texas A&M University, College Station, TX, U.S.A.

Introduction

Series of geophysical studies on gravity, magnetics, seismic structures and radiometric ages of the Japan Sea have been performed, but the tectonic evolution of the Japan Sea has not been fully understood yet due to various complexities of its formation processes. This study focuses mainly on clarifying details of geophysical characteristics of main basins in the Japan Sea: the Japan Basin and the Yamato Basin. These two basins differ considerably in topography, geological and geophysical characteristics as well as seismic structures. Three major results are described in this paper. Firstly, the isobase map of the Japan Sea which reveals the topographic distribution of acoustic basement is obtained. Secondly, the relation between topography and gravity based on loading responses using an admittance function shows that the central part of the Japan Sea is partly supported by elasticity of the plate. Thirdly, a contour map of the magnetic anomalies is obtained in the northeastern part of the Japan Basin where the presence of weak magnetic lineations trending N60°E-N40°E had been identified. Some discussions are attempted on formation models of the Japan Sea by taking into consideration available data and their analyses.

New Acoustic Basement Topography

Several isobase maps of sediments in the Japan Sea which reveal acoustic basement features (Beresnev and Kovylin, 1968; Hilde and Wageman, 1975; Ludwig, et al., 1975; Ishiwada, et al., 1984; Tamaki, 1988; Seama and Isezaki, 1990) were referred to for the purpose of constructing a new isobase map. Figure 1 shows a new isobase map: the thickness of a sediment layer below the ocean floor. Acoustic basement features which can be made clear only through scraping the sediment layer off the top of basement differ obviously for the Japan and the Yamato basins. The feature of the Japan Basin is fairly rugged compared with the relatively smooth basement of the southern part of the Yamato Basin. The Yamato Basin is mostly filled with Neogene and Quaternary terrigeneous and hemipelagic sediments of 3,000-5,000m (Tamaki and Pisciotto, et al., 1990). Geological classification of sedimentary layers of the Japan Basin, however, has not been achieved yet. One of isobase maps derived from seismic reflection data by the recent Japan-Russian Japan Sea Joint Program (1989-1991) was utilized to

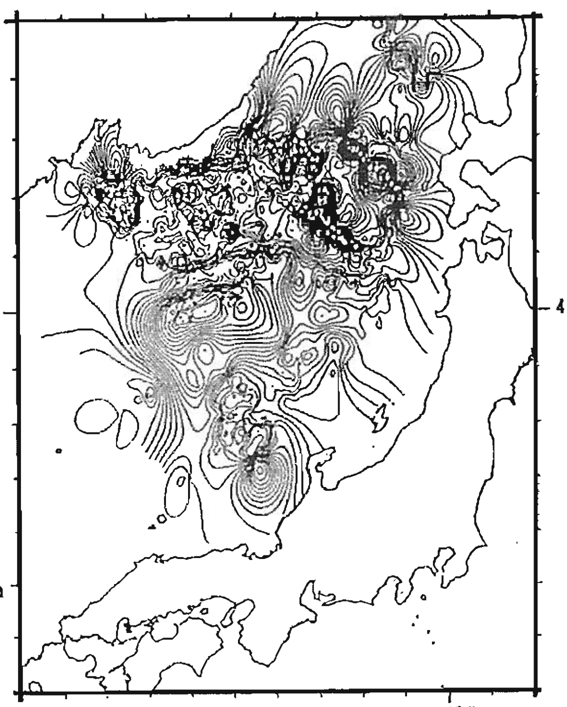

Fig.1 Isobase map of the Japan Sea. Some parts of counter lines are smeared inevitably due to a large scale reduction. More details will be presented in our future article.

construct a new isobase map of this region. This kind of isobase map is a basic tool for consideration of the loading of sediment mass in order to clarify responses of crust on gravity and magnetic lineation patterns of the Japan Sea. For instance, it is necessary to remove loading of sediment mass in order to obtain the relationship between the depth of the oceanic basement as proposed by Crough (1983):

[Basement depth after sediment loading correction (m)]
= [bathimetric depth (m)] + 600 × [two-way travel-time in sediment (sec)]

Gravity and Crustal Response

The thickness of elastic plates has been investigated using both topography and gravity anomalies. In general, the oceanic lithosphere has an elastic flexural rigidity against loads such as volcanoes, islands, seamounts and others force to bend the plate. The thickness of an elastic plate can be estimated from its flexure. It is well established that the gravity observed at the sea surface can be correlated with topographic features. There are typically three types of models for mechanical compensation. This study utilizes the admittance functions given by Louden (1981) to investigate the compensation mechanism of the Japan Sea. Three types of models are tested. The first is a model without gravitational compensation in which the gravity field anomaly is solely produced by topography of the sea floor. The second is a local isostasy model introduced by Airy (1855) in which compensation is attained by thickening the crust. The third is a plate model of elastic strength. The elastic plate is assumed usually $\frac{1}{2}$ ~ $\frac{1}{3}$ of the seismological thickness of the plate.

Results

The response of gravity in the Japan Sea indicates different features in the two basins. The southern part of the Yamato Basin has a 14*km* thick crust floating isostatically on the mantle material (Fig.2). The central and the northern parts of the Yamato Basin can be treated as the thin and elastic plate model. The thickness of the crust gradually decreases from the center to the north. The northern part of the Yamato Basin is the boundary area between the Yamato Basin and the Japan Basin. The crust of the Japan Basin (8-9*km* thick) is supported by its own elastic rigidity, in addition to regional isostatic bouyancy. The results of the calculations are plotted in Figure 2 showing a relation between admittance versus wave number with $\pm 1\sigma$, where σ is standard deviation. Similar results, i.e., the 14*km* crust in the southern part of the Yamato Basin and the 8-9*km* crust of the Japan Basin have been obtained by seismological experiments (DELP 1985 and Japan-Russian Japan Sea Joint Program) compatible to the present calculation.

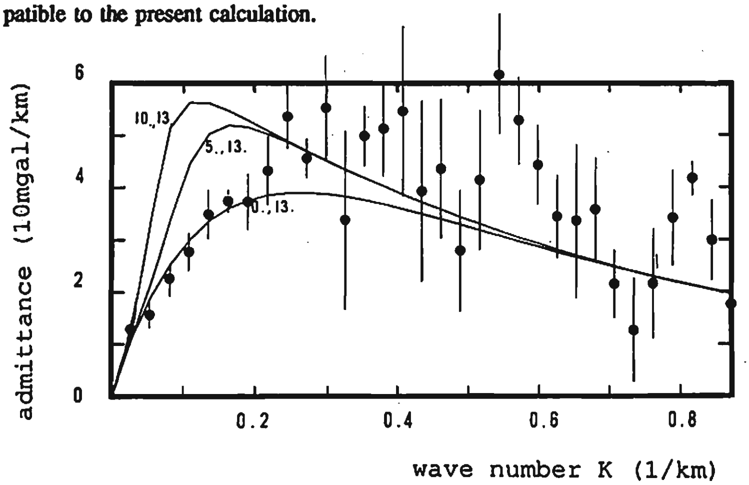

Fig.2 Typical example of a relation between observed (solid circles) and calculated (solid line) admittance. Numbers attached are thickness of elastic plate and crustal thickness (e.g. 0.,13. for the bottom curve).

Re-examination of Magnetic Anomalies

Sets of data from NGDC cover the data obtained from scientific cruises performed until 1986 in the Japan Sea. Magnetic anomaly data are systematically shifted from zero level due to biasing of local IGRF (Internat.Geomag.Ref.Field) (Isezaki, 1973; Matumoto and Isezaki, 1986). All refined data calculated on a basis of IGRF85 were used. Magnetic anomalies from ETOPO5 and SEASAT reveal some lineation patterns in this area.

Four steps used for analyzing magnetic data and some details are described as follows: (1) we confirm that the magnetic anomaly profiles are independent of acoustic basement features which is newly obtained through this study based on seismic profiles. (2) We pick up profiles in which anomalies variation resemble each other in the basin areas, and select the representative profiles in order to compare to a magnetization model of basement. (3) We try to make a model from these representative profiles using a magnetic modeling program revised by J. L. Labreque (1986) and the "Geologic Time Scale" given by Harland, et al. (1989). The magnetic modeling program has 33 parameters and all of them are changeable. Parameters changed to make better fitting are mainly 1) the strength of magnetization, 2) the thickness of a magnetized layer, and 3) the half spreading rate. (4) We make a grid data of magnetic anomalies in the regions where lineation patterns can be seen obviously. We recalculate the trend of lineations by stacking line profiles. Grid data which cover the area of 30.0°N-48.0°N and 127.0°E-143.0°E are obtained using Brigg's method (1974) and Akima's method (1970), based on the 1986-version NGDC dataset. A region selected for the present study is spread within the rectangle of 40.0°N-43.0°N and 130.0°E-138.0°E.

Results

It is attempted to compare 3-dimensional graphic images with 2-dimensional profile maps of the basins in the Japan Sea. It seems that there are many faults and fracture zones within the basement because the patterns of profiles are changing apparently among track lines. Many profiles must be also distorted by sckewness, some tectonic motions of later stage after magnetization, and/or thermal events due to later reheating. The Japan Basin is devided into two parts - the northeastern and the southwestern parts. Correlating magnetic profiles with the opening sea-floor model, five cases listed in Table 1 can be tested. Comparison of the calculated profiles with field observation data is tried in order to find out best fitting of the field data to these models.

Table 1

No	Anomaly number	Chron age (Ma)	Half spreading rate (*cm/yr*)
(1)	12-17	31-38	4.0
(2)	13-20	34-45	6.0
(3)	20-24	43-57	2.5-3.0
(4)	5C-5D	16-19	9.0
(5)	5D-6AA	18-23	7.5

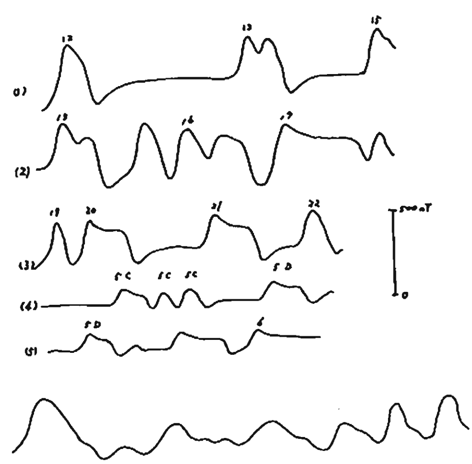

Fig.3 Magnetic anomaly patterns calculated from basement magnetization (top (1) through (5)) based on assumption given in Table 1 as compared to magnetic profile stacked (bottom). Details are given in the context.

The comparison of the results from the northeastern and from the southwestern parts of the Japan Basin shows that the model No.(4) seems to be best fit to the stacked magnetic anomaly pattern (bottom curve) in this area. Figure 3 shows five model profiles (top part of five) and one of magnetic profiles in the studied area. The age estimated by using magnetic modelling is also compatible with other geophysical data: heat flow data and radiometric data (ODP reports in preparation by Tamaki; private communication).

Discussions

The formation process of the Japan Sea is thought to have occurred by the following two steps; the Japan Basin was initially formed by normal sea-floor spreading after the separation of Japanese landmass from Siberia and the spreading propagated westward at about 15-25 Ma (late Oligocene to early Miocene). The propagation of the spreading center westward was likely to have occurred in view of magnetic lineations cut by hidden faults and radiometric ages of ODP cores (ODP reports in preparation by Tamaki; private communication). The complexity of the magnetic lineations can be correlated to later destruction of the crust. On the contrary, the Yamato Basin was intruded by magma among the Yamato Ridge (continental fragments) and the Japanese mainland during and after the sea-floor spreading of the Japan Basin. However, according to the presence of the thrust faults and a thrust type of earthquake mechanisms on the eastern margin of the Japan Sea, and the presence of a compressional stress field at present imply the change in stress field after the formation of the Japan Sea: extension to compression. There is a difference in the avarage bathymetric depth; the Japan Basin is deep and the Yamato Basin is slightly shallow. Also there is a difference of acoustic basement features; the Japan Basin has a rugged surface and the Yamato Basin is smooth. Differences in the depth of the Mohorovicici's discontinuity indicates in the Japan Basin the Moho depth is increasing westward compared to a fairly flat distribution of the Moho depth in the Yamato Basin. The correlation between gravity and topography shows that the southern part of the Yamato Basin has a crust of $14km$ thickness compatible with the result of seismic structures, and the southern part of the Yamato Basin is supported isostatically. The central to northern part of the Yamato Basin and the Japan Basin are compensated partly by the elasticity of the crust. This means that the topographic displacement due to the load of the Yamato Ridge and other highs can not be explained only by the Airy type isostasy but a combination of isostasy and the elastic rigidity. The average thickness of the crust is gradually decreasing from the north of the Yamato Basin to the Japan Basin. The result seems to be consistent with the seismic structures obtained to date.

Conclusions

A number of geophysical characteristics of the Japan Sea back-arc basin are clarified by the present study as well as many geoscientific knowledges and facts obtained by numerous studies in this area. Major concerns of the present authors are: (1) Revision of isobase maps from the entire Japan Sea area with special stress on the isobase map of the Japan Basin (the northern part of the Japan Sea) by obtaining seismic reflection data by the courtecy of USSR (Russian) - Japan joint efforts of 1989-1991. (2) Identification of some magnetic lineation patterns in the northeastern corner of the Japan Basin for which a set of new magnetic data was offered by the courtecy of Ocean Research Institute, Univ. Tokyo. The estimated age of the ocean floor opening as well as the spreading rate have been obtained by the model experiment and the age estimation is in accordance with the age determination from the recent ODP Leg127/128 results. (3) The visco-elastic equilibrium attained by the crustal part overlying mantle material could be deduced by the use of the admittance function technique to reveal that the main part of the Yamato Basin is isostatically compensated and that the transition zone between these two basins is supported partly by elastic strength of the crust. These findings will be incorporated into our present knowledge of the geophysical feature of this basin area to construct a new view on the evolution and dynamics of the Japan Basin.

References

Airy, G. B. (1855) Philos.Trans.R.Soc., 145.
Akima, H. (1970) J.Acm., 17, 589.
Beresnev, A. F. and V. M. Kovylin (1968) P.P.Shirstitute of Oceanology, USSR Academy of Sciences, 86.
Briggs, I. G. (1974) J.G.R., 39, 39.
Crough, S. T. (1983) J.G.R., 88, 6449.
Harland, W. B., et al. (1989) A Geologic Time Scale, Camb.Univ.Press, 263.
Hilde, T. W. C., S. Uyeda, and L. Kroenke (1977) Tectonophy., 38, 145.
Hilde, T. W. C. and J. M. Wageman (1975) Island Arcs, Univ.West.Aust.Press,123.
Hirata, N. and H. Kinoshita(1991) Month Earth, 3, 190.
IAGA Division I Working Group 1 (1987) J.G.G., 39, 773.
Ingle Jr, J. C. et al. (1990) Proc. ODP, Init. Repts., College Station, 652.
Isezaki, N. (1973) Oceanographical Magazine, 24, 107.
Isezaki, N. and S. Uyeda (1973) Marine Geophys. Res., 2, 51.
Isezaki, N. (1986) J.G.G., 38, 403.
Isezaki, N. and Y. V. Shevaldin (1991) Japan-USSR Monograph Series 1.
Ishiwada, Y., E. Honza, and K. Tamaki (1984) Proc.27th Inter.Geol.Congr.,23, 43.
Japanese DELP Research Group (1987) Bull. Earthq. Res. Inst., 62, 339.
Katao, H. (1988) Bull.Earthq.Res.Inst., 63, 51.
Kinoshita, H. and S. Uyeda (1990) DELP News.
Kobayashi, K. and N. Isezaki (1976) Geophys. Monogr. Ser. 19, 235.
Kobayashi, K., K. Tamaki, M. Nakanishi, N. Isezaki, and K. Sayanagi (1986) EOS, 67, 44, 1227.
Kobayashi, K. (1988) Preliminary Report of the Hakuho Maru Cruise KH86-2, Ocean Res. Inst., Univ. Tokyo, 129.
Kono, M. (1986) J.G.G., 38, 411.
Kuramoto, S. (1989) Month. Earth (in Japanese), 11, 503.
Lallemand, S., P. Huchon, J. P. Brun, X. Le Pichon, C. C-Rooke, and J. C. Tom (1991) J.G.R., 96, 4367.
Labreque, J. L. (1986) Program Modelf.
Leg 127 Shipboard Scientific Party (1989) Nature News & View.
Louden, K. E. (1981) Geophy.J.R.astr.Soc., 64.
Ludwig, W. J., S. Murauchi, and R. E. Houtz (1975) Geol.Soc.Am.Bull., 87, 651.
Matsumoto, K. and N. Isezaki (1989) B.C.thesis (in Japanese), Kobe University.
Seama, N. and N. Isezaki (1990) Tectonophy., 181, 285.
Tamaki, K. (1986) J.G.G., 38, 427.
Tamaki, K. (1988) Bull. Geol. Surv. Japan, 39, 5, 269.
Tamaki, K. and K. Kobayashi (1988) Mar. Sci. Mon. (in Japanese), 20, 705.
Tamaki, K., K. Kobayashi, N. Isezaki, K. Sayanagi, M. Nakanishi, and C. H. Park, (1988) preliminary Report of the Hakuho Maru Cruise KH86-2, 7.
Tamaki, K. and K. Pisciott, et al. (1990) Proc. ODP, Init. Repts. 127, College Station, 844.

AUTHOR INDEX